

THESIS



3 1293 01591 3944

This is to certify that the

thesis entitled

## PERMEATION OF TOLUENE VAPOR THROUGH GLASSY POLY(ETHYLENE) TEREPHTHALATE FILMS

presented by

Ruben J. Hernandez Macias

has been accepted towards fulfillment of the requirements for

M. S. degree in Chemical Engineering

Date November 9, 1984

MSU is an Affirmative Action/Equal Opportunity Institution

professor

**O**-7639



RETURNING MATERIALS:
Place in book drop to
remove this checkout from
your record. FINES will
be charged if book is
returned after the date
stamped below.

JAN 1 1 2000
21 AUB D 3 2002

# PERMEATION OF TOLUENE VAPOR THROUGH GLASSY POLY(ETHYLENE) TEREPHTHLATE FILMS

Ву

Ruben J. Hernandez Macias

### A THESIS

Submitted to
Michigan State University
in partial fulfillment of the requirements
for the degree of

MASTER OF SCIENCE

Department of Chemical Engineering

Copyright by

Ruben J. Hernandez Macias

1984

#### ABSTRACT

## PERMEATION OF TOLUENE VAPOR THROUGH GLASSY POLY(ETHYLENE) TEREPHTHALATE FILMS

By

#### Ruben J. Hernandez Macias

Biaxially oriented poly(ethylene) terephthalate films were permeated in both continuous-flow and accumulative methods with a toluene vapor-nitrogen mixture. A continuous flow apparatus was developed and built for this purpose. The influence of vapor toluene concentration and temperature on the diffusion coefficient and permeability constant was studied for one type of film. The permeation behavior of the toluene/poly(ethylene) terephthalate system appeared to be Fickian at 23° C. While the diffusion coefficient was dependent only on toluene concentration at ambient temperature, a minimum threshold value of concentration was detected. An expression based on free volume theory was developed to predict the experimental data. The diffusion coefficient appeared to follow an Arrhenius expression with temperature. Permeability data suggested that an increasing temperature and previously exposing the film to toluene vapor can affect drastically the permeability properties of poly(ethylene) terephthalate with organic vapors. Different permeability constant values were obtained, depending on the method of the test.

To my parents and my wife.

#### **ACKNOWLEDGMENTS**

I wish to express my appreciation to Dr. K. Jayaramam for his guidance throughout my research and to Dr. Jack Giacin from the School of Packaging for his continuous support, guidance, and use of his laboratory.

I wish to thank Eastman Kodak Co. for providing sample films of poly(ethylene) terephthalate and Perkin-Elmer Co. for their analysis on the Differential Scanning Calorimeter. I am further grateful to Dr. Chester Mackson, Director of the School of Packaging, for providing a research assistantship in support of this work and for the use of laboratory facilities.

I also want to thank Larry Baner for sharing with me his expertise on gas chromatography.

I acknowledge financial support for this study from a grant from MSU Foundation, from the School of Packaging, and support provided by Mobil Chemical Company Films Division.

## TABLE OF CONTENTS

		Pag
1.	List of Tables	vii
2.	List of Figures	×
3.	Nomenclature	xii
	3.1 Nomenclature used in Literature Review	xii xiv
4.	Introduction	1
5.	Literature Review	3
	5.1 Diffusion coefficients	3
	5.2 Ideal diffusion and sorption of fixed gas	7
	5.3 Characterization of the diffusion process	8
	5.3.1 Glassy state	8 10 12
	5.4 Fickian and non-Fickian diffusion	13
	5.5 Effect of molecule orientation on diffusion	18
	5.6 Permeability theories	22
	5.6.1 Fujita free-volume theory	22 27 28
6.	Materials and Methods	35
	6.1 Materiale	35

																					Page
	6.2	Experi	menta	1 pro	ced	lure	<b>s</b> .	• •	•	•	•	•		•	•	•	•	•	•	•	
		6.2.1	Cont	1nuo	ıs g	as	f1 o	w pe	ərme	ea t	:10	n a	арр	ara	atı	ıs					39
		6.2.2		ation	_			-													49
		6.2.3		1 s1 or																	51
		6.2.4		mulat																	54
		6.2.5		ity g																	55
		6.2.6		brati																	58
		6.2.7		erent																	59
		••••	• • • • • • • • • • • • • • • • • • • •	0. 0		-	~	9	<b>-</b>			<b>.</b>	J	•	•	•	•	•	•	•	
7.	Resul	ts and	disc	ussic	on .	•	• •	•	• •	•	•	•	•	•	•	•	•	•	•	•	60
	7.1	Permeat	ti on	of to	ol ue	ne	thr	ougt	n PE	ΕT	•	• (	•	•	•	•	•	•	•	•	60
		7.1.1	Expe	rimer	nt l			•						•						•	61
		7.1.2		rimer																	63
		7.1.3		rime																	65
		7.1.4																			68
		7.1.5	Expe	rimer	nts	5 a	nd (	5	• •	•	•			•	•	•	•	•	•	•	
		7.1.6																			
		7.1.7																			
		7.1.8																			
		7.1.9		tion																	-
														•	•	•	•	•	•	•	02
		7.1.10		erati																	82
			camp	ישוים נו	11.0	UI		•	• •	•	•	•	• •	•	•	•	•	•	•	•	02
	7.2	D1 scuss	s1 on	• •		•	• •	• •		•	•	•		•	•	•	•	•	•	•	84
		7.2.1	Debo	rah r	umb	er				_	_			_		_	_	_		_	84
		7.2.2		erati																	85
		7.2.3		eant										<del>0</del> 1		- 1 6	3111	•	•	•	05
		1.2.3		ustor																	88
		7 0 4																			
		7.2.4		der										•	•	•	•	•	•	•	99
		7.2.5		ct of																	100
			to t	ol ue	ne v	apo	r.	•	• •	•	•	•	• •	•	•	•	•	•.	•	•	103
8.	Conc	lustons		• •		•		•		•	•	•		•	•	•	•	•	•	•	105
	8.1	Literat	ture	revie	ew c	ons.	i de	rati	ion	S	•	•		•	•	•	•	•	•	•	105
	8.2	Equ1 pm	ent c	onsi	dera	tic	ns	•		•	•	•		•	•	•	•	•	•	•	106
	8.3	Permea	tion	proce	<b>9</b> SS	con	sid	era	tio	ns	•	•		•	•	•	•	•	•	•	106
^	Door																				110

																				<u>Page</u>
10.	Appendices																			
	Appendix I:	: Sa	mple	cal	cula	atio	ns	•		•	•	•	•	•	•	•	•	•	•	112
	Appendix II		odel alcul									•	•	•	•		•	•	•	114
	Appendix II	II: Mo	del	for	lag-	-tin	ne m	eth	od	•	•	•	•	•	•	•	•	•	•	118
	Appendix IV	/: Mc	del	for	sma]	1-1	:ime	ap	pro	ıtxo	nat	t1 c	ח	me	th	od	i	•	•	120
	Appendix V:	: Sn	nall-	time	met	thod	d ca	1cı	ılat	:10	n	•	•	•	•	•	•	•	•	122
	Appendix VI	: DS	SC p1	ots				•		•	•	•	•	•	•	•	•	•	•	125
11.	Literature	ci te	i					•		•	•	•	•	•	•	•	•	•	•	130
12.	Materials b	16110	ograp	hy .				•						•						136

## LIST OF TABLES

Table		Page
1	Vapor-organic polymer permeation system	25
2	Density and percent of crystallinity of the PET sample films	36
3	Some properties of PET	38
4	Conditions at which the gas chromatograph was normally run	48
5	Conditions at which the gas chromatograph was run for calibration	59
6	Data for Experiment 1	63
7	Data for Experiment 2	65
8	Data for Experiment 3	68
9	Data for Experiment 4	71
10	Data for Experiments 5 and 6	72
11	Data for Experiment 7	75
12	Data for Experiment 8	78
13	Data for Experiment 9	79
14	Summary data for diffusion of toluene vapor through PET	81
15	Solubility data, toluene vapor-PET	82
16	Value of D <sub>s</sub> as a function of temperature	87
17	Value for the Arrhenius equation	88
18	Values of the weight fraction as a function of toluene partial pressure plotted in Figure 20	93

Table	Page
19	Values of mutual diffusion coefficient as a function of w
20	Values of w <sup>-1</sup> and [1n D/0.23 D <sub>0</sub> ] <sup>-1</sup>
21	Comparison of experimental and calculated values of D
22	Permeability constants in g.mil/day.m <sup>2</sup> .100 ppm at 23°C, 90 ppm of toluene
23	Permeability constant for seleced films
A-1	Values for Experiment 4
A-2	Values for Experiment 1
A-3	Values for Experiment 2
A-4	Values for Experiment 4
A-5	Values for Experiment 7

## LIST OF FIGURES

<u>Figure</u>		Page
1	Volume-temperature relation (adapted from Haward, 1973)	9
2	Fickian permeation curve (adapted from Fujita, 1961)	15
3	Non-Fickian permeation curve (adapted from Fujita, 1961)	15
4	Concentration-penetrant activity diagram (adapted from Hopfenberg and Frisch, 1969)	17
5	General temperature—penetrant concentration diagram (adapted from Vrentas et al, 1975)	19
6	Schematic of the cell for continuous gas flow method and photograph	40
7	Experimental process flow diagram and photograph	43
8	Plumbing between the sampling valve and the sample stream (adapted from Hewlett Packard 5830A gas chromatograph, Instrument Manual)	. 47
9	Schematic representation of a quasi-isostatic cell	56
10	Experiment 1 Total permeated toluene Q versus time	62
11	Experiment 2 Total permeated toluene Q versus time	64
12	Experiment 3 Flow rate of permeated toluene Q versus time	66
13	Experiment 3 Total permeated toluene Q versus time	67
14	Experiments 4 and 9 Flow rate of permeated toluene Q versus time	69
15	Experiment 4 Total permeated toluene Q versus time	70
16	Experiments 7 and 1 Total permeated toluene Q	73

Figure		Page
17	Experiment 8 Total permeated toluene versus time	77
18	Diffusion coefficient as a function of permeant concentration at 23 °C	80
19	Solubility equilibrium at 23°C	83
20	Penetrant partial pressure versus weight fraction at 23°C and solution equilibrium	92
21	Plot of [ln D/0.23D <sub>0</sub> ] <sup>-1</sup> versus W <sup>-1</sup> for toluene/PET at 23°C	96
22	Values of diffusion coefficient versus toluene concentration, predicted and experimental	100
A-1	X versus time for Experiment 4	117
<b>A-</b> 2	DSC plot for Sample a	126
<b>A-</b> 3	DSC plot for Sample b	127
A-4	DSC plot for Sample c	128
A-5	DSC plot for Sample d	129

## NOMENCL ATURE

## 3.1 Nomenclature used in Literature Review

Symbol		<u>Units</u>
Ad b	proportional parameter in the Langmuir isotherm	mol.cm <sup>2</sup> /mol.sec
Bd	parameter for the free-volume theory	dimensionless
C	•	cc/cc
	concentration of permeant	
Cp <sup>B</sup>	amount of permeant contained per unit	g/cc
C <sub>P</sub> M	of volume of polymer  amount of permeant contained per unit  of total mass	g/g
C <sub>P</sub> V	amount of permeant contained per unit of volume of mixture	g/cc
C'A	parameter in the Langmuir isotherm	concentration
D	mutual diffusion coefficient	cm <sup>2</sup> /sec
D#	intrinsic diffusion coefficient	cm <sup>2</sup> /sec
DLag	diffusion coefficient from lag time	cm <sup>2</sup> /sec
DPV	volume-fixed diffusion coefficient of the permeant	cm <sup>2</sup> /sec
DPB	polymer-fixed diffusion coefficient of the permeant	cm <sup>2</sup> /sec
D <sub>P</sub> M	mass-fixed diffusion coefficient of the permeant	cm <sup>2</sup> /sec
D <sub>T</sub>	thermodynamic diffusion coefficient	cm <sup>2</sup> /sec
DO	self diffusion coefficient	cm <sup>2</sup> /sec

Symbol		<u>Units</u>
D <sub>0</sub>	<pre>pre-exponential factor or limiting diffusion coefficient</pre>	cm <sup>2</sup> /sec
D <sub>01</sub>	<pre>pre-exponential factor for the self- diffusion expression</pre>	cm <sup>2</sup> /sec
(DEB)B	Deborah number	dimensionless
ED	Activation energy for diffusional process	cal/mole
EP	Activation energy for permeation process	cal/mole
Eθ	Activation energy for lag time	cal/mole
f	average of free volume per unit of volume	dimensionless
	thickness of the film	cm or mil
v <sub>B</sub>	specific volume of polymer	cc/g
۷p	specific volume of permeant	cc/g
w	mass fraction	dimensionless
×	mole fraction	dimensionless

## Other Subscripts

B polymer

P penetrant molecule

## Other Superscripts

B polymer

P penetrant molecule

## Greek Letters

Symbol		<u>Units</u>
α	numerical factor to correct for overlapping free volume	dimensionless
$\overline{\alpha}$	amorphous volume fraction	dimensionless
β	polymeric continuous phase volume fraction	dimensionless
θ	lag time	time
θο	pre-exponential factor	time
λm	mean relaxation time	sec.
μ	viscosity	g/cm.sec
μ <sub>n</sub>	chemical potential of permeant	
μ <sub>p</sub> ξ	factor relating critical volume	dimensionless
ρ	density	g/cc

## 3.2 General Nomenclature

Symbol		<u>Units</u>
ap	activity coefficient	
c	permeant concentration in the gas phase	$g \times 10^6/cc$
F	flux of toluene through film	g/time area
f#	free volume fraction at zero penetrant	dimensionless
	concentration	
Р	partial pressure	atm.
p <b>pm</b>	parts per million	$g \times 10^6/cc$
P	permeability constant	g.mil/m <sup>2</sup> .day.
		100 ppm
σ	total accumulated toluene	g
R	gas constant	
t	time	time

Symbo	1	<u>Units</u>
Т	temperature	•K
٧o	volume of the cell lower chamber	cc
W	weight fraction of toluene in PET	dimensionless

## Greek Letters

Symbol

	_	
Υ	average free volume per unit volume of solvent	dimensionless
φ <sub>a</sub> θ <sub>D</sub>	amorphous fraction of PET	dimensionless
חס	characteristic diffusion time	sec

<u>Units</u>

#### INTRODUCTION

with the increased use of polymers in areas such as pharmaceutical, food and beverage packaging, both as rigid containers and flexible films, knowledge of the diffusivity properties of gases and subcritical vapors in the polymers will play an increasingly important role in the selection of a packaging system for a particular end use application and for engineering applications. Poly(ethylene) terephthalate, PET, has gained an increasing importance in the packaging sector because of its aroma barrier properties.

While there is a considerable amount of data on the diffusion of oxygen, carbon dioxide and water vapor through PET, there is a lack of data on the diffusion of organic molecules through poly(ethylene) terephthalate, particularly below the glass transition temperature (Tg) and on the effect of thermal-mechanical chain orientation conditions on the diffusion coefficient of organic penetrants through PET barrier membranes. Such knowledge would lead to a better understanding of diffusion in glassy polymers for the case of permeant molecules that have strong thermodynamic interactions with the polymer and for penetrant/polymer systems when a concentration-dependent diffusion coefficient is observed. Further, this would provide package design criteria. Thus, studies on PET films have both practical and theoretical importance. The difficulty of the experimental procedure and the length of time required to collect data are characteristic of

the organic vapor-PET barrier membrane system, and justify, in part, the present lack of data.

An experimental procedure was therefore developed in order to conduct more operator—independent experiments, having good control of the variables. The objectives of this research were:

- 1. Review past experimental methods and results, and current theory on polymer-organic penetrant diffusion systems.
- 2. Assemble a continuous-flow, automatic sampling apparatus to measure the diffused penetrant.
- 3. Carry out diffusion experiments on the penetrant barrier system of toluene vapor-PET, analyzing the results and effects on the film.
  - 4. Make recommendations for future work.

#### LITERATURE REVIEW

The literature review encompasses studies by previous investigators on the objectives set forth in this investigation. These included the fundamental aspects on Fickian and non-Fickian diffusion in glassy polymers, methodology, experiments on permeation of organic vapor and studies which considered the permeability of PET specifically.

#### 5.1 <u>Diffusion Coefficients</u>

Diffusion is defined as the process in which components are transported from one part of a mixture to another as a result of random molecular motion. For polymer-penetrant systems diffusion, two experimental methods are typical. They are the sorption method and the permeation method.

In a sorption experiment, a given polymer is exposed to a gas or vapor of a given penetrant substance at a given pressure and temperature and the gain or loss in weight of the film is measured as a function of time. In a permeation experiment, the penetrant flow through a film of a given polymer or the total amount flowed through the film is measured as a function of time under the condition that the concentration of the penetrant in one side of the film be different from the concentration of the other side (Fujita, 1961).

The behavior of a two-component system, satisfying the condition

of zero volume change on mixing and independent of pressure is given by Fick's second law of diffusion:

$$\frac{\partial c_{p}}{\partial t} = \text{div. (D grad } c_{p}) \tag{1}$$

When diffusion is only considered along the x-axis, Equation 1 becomes

$$\frac{\partial c_{\mathbf{p}}}{\partial \mathbf{t}} = \frac{\partial}{\partial x} D \frac{\partial c_{\mathbf{p}}}{\partial x} \tag{2}$$

Where D is the mutual diffusion coefficient and is equal to  $D_P^V$ , the volume-fixed diffusion coefficient of the permeant, P, since the polymer film is a section fixed with respect to the diffusant.

The concentration  $c_p$  is here expressed as the amount of permeant contained in unit volume of mixture, V; or in unit basic of volume of polymer, B; or in unit basic of total mass, M. It can be written as  $c_p^V$ ,  $c_p^B$ ,  $c_p^M$ . The same holds for expressing the polymer concentration  $c_8^V$ ,  $c_8^B$ ,  $c_8^M$ .

This allows for distinguishing the different diffusion coefficients  $D_B{}^V$ ,  $D_P{}^B$ ,  $D_P{}^M$  to indicate the frame of reference to which they refer. The relations between them are (Crank, 1979):

$$D_{P}^{B} = D_{P}^{V}(v_{B} c_{B}^{V})^{2} = D_{P}^{B}(1-v_{P} c_{P}^{V})$$
 (3)

$$D_{P}^{M} = D_{P}^{V}(c_{B}^{V}/c_{B}^{M}) = D_{P}^{V}(1-c_{P}^{V})/(1-c_{P}^{M})$$
 (4)

Where  $v_B$  and  $v_P$  denote the constant volumes of the unit amount used in defining the concentration of polymer, B, and penetrant, P.

When a difference of mass and size between the molecules of a two-component system exists, a hydrostatic pressure tends to build up in

the region of transfer. This pressure is relieved by a compensating bulk flow. The existence of bulk flow can be demonstrated in the case of gases, when diffusion occurs across a porous plate which offers considerable resistance.

This also has been demonstrated in selected polymer-solvent systems (Richards, 1946).

The overall rate of transfer of a component across a volume-fixed section may be expressed as the combined effect of bulk-flow and true diffusion, resulting from the random motion of non-uniformly disturbed molecules. The intrinsic diffusion coefficient  $(D^*p)$ , expressed in terms of the rate of transfer of component P across a fixed section does not consider the bulk-flow through it, but only diffusion. The relation between  $D_p^V$ ,  $D^*p$  and  $D^*p$  is given by:

$$D_{P}^{V} = V_{P}^{V} C_{P}^{V} (D*_{B} - D*_{P}) + D*_{P}$$
 (5)

In the use of vapor diffusion through a polymer film, the intrinsic diffusion coefficient of the polymer  $D*_B$  is zero and (Hartley and Crank, 1949):

$$D_{P}^{*} = D_{P}^{V}/(1-V_{P} C_{P}^{V}) = D_{P}^{V}/V_{B} C_{B}^{V}$$
 (6)

From equations 3 to 6, D,  $D_P^V$ ,  $D_P^B$ ,  $D_P^M$  and  $D*_P$  converge to the same value  $D_0$  at the limit of zero penetrant concentration.

Another coefficient, the thermodynamic diffusion coefficient  $D_{\mathsf{T}}$  is defined in section 5.6.1.

The self-diffusion coefficient of a diffusing particle of radius  $r_1$  in a pure solvent of viscosity  $\mu$  is given by the Stoke-Einstein equation (Bird et al. 1960):

$$D_{1} = \frac{1}{6\pi r_{1}} \frac{kT}{\mu} \tag{7}$$

Where T is the absolute temperature and k is the Boltzmann constant.

Cohen and Turnbull (1959) expressed the self-diffusion coefficient as a function of the free volume parameters.

Vrentas and Duda (1977a), following Cohen and Turnbull, expressed the self-diffusion coefficient and applied it to a solvent-polymer system:

$$D_{1} = D_{01} \exp \left[-\alpha (w_{1} \hat{v}_{1}^{*} + w_{2} \xi \hat{v}_{2}^{*})/\hat{v}_{FH}\right]$$
(8)

Where  $D_{01}$  is the pre-exponential factor

is a numerical factor introduced to correct for overlapping of free volume

Îs the specific critical hole-free volume of component

 $\hat{\mathsf{V}}_{\mathsf{FH}}$  is the average hole—free volume per gram of mixture

ξ relates the critical volume of jumping units of two components and can be determined experimentally

is the fraction mass of polymer and solvent respectively.

Vrentas and Duda (1977b) related the self-diffusion coefficient to the mutual diffusion coefficient D, by:

$$D = \frac{D_p x_B + D_g x_p}{RT} \left( \frac{\partial \mu_p}{\partial \ell n x_p} \right)_{T, P}$$
 (9)

Where  $D_P$  and  $D_B$  are the self-diffusion coefficient of the penetrant and polymer respectively

 $x_{\rm D}$  and  $x_{\rm R}$  are the hole fractions

 $\mu_{p}$  is the chemical potential of penetrant that can be determined from the thermodynamic theory of Flory

### 5.2 Ideal diffusion and sorption of fixed gas

Henry's law relates the concentration of penetrant in the polymer C and the partial pressure of the penetrant in the gas phase:

$$C = sp \tag{10}$$

where C is the concentration of permeant in the gas phase, s is the solubility coefficient, and p is the partial pressure.

The relation between permeability, diffusion coefficient D, and solubility s is given by Barrer (1939):

$$\overline{P} = s.D$$
 (11)

where  $\overline{P}$  is the permeability constant.

D varies with temperature in the following way:

$$D = K \exp \left(-E_D/RT\right) \tag{12}$$

where K is the pre-exponential factor,  $E_D$  is the activation energy, T is the absolute temperature, and R is the gas constant. Barrer (1939) also showed that the lag time  $\theta$ , defined in Appendix III, is related to D by

$$\theta = \frac{\ell^2}{6n} \tag{13}$$

where & is the thickness of the film.

Both 
$$\theta_0$$
 and  $\overline{P}_0$  follow the Arrhenius law with temperature:  
 $\theta = \theta_0 \exp(-E_\theta/RT)$  (14)

and

$$\overline{P} = \overline{P}_0 \exp \left(-E_{\overline{P}}/RT\right) \tag{15}$$

where  $\theta_0$  and  $\overline{P}_0$  are the pre-exponential factors, and  $E_{\theta}$  and  $E_{\overline{p}}$  the activation energies.

#### 5.3 Characterization of the diffusion process

PET is a linear polyester with a melting point of 255°C and a glass transition temperature (Tg) of 69°C. Since this study was carried out at room temperature (about 23°C), the polymer was in its glassy state. Moreover, the PET samples were partially crystalline with about 25% of crystallinity, and biaxially oriented at 100°C.

Brief statements dealing with glassy polymers and crystallinity concepts are presented only to facilitate an understanding of the diffusion process.

#### 5.3.1 Glassy state

Polymer glasses consist essentially of long chain molecules which have a random configuration and which are packed together to fill space. The precise properties are below the temperature at which the polymer hardens and becomes a glass. This temperature is the glass transition temperature, Tg (Haward, 1973).

Figure 1 shows schematically how the glassy state is related to the crystalline state and the melt. This is an isobaric volume—temperature diagram, where the process of the glassy solidification can

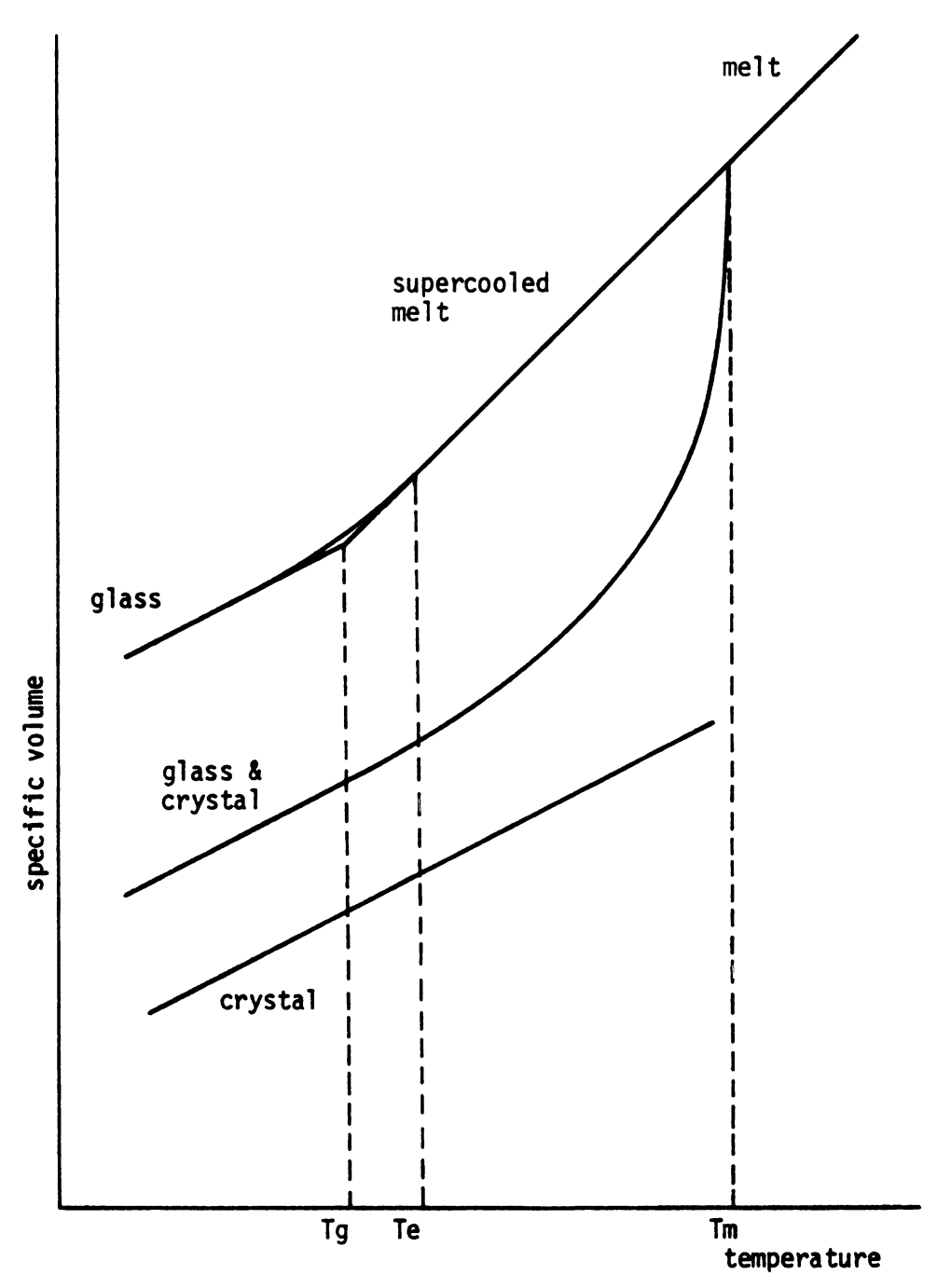


Figure 1. Volume-temperature relation. Tm, melting point; Tg, glass transition temperature; Te freezing-in temperature. Adapted from Haward (1973).

be examined. A glass is a "frozen-in" supercooled liquid. Here the concept "frozen-in" indicates that we are dealing with an inhibited, non-equilibrium state (i.e., the inhibition of a kinetic process). However, the origin of the glass-rubber transition remains obscure and the molecular explanation that has been advanced by a number of workers does not have universal approval. A comprehensive review of the glassy state of polymers is given in the book edited by Haward (1973).

#### 5.3.2 Crystallinity

The concept of degree of crystallinity or crystallinity arises from the observation that many properties of polymers are intermediate between those expected of a purely crystalline and of a purely liquid (or amorphous) material. The concept of crystallinity assumes the existence of a two-phase system, when the properties of each phase are assumed to be independent of the presence and amount of the other. An observed property such as density is considered to be additive.

The longest dimension of the crystallites in polycrystalline materials is usually about 5 nm, which is a small fraction of length of a fully extended polymer molecule. A long polymer chain can traverse successively through disordered, random regions through bundles of organized regions called micelles, then an amorphous region again and so on. For a polymer that can be extended to a length of 5000 nm with crystal and amorphous domains averaging 10 nm a single polymer thread might tie together a hundred or more crystallites. But the abrupt change in density from crystal to amorphous region at the end of the

micelle is unlikely. If some of the chains can fold on themselves, the transition to the amorphous region can be accommodated. Such chain folding has been shown when drawn PET is annealed (Dumbleton, 1969).

Mechanical properties of polymers of low percent crystallinity (<25%) may be explained in terms of an essentially amorphous polymer with the crystallites acting as massive cross-links of about 5 to 50 nm in diameter. The cross-links restrain the movement of the amorphous network just as covalent cross-links would, but unlike the covalent bonds, the crystal cross-links can be melted or mechanically stressed beyond a low yield point.

Quiescent crystallization of a polymer from the melt or solution often results in a peculiar form of crystallite growth with a preferred chain orientation relative to a center (nucleus). Polarized light reveals that the polymer chains are oriented tangentially around each nucleus despite the fact that the area, called a spherullite, consists of a multitude of crystallites and is not a single crystal (Rodriguez, 1982).

Misra and Stein (1979) studied the stress-induced crystallization of PET, upon stretching PET above and below Tg. When PET was stretched above Tg they found an increase in crystallinity for samples stretched at 80°C and beyond 80% strain. Only strain-induced crystallization was found to take place at this temperature. With an increase in the temperature (from 80 to 110°C) there is a decrease in the extent of rodlike superstructures and their size. Stretching to

175% elongation increased the number and size of spherulites; however on stretching to 350% elongation, a fibrillar morphology was attained.

At low elongation levels, a rodlike superstructure exists that does not contribute to crystallinity but is highly oriented in the direction of normal stretching. At high elongation levels (above 200%) the rods change into ellipsoidal spherullites which are elongated normal to stretching. The ellipsoids can be considered to be composed of rods oriented preferentially in the direction normal to stretching.

#### 5.3.3 Glass transition temperature and Fickian diffusion

The importance of the glass transition temperature, Tg, in the mass transport of a penetrant-polymer system was described by Meares(1954), and is now very well recognized.

The glass transition temperature (Tg) of any amorphous substance, whether polymeric or not, is defined as the point where the thermal expansion coefficient undergoes a discontinuity. Decrease in temperature is accompanied by collapse of free volume which is made possible by configurational adjustments. Eventually, the free volume becomes so small that further adjustments are extremely slow or even impossible. In polymers, there may be more than one discontinuity in the thermal expansion coefficient. The largest discontinuity is usually associated with the loss of the molecular mobility which permits configurational rearrangements of the chain backbones; this is "the" glass transition (Ferry, 1970).

The sorption of gases above Tg indicates that the heat of solution must include along with the heat of interaction between the

which is endothermic, therefore accounting for the endothermic and slightly exothermic heats of solution. The exothermic heats of solution below Tg can be explained by the inclusion of the exothermic heat of adsorption for the "hole filling" in the heat of solution. The diffusion process above Tg requires a larger zone of chain activation than below Tg which is consistent with the higher surge of activation reported above Tg (Hopfenberg and Stannet, 1973).

The glass transition temperature is very important in the mass transport of organic penetrant-polymer systems. For example, Fujita (1981) and Meares (1965) claimed that the free volume theory (described on page 22) is only valid well above Tq.

#### 5.4 Fickian and non-Fickian diffusion

When D is only a function of concentration, diffusion is called Fickian. When D also varies with time, diffusion is often called non-Fickian. Organic vapors are usually freely absorbed by polymers and the sorbed molecules diffuse by a random exchange of places with polymer segments. The micro-Brownian motion of the chain segment is very retarded compared with that of the sorbed molecule. This absorption causes the polymer to swell and so changes the configurations of the polymer molecules. These configurational changes are not instantaneous but are controlled by the retardation times of the chains. If these are long, stresses may be set up which relax slowly. Thus the absorption of a vapor is accompanied by time-

dependent processes in the polymer which are slower than the micro-Brownian motion which promotes diffusion (Meares, 1965).

At temperatures well above Tg the micro-Brownian motion of polymer is sufficiently active even in the undiluted state of a given polymer to enable equilibrium to be reached rapidly. At such temperatures the chains in any volume element of the polymer may take up almost instantaneously an equilibrium conformation consistent with the sorbed state when a vapor diffuses into the solid. In this case the time-dependence of D due to internal stresses also should disappear, since the stress set up by swelling immediately decays by a rapid chain relaxation. Then at temperatures well above Tg the diffusion coefficient of a polymer-organic vapor system becomes free of any time-dependent effect and depends only on the diffusant concentration (Fujita, 1981).

Fujita (1981) described a Fickian permeation as having the following characteristics (see figures 2 and 3):

- a. Plots of Q vs. t are convex toward the time axis and approach asymptotically a straight line as t increases. This behavior is valid irrespective of the focus of D as a function of concentration. Q is the total amount of material permeated at time t.
- b. On the asymptotic linear portion, the rate of permeation dQ/dt is independent of time, and so the permeation is said to be in the steady state. In this state, the concentration distribution in the film no longer changes with time.
- c. The time lag (0) for permeation is defined as the intercept of the time axis of the steady-state portion of a permeation curve.

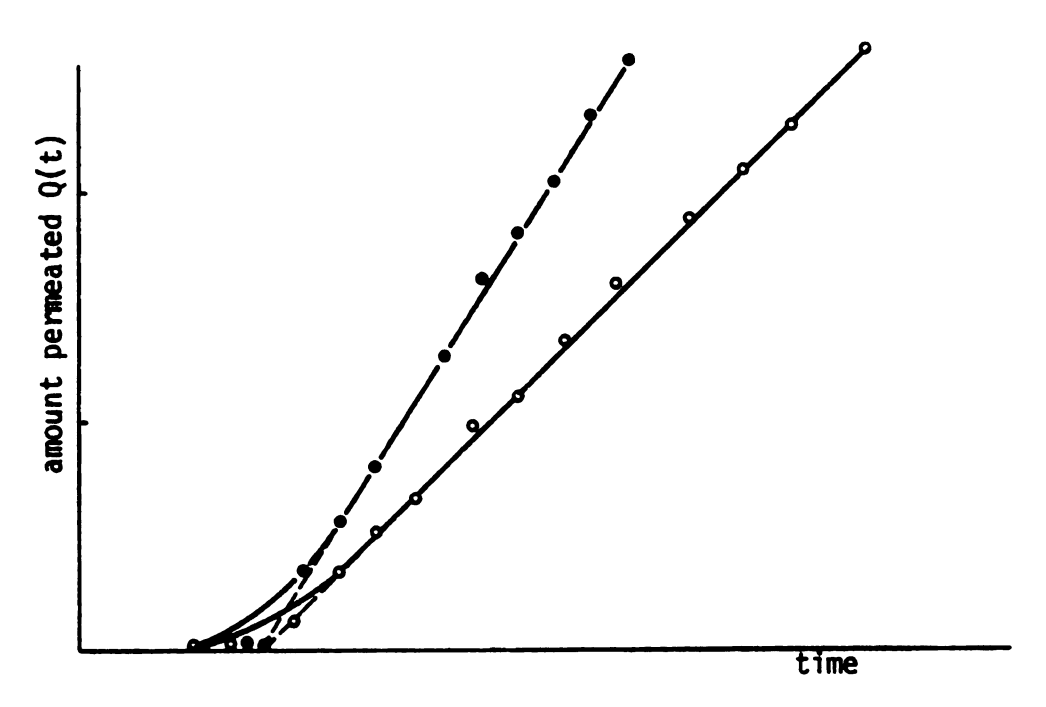


Figure 2. Fickian permeation.
Adapted from Fujita (1961)

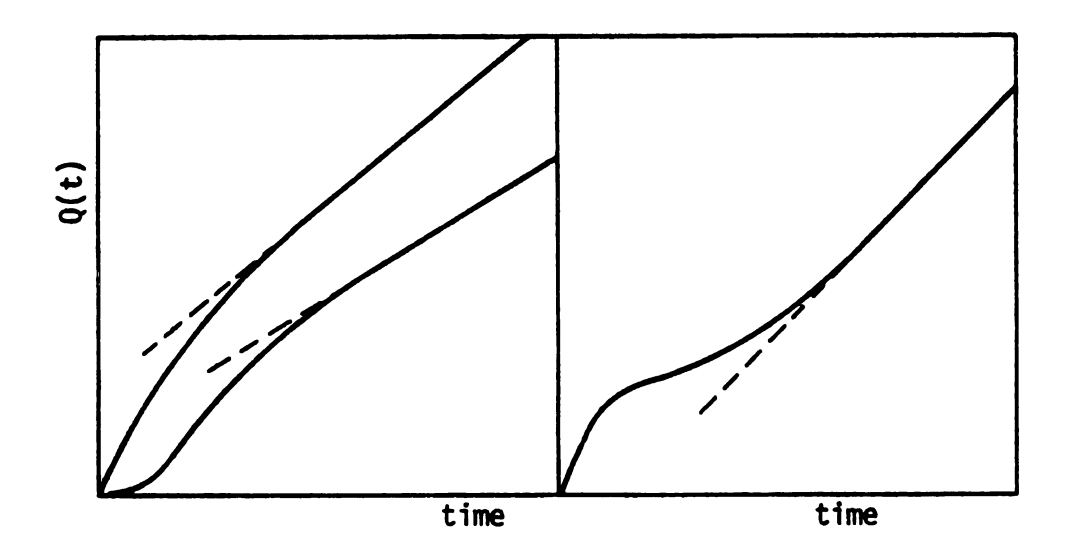


Figure 3. Non-Fickian permeation.

Adapted from Fujita (1961)

Figures 2 and 3 show schematic representations of a Fickian permeation and a non-Fickian permeation curve respectively.

Alfrey et al (1965) made a more quantitative classification of diffusion processes using data from a sorption experiment. Denoting by Q the amount of diffusant sorbed, when fitting Q to  $kt^n$ , where k is a constant and t is time, there exist the following cases depending on the value of n. Fickian diffusion is characterized by n = 1/2, non-Fickian diffusion is defined when n is between 1/2 and 1. Three situations are differentiated by Alfrey et al based on polymer chain relaxation rates and diffusion rates:

- Fickian diffusion or case I in which the rate of diffusion is much less than that of relaxation, and the system is controlled by the diffusion coefficient. In this case n = 1/2. Here the diffusion coefficient may depend on concentration for the specific penetrant-polymer system.
- Case II in which the relaxation process is much slower than the diffusion rate is characterized by n = 1, and the kinetics can be reduced to only the velocity of the advancing front of the diffusant in addition to the equilibrium swelling factor. This is an apparent Fickian process.
- Non-Fickian or anomalous diffusion occurs when diffusion and relaxation rates are of the same order.

A more complete generalization, although very qualitative, has been described by Hopfenberg and Frisch (1969). The relations between the various transport features are easily understood by examining the various regions of temperature—activity presented in figure 4, which was described by the authors.

Vrentas, Jarazebsky and Duda (1975) presented a general temperature-penetrant concentration diagram in function of the Deborah

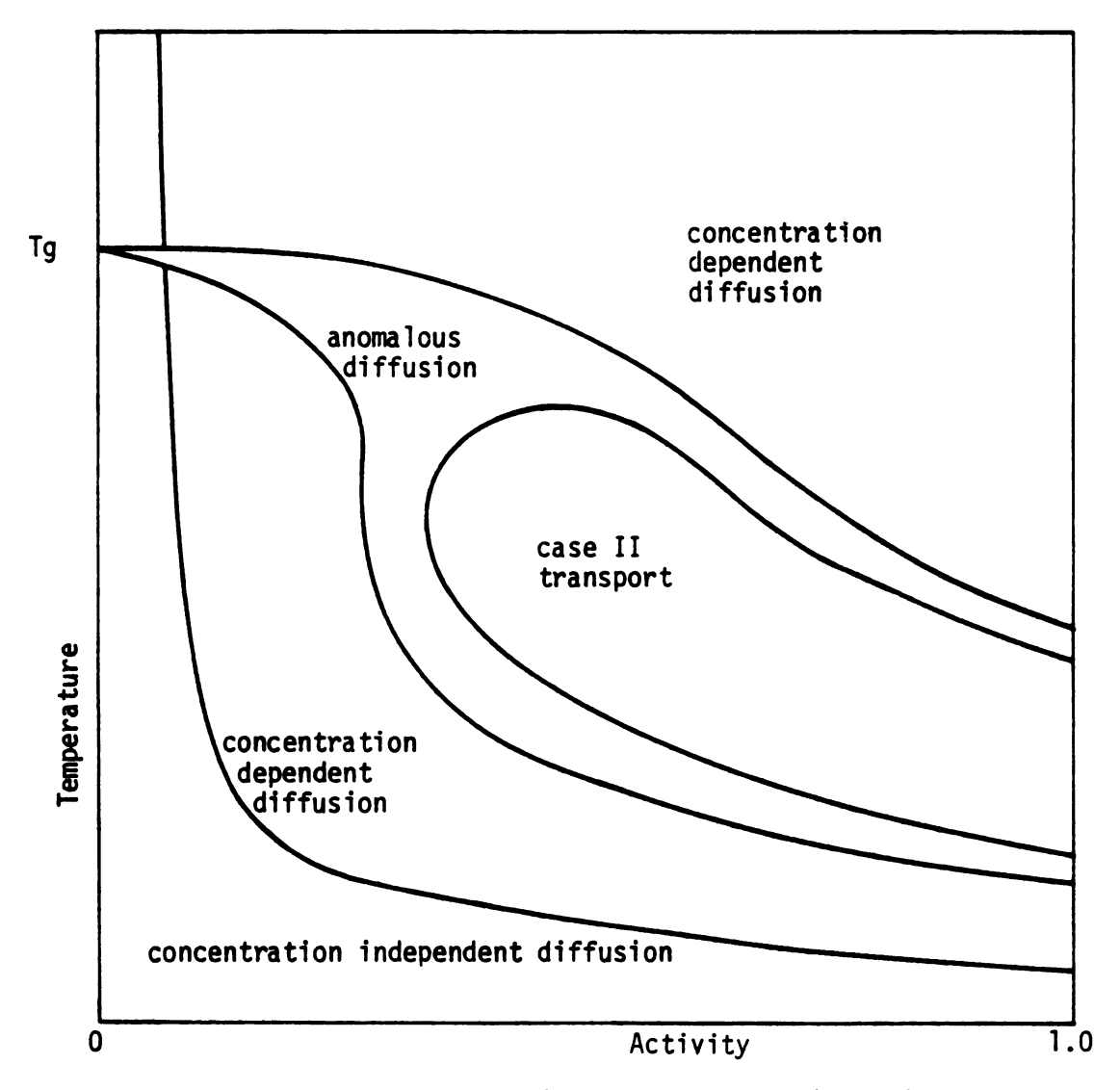


Figure 4. Transport features in the various regions of the penetrant activity. Adapted from Hopfenberg and Frisch (1969).

number (see figure 5). Based on viscoclastic fluid theory the Deborah number is defined as

$$(DEB)_D = \lambda_m \theta_D$$

where  $\lambda_m$  is the mean relaxation time for the polymer-solvent system at the condition of interest and  $\theta_D$  is a characteristic diffusion time, one-dimensional mass transfer in polymeric film.

### 5.5 Effect of molecule orientation on diffusion

Biaxial, or planar, orientation occurs when a film or sheet is drawn in more than one direction, commonly along two axes at right angles to one another. Biaxially oriented film possesses superior tensile properties, improved flexibility and toughness, and increased shrinkability. There are three components to this process: 1) the instantaneous elastic deformation caused by valence—angle deformation, 2) the molecular—alignment deformation caused by uncoiling, and 3) the nonrecoverable viscous flow caused by molecules sliding past one another. The orienting component, and ideally the major component of the stretching process, is given by 2). The alignment process depends upon the temperature of the orientation above Tg, the rate of stretching, percent of stretching and quench rate (Encyclopedia of Polymer, vol. 2).

As a consequence of high orientation of polymer chain in amorphous conformation, which favor closer packing than is possible in a completely randomized amorphous polymer, the density is higher and hence the fractional free volume smaller than in an equilibrium amorphous

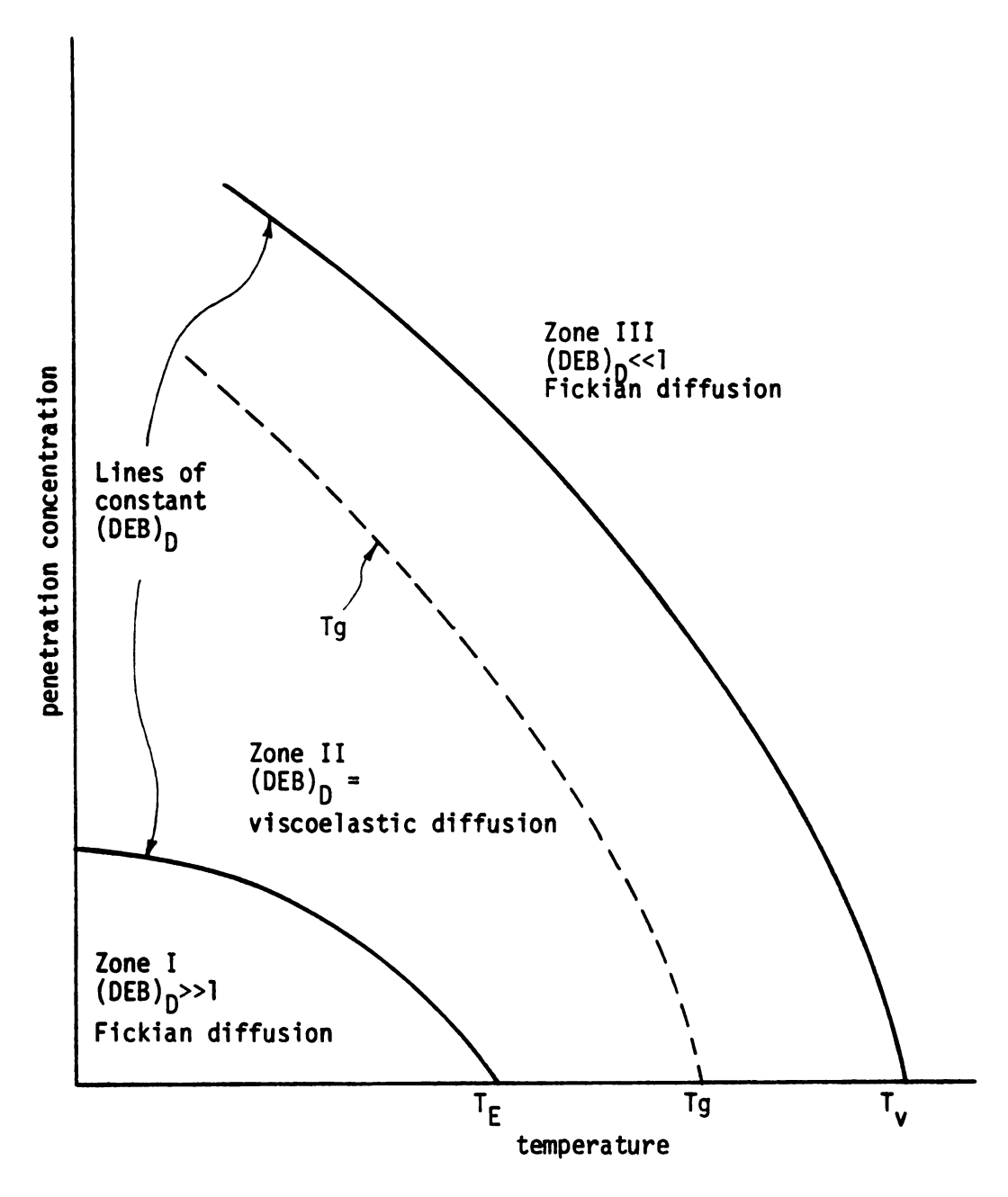


Figure 5. General temperature-penetrant concentration diagram. Adapted from Vrentas et al (1975).

state. Such an effect is reflected in a decreased sorption and diffusion coefficient (Peterlin, 1975).

When Lasoski and Cobb (1959) oriented PET, they observed that the orientation increased slightly with the density. Amorphous films (density 1.330) were oriented uniaxially 300% and biaxially 300 x 300%, with concomitant increases in density to 1.340 (5% of crystallinity) and 1.348 (10% of crystallinity) respectively, due to crystallization during orientation. Their studies with PET showed a significant reduction in moisture permeability following orientation. This difference was greater at low degrees of crystallinity (10%) and diminished as the degree of crystallinity increased. Beyond a density 1.380 (40% of crystallinity), no difference in water vapor transmission was detected. Experiments were carried out with 300% uniaxially and 300 x 300% biaxially oriented film samples.

Further, G. S. Park (1981) pointed out that orientation of polymer molecules takes place during the absoption-desorption process due to penetrant molecules. Drechsel et al (1953) studied the sorption and desorption of acetone by films of cellulose nitrate (Tg above 100°C) at 30°C by following the weight of vapor takeup or loss as a function of time. A striking result was that for successive sorption-desorption cycles, the rate of sorption decreased markedly by as much as a factor of 16 for five cycles. When the sorbed fractional amount versus square root of time was plotted, a slower and more sigmoid sorption curve was obtained after each sorption-desorption cycle. Studies of the optical anisotropy of the films showed that the orientation of the polymer

molecules normal to the plane of the film was increased by the diffusion process and it was concluded that this accounted for the decreased rate for successive sorption-desorption cycles and provided an explanation for the diffusion anomalies. A possible cause of this orientation was the observed anisotropic swelling, combined with slow movement of the polymer segment.

Similar phenomena have been reported by Long and Kokes (1953) working with benzene and polystyrene, although smaller effects were obtained. The rate of sorption and desorption of vapor of benzene in films of polystyrene were studied at 30°C and 40°C and at a variety of pressures. They found that at 30°C and pressures up to 50 mm Hg the plot of uptake or loss of vapor into the film versus time showed a decrease for successive sorption steps. This decrease was apparent for the second and third cycles. However, the fourth and fifth cycles were essentially unchanged. Again, measurement of the optical berefringence of the film used in the experiment showed that the successive cycles caused an increase in orientation parallel to the direction of diffusion.

Overbergh et al (1975) reported crystallization of isotactic polysterene induced by dichloromethane and acetone. They found that crystallization was diffusion controlled.

Makarewicz and Wilkes (1978) studied the diffusion of acetone, benzene, dioxane, methylene chloride and nitromethane in both the vapor and liquid phases, through unoriented and amorphous PET. They found that both vapor and liquid induced crystallization in initially amorphous and

unoriented PET. This strong effect took place while the organic molecule diffused through PET at 24°C. They also studied the diffusion of methylene chloride and dioxane liquid in oriented and non-oriented PET. The weight uptake kinetics were significantly slower in the oriented cold drawn material than in the unoriented.

A very interesting result was reported by Misra and Stein (1979) on the relationship between percent strain and the degree of induced orientation in PET. They showed that birefringency, and consequently orientation, varied almost linearly with percent of strain, and that birefringency decreased exponentially with increasing orientation temperature. Birefringency measurements were carried out at ambient temperature.

# 5.6 Permeability theories

#### 5.6.1 Fuiita free-volume theory

The free volume is defined as the volume within the cage of a molecule minus the volume of the molecule itself. One may visualize it as a "hole" opened up by thermal fluctuations of molecules and more specifically one may think of this "hole" as the space among molecules in a polymer film. Fujita (1961), reinterpreting Cohen and Turnbull's ideas (1959) to a two-component mixture, such as the polymer systems considered in this work, expressed the probability of finding such a "hole" exceeding a given value by:

$$P(B_d) = \exp(-B_d/f) \tag{16}$$

Where f can be regarded as the average free volume per unit of volume of the system (i.e., the average fractional free volume of the system).

 $B_d$  is defined as the value of a "hole" corresponding to the minimum size required for a given diluent molecule to permit a "considerable" displacement into the polymer. Also according to Fujita the thermodynamic diffusion coefficient  $D_T$  is given by the expression:

$$D_{T} = RTA_{d} \exp(-B_{f}/f) \tag{17}$$

Where R is the universal gas constant, T is the absolute temperature and  $A_d$  is a proportionality constant. Although  $A_d$  and  $B_d$  are not very well defined, they depend on the size and shape of the penetrant molecule. They are considered to be independent of temperature and penetrant concentration.

Hayes and Park (1956) related the intrinsic diffusion coefficient D\*p and the thermodynamic diffusion coefficient by

$$D_{T} = D*_{p}(d \ln C_{p}/d \ln a_{p})$$
 (18)

Where ap is the activity of the penetrant in the given polymerpenetrant system.

From equations 18 and 5 one obtains:

$$D_p^V = D_T(d \ln a_p/d \ln C_p)(1-V_p C_p^V)$$
 (19)

For our polymer-penetrant system,  $D_{p}^{V}$  is equal to the mutual diffusion coefficient D.

$$D = RTA_{d}(dln a_{p}/dln C_{p})(1-v)exp(-B_{f}/f)$$
 (20)

Where v is the volume fraction of the penetrant dissolved in the polymer-penetrant mixture and is expressed in cubic centimeters of liquid penetrant per cubic centimeter of mixture, and C is expressed as g of penetrant per cubic centimeter of polymer.

din ap/din vp should be determined experimentally and in some cases is equal to one (Stern and Kulkarni, 1983). Fujita's free-volume approach provides a fairly reasonable explanation of the principal features of the concentration and temperature-dependence of D, which are characteristic of diffusion of organic vapors and gases in amorphous polymers above Tg.

Vrentas and Dudas (1977) claimed that Fujita's approach represents a special case of a more generalized free-volume theory that can be applied at all temperatures, but its application to temperatures below Tg has not been shown. Table 1 gives a partial list of organic vapor-polymer systems above Tg, supporting Fujita's free-volume theory (Fujita, 1981).

Stern, Fang and Frisch (1972) extended Fujita's free-volume theory to small molecules and for high pressure. They showed that the dependence of permeability coefficient on pressure reflected how the free volume of the polymer is affected by this pressure. Permeability coefficients for 1,1 difluoroethylene ( $C_{2H_2F_2}$ ) and fluoroform ( $C_{2H_3}$ ) in polyethylene were determined at pressures up to 35 atm and at temperatures between -18° and 70°C.

Fang et al (1975) discussed the application of free-volume theory to the permeation of a gas and liquid mixture through polymeric membranes. Engineering analyses of the gas separation processes by selective permeation have generally been based on assumptions that the mass transfer coefficients for the components of the permeating gas mixture are independent of each other, and that the permeability

TABLE 1. Organic vapor/polymer permeation systems

Polymer	Penetrant	Reference
Polyisobutylene	propane	Prager and Long (1951)
Polyvinylacetate	methyliodide	Richman and Long (1960)
Natural rubber	benzene	Barrer and Fergusson (1958
Polymethyl acrylate	benzene	Kishimoto and Enda (1963)
Non cross-linked rubber	benzene	Hayes and Park (1955)
Polyvinyl acetate	methanol	Kishimoto and Matsumoto (1964)
Polyvinyl acetate	allyl chloride	Meares (1958)
Cross-linked natural rubber	methane, ethane, ethylene, butane, propane	Barrer and Skirrow (1958)
Polyvinyl acetate	acetone, benzene, methanol, propanol, propyl chloride, allyl chloride, carbon tetrachloride, propylamine	Kokes and Long (1953)

coefficients are independent of gas pressure. These assumptions are fully valid only for very dilute systems and are applicable, for example, to the mixed permeation of gases with low critical temperature, which exhibit very low solubilities in polymer even at high temperatures. The permeation of mixtures of more soluble gases cannot be modeled adequately on the basis of these assumptions. The authors described an application of free-volume concepts to the permeation of binary gas and liquid mixtures. Theoretical predictions were made and compared with the results of experimental studies for a mixture of ethane-butane in PE at 1 atm and 30°C; for N<sub>2</sub>0-CO<sub>2</sub> in PE at 28 atm and 30°C: for hexane-benzene also in PE at 25-40°C. The result showed very satisfactory agreement between predicted and experimental results. The model basically assumes that the transport of the components of a mixture in a polymer, at a given temperature and hydrostatic pressure, depends on the free volume of the system, and that the effect of these components on the free volume is additive. The application of this model is, however, restricted to amorphous polymers.

In an excellent study, Kulkarni and Stern (1983) have determined the diffusion and solubility coefficients for  $\mathrm{CO}_2$ ,  $\mathrm{CH}_4$ ,  $\mathrm{C}_2\mathrm{H}_4$  and  $\mathrm{C}_3\mathrm{H}_8$  in polyethylene at temperatures of 5, 20 and 30°C and at gas pressure up to 40 atm. The concentration dependence of the diffusion coefficients was represented satisfactorily by Fujita's free-volume model, modified for semicrystalline polymers, when the solubility of all the penetrants in polyethylene was within the limit of Henry's law.

They found semiempirical correlations for the free-volume parameters in terms of physicochemical properties of the penetrant gases and the penetrant-polymer systems. This study represents one serious attempt to predict the diffusion and permeability coefficient of other gases and a mixture of gases in polyethylene, as a function of pressure and temperature.

Stern and Kulkarni (1983), as a continuation of the above study, also measured permeability coefficients for the same systems at the same conditions. The temperature and pressure dependence of the permeability coefficients was represented satisfactorily by an extension of Fujita's free-volume model of diffusion for small molecules. The experiments were carried out under steady-steady conditions, and agreed pretty well with the model, providing further support to this theory and proving that it can be applied to small molecules other than organic vapors.

# 5.6.2 Dual-model theory

Since solution of probe molecules in perfectly crystalline regions of a polymer is not expected, and the diffusion coefficient of foreign molecules is also expected to be very small, crystalline polymers can be considered as a heterogeneous medium for the diffusion process. Accordingly, such crystallites act rather similarly to impermeable filler particles. They differ from such filler particles in that the degree of crystallinity may be changed by heating, straining, cooling and annealing and that the crystal should always be fully wetted by polymer chains with amorphous regions (Barrer, 1981).

Van Amerongen (1947) was among the first to demonstrate the effect of crystallization on the diffusivity coefficient, working with gutta percha.

Michaels et al (1964), studying the diffusion of He, Ar and ethane through linear polyethylene films, found that irrespective of thermal history and level of crystallinity, solubility constants and heats of solution of argon and ethane are normal, varying linearly with amorphous volume fraction.

#### 5.6.3 Immobilized dual-sorption model

Michaels et al (1963a) proposed a dual model to explain sorption of gases in PET. Based on suggestions of Barrer et al (1957), they proposed that sorption of gases in glassy amorphous and crystalline polymers generally take place by two independent processes operating concurrently, namely, ordinary dissolution obeying Henry's law and a "hole-filling" process obeying a Lagmuir expression. They were able to quantitatively separate the two processes and found that the solubility of gases below and above Tg followed different patterns which were explained as resulting from the disappearance of "holes" existing in the glassy amorphous polymer when the glass transition temperature was traversed. They worked with He,  $N_2$ ,  $O_2$ , Ar,  $CH_4$ ,  $CO_2$  and  $C_2H_4$  at temperatures between 25 and 135°C and pressure up to 200 psia.

What follows is a brief description of the dual-mode sorption model (Michaels et al, 1930a). See also Hopfenberg and Stannet (1973).

The total concentration of the sorbate in the polymer, C, consists of two thermodynamically distinct molecular populations,

namely, molecules "adsorbed" in the "holes"  $(C_A)$  and molecules dissolved in the amorphous polymers  $(C_D)$ , therefore

$$C = C_A + C_D \tag{21}$$

This model hypothesizes that adsorbed completely immobilized and that the transport law should be written as  $J = -D\partial C_D/\partial \times$ 

Where J is the diffusive flux of gas and  $\mathbf{C}_{D}$  is given by a Henry's law expression

$$C_{D} = s p \tag{22}$$

Where s and p are the same as equation 10.

CA is represented by a Langmuir expression:

$$C_{A} = \frac{C'_{A}.b.p}{1+b.p} \tag{23}$$

Where C'A and b are the parameters in the Langmuir isotherm, C'A is the hole saturation constant and b is the hole affinity constant.

Combining equations 21, 22 and 23, we have

$$C = \frac{C'_{A}bp}{1+bp} + sp \tag{24}$$

Michaels et al (1963a) determined the constants  ${\rm Cl}_{\rm A}$ , b and s for  ${\rm CO}_2$ -PET up to 12 atm at 25°C.

Based on previous studies on gas flow in polyethelene that provided information on the effects of crystallinity in impeding the diffusion of small molecules, Michaels et al (1963b) undertook an investigation to determine whether the model developed for diffusion of gases in rubbery crystalline polymers could be applied to diffusion in a glassy crystalline polymer. Working with gases in glassy and rubbery

PET they found that diffusion was impeded purely geometrically by the presence of the crystallites. They proposed a model for diffusion in the amorphous and crystalline polymers based on the dual theory of sorption.

The diffusion coefficient D due to the presence of crystallites is expressed by

$$D = D^{0} \overline{\alpha}$$
 (25)

where D<sup>O</sup> is the diffusion coefficient in completely amorphous PET and is the amorphous volume fraction.

At low pressure, when Henry's law is obeyed for the overall sorption process, the actual diffusion coefficient is given by

$$\frac{D'}{[1 + bC'_A/S]} \frac{\partial^2 C_D}{\partial x^2} \frac{\partial C_D}{\partial t}$$

Where the parameters  $C^{1}_{A}$ ,  $C_{D}$  and s are defined above.

Michaels et al (1963b) found that gas diffusion in glassy PET was Fickian, and when sorption obeyed Henry's law, D is independent of concentration.

In order to explain transient permeation in glassy polymers below Tg, Paul and Koros (1970) generalized the dual sorption model by introducing the notion of partial immobilization through the use of a simple flux relation, which might be viewed as the sum of two separate but parallel processes. While the dual-sorption theory pictures gaseous species held by the Langmuir mode as being completely immobilized, the proposed model is extended to accommodate different degrees of partial immobilization of gases sorbed by this mode. The

flux J is given now by

$$J = -D_D \frac{\partial C_D}{\partial x} - D_A \frac{\partial C_A}{\partial x}$$
 (27)

Where  $D_D$  and  $D_A$  are the diffusion coefficients for gas molecules sorbed by each of the two mechanisms, i.e., "dissolved" in accordance with Henry's law and "adsorbed into holes" according to Langmuir's isotherm, respectively.

The predictions of the model are that (i) total immobilization results in constant permeability with a lag time which strongly decreases with pressure, (ii) no immobilization results in a constant lag time with a permeability which decreases strongly with pressure, and (iii) incomplete immobilization results in both the permeability and lag time decreasing with pressure but neither as strongly as in the other limiting cases.

After simplifying the formulation first suggested by Petropoulos (1970), Paul and Koros solved equation 32 and obtained the following expression for permeability.

$$\overline{P} = Ds \left(1 + \frac{FK}{1 + bp_2}\right) \tag{28}$$

Where

$$F = \frac{D_A}{D}$$
 and  $K = \frac{C'_A}{D.s}$ 

and for the lag time the expression is now

$$\theta = \frac{\ell^2}{6D} f(\xi) \tag{29}$$

Where  $F(\xi)$  is an expression given by Paul and Koros (1976).

Koros and Paul (1978) performed transient and steady-state permeation experiments with  $\rm CO_2$  in semicrystalline PET at temperatures between 25 and 115°C over the pressure range from 1 to 20 atm. The pressure dependency of lag time and permeability disappeared completely above Tg and Fick's law with concentration-independent diffusion coefficient applied. In the glassy state, they used the partial immobilization model to fit experimental data. They calculated D (or  $\rm D_D$ ) and  $\rm D_A$  at different temperatures. Their predictions of the lag time agree quite well with the experimental ones at temperatures below 85°C. This paper supported the idea that there are two distinct modes into which  $\rm CO_2$  can be sorbed in glossy PET, and that the  $\rm CO_2$  molecules in these two thermodynamically distinct populations have different diffusional mobility.

It should be pointed out that the formulation proposed by Petropoulos (1970) takes into account the thermodynamic diffusion coefficient  $D_T$ , and that it was considered independent of the penetrant concentration. The formulation of Paul and Koros (1978) takes into account the mutual diffusion coefficient  $D_D$  and also was considered concentration—independent.

There is no plasticization of the polymer by gases.  $D_T = D$  only when F = 0. There is no a priori guide to which of the two formulations to use and the judgement must come from experimental data.

Paul and Kemp (1973), based on a modified immobilized dualsorption model initially proposed by Paul (1969), compared theoretical prediction with experimental time lag values obtained for various gases (He,  $N_2$ ,  $CO_2$ ) in a model membrane synthesized by dispersing highly adsorptive molecular sieves of crystalline aluminosilicate into silicone rubber. They modified the following equation:

$$\theta = \frac{2}{6D} \left[ 1 + Kf(y) \right] \tag{30}$$

in order to take into consideration the heterogeneous nature of the membrane.

$$\theta m = \frac{\ell^2}{6D_m} \left[ 1 + \frac{(1-\beta)}{\beta} kf(y) \right]$$
 (31)

$$C = \beta sp + (1-\beta) \frac{C'_A.b.p}{1 + b.p}$$
 (32)

$$Dm = D \frac{Pm}{\beta . \overline{P}}$$
 (33)

Where  $\theta_{m}$  is the lag time of the heterogeneous phase

Dm is the effective diffusion coefficient

β is the polymeric continuous phase volume fraction

Pm is the permeability of the filled membrane

The effect of immobilizing adsorption is to increase the time lag beyond that expected in the absence of this process, but there will be only minor effects on the steady-state permeation rate. This shows that in this case the lag time method may lead to erroneous calculation of D. On the other hand, this effect can be utilized in a beneficial fashion to design very effective protective coating, packaging material, time-released mechanisms, etc. for special situations. It

should be pointed out that the polymer phase in their study is above Tg and that the probe molecules are gases above critical temperature.

#### MATERIALS AND METHODS

#### 6.1 Materials

# PET film samples

Film samples were provided by Eastman Kodak Company.

Commercial PET samples were oriented at three different elongations and at three different temperatures. That process gave nine different samples that were characterized as follows.

The initial dimension of all samples was  $4 \times 4$  inches, and the orientation was done at a strain of 350%/sec based on the initial dimensions. This corresponded to a pull rate of 14 in./sec. biaxially oriented.

The films were stretched 200, 300 and 400% of the initial dimensions at 90, 100 and 115°C.

Three sheets were used for each of the nine points.

Table 2 shows values of crystallinity obtained from density studies.

No further data, such as molecular weight, were provided for polymer characterization.

Samples were maintained in an organic vapor-free atmosphere until the moment of the experiment.

All experiments performed in this work were done with 4X  $100^{\circ}$ C A, B and C films.

TABLE 2. Density and percent of crystallinity of the PET sample films

E41-	Pancity a/co	Crystallinity %
Film	Density g/cc	orystallinity A
2 × 90°C "C"	****	
3 x 90°C "A"	1.361	23
4 × 90°C "A"	1.358	20
4 × 90°C "C"	1.360	22
2 × 100°C "A"	1.362	24
3 × 100°C "C"	1.368	28
3 × 100°C "C"	1.367	28
3 × 100°C "B"	1.367	29
4 × 100°C "A"	1.366	27
4 × 100°C "A"	1.367	28
4 × 100°C "C"	1.366	27
4 × 115°C "B"	1.369	30
3 × 115°C "B"	1.373	33
2 x 115°C "B"	1.370	30

Poly(ethylene) terephthalate, PET,

is a linear polyester.

The properties of PET film result from an ordered structure produced by means of molecular chain orientation and crystallization.

Table 3 shows the properties of PET.

## Toluene

Toluene with purity greater than 99.8%, boiling point of 110-111°C from Burdick and Jackson Laboratory Inc. was used as the permeant.

#### Nitrogen gas

High purity dry nitrogen 99.98% was provided by Union Carbide Corporation, Linde Division, Daudery, Connecticut.

As Rodriguez (1982) points out, the characterization of a partly crystalline polymer is much more complex than mere specification of the fraction that is crystalline. Among the factors that should be taken into consideration are:

Crystallite size and distribution

Constraints on amorphous region (matrix) that perturb it from its truly disordered condition

Presence of voids and surface stress

Polymer chain chemistry, where induced chain irregularities prevent the system from attaining its lowest energy state

Chain length, chain ends, and

Distribution of spherulite sizes.

TABLE 3. Properties of PET

Property		Source
Glass transition temperature, °C	80.7	This work
ensity at 30°C, g/cc		
-amorphous phase	1.331	Cobbs and Burton (1953)
-crystalline phase	1.470	Cobbs and Burton (1953)
ensity at 23°C, g/cc		
- amorphous phase	1.333	Daubeny et al (1955)
-crystalline phase	1.455	Daubeny et al (1955)
ensity values		
- amorphous phase	1.333	Kodak
- crystalline phase	1.455	Kodak
Melting point, °C	232	This work
lean relaxation time at 25°C, sec	$1 \times 10^{10}$	Meredith and Hsu (1962)

However, collecting all this information would be almost impossible. This limits the author's ability to explain all the experimental results in terms of theoretical understanding. Not only the complexity of the information required but also the lack of adequate theory allows for only approximate values of the diffusion coefficient to be obtained.

# 6.2 Experimental Procedure

# 6.2.1 Continuous gas flow permeation apparatus Scope

The diffusion-detection system which is illustrated in Figure 7 was developed, assembled and tested as part of this project. It allows for the continuous collection of permeation data of an organic vapor or gas through a film from the initial time zero to a steady-state condition, as a function of temperature and permeant concentration.

#### Description

The film to be tested was mounted between two stainless steel disk-shaped plates forming a cell with two chambers, each having a volume of 5 cc (see Figure 6). The assembled cell was placed horizontally in a constant temperature bath and a constant concentration and constant flow of permeant was flowed through both upper chambers. A constant flow of nitrogen was passed through both lower chambers, removing permeant vapor at a constant rate and conveying it to the detection apparatus which consisted of a gas

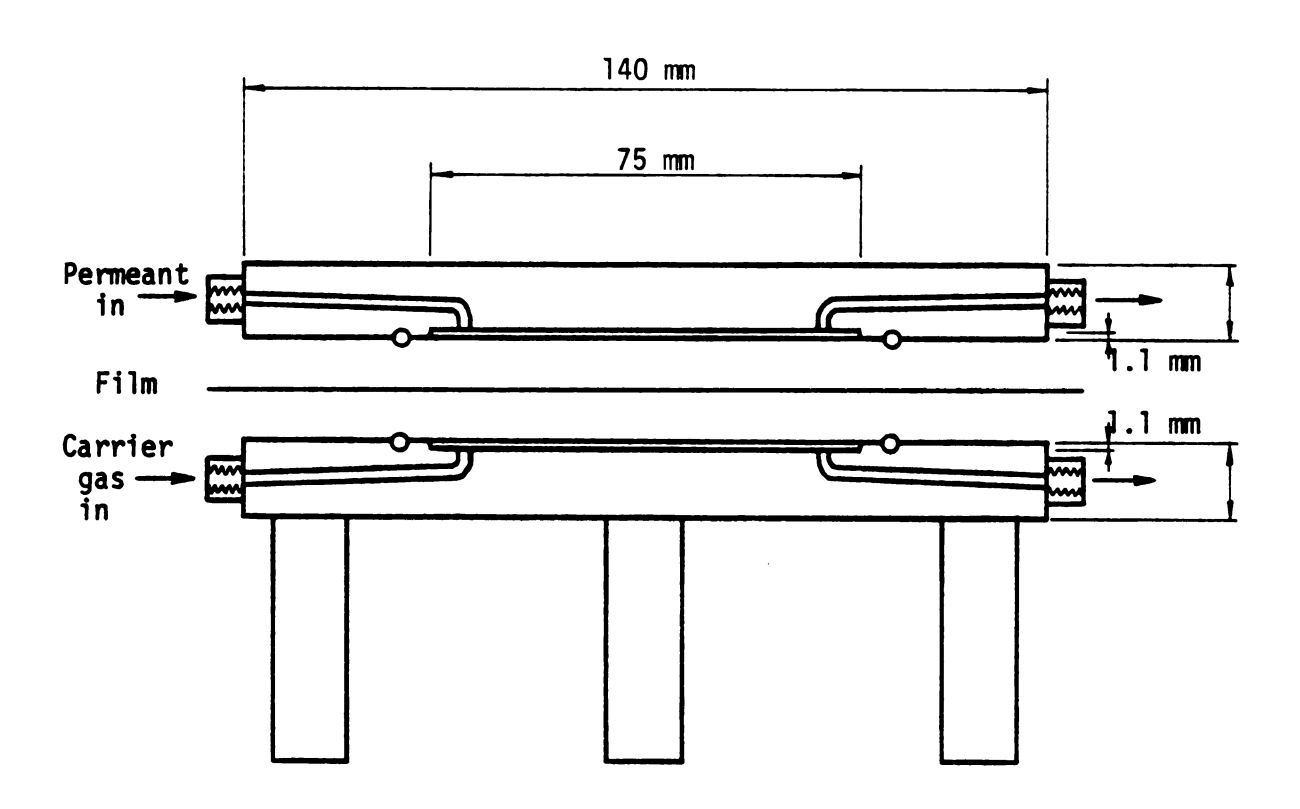


Figure 6A. Schematic of the cell for continuous gas flow method.

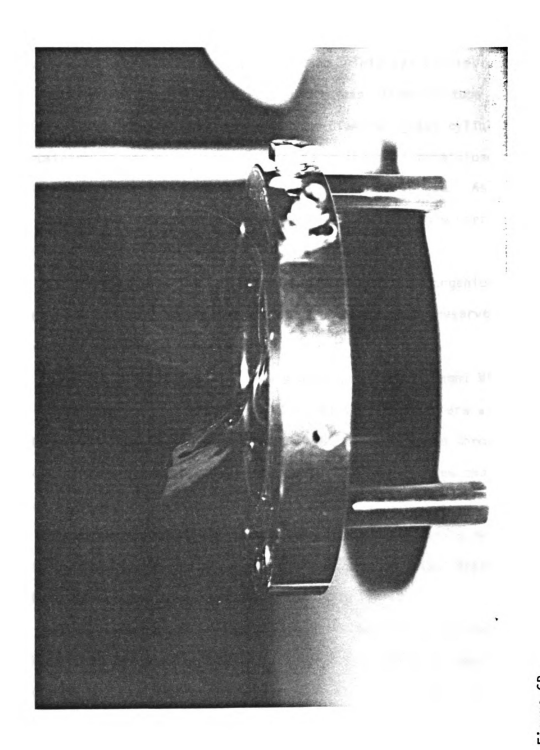


Figure 6B.

chromatograph (Figure 7), with flame ionization detection interfaced to the permeability cell via a computer-aided gas sampling valve. A constant concentration permeant vapor was produced by bubbling nitrogen gas at 1 atm through liquid toluene. This was carried out by assembling a vapor generator consisting of a gas disperser tube (G) of Pyrex (ASTM 40-60) 250 mm long and a 250 mm diameter glass cylinder (D) containing the organic liquid. This produced a mixture close to the saturation vapor pressure of toluene in the carrier gas. As shown, this stream can be mixed with another stream of pure carrier gas nitrogen to obtain a lower vapor concentration.

Before being directed to the permeation cell, the organic vapor/nitrogen mixture was passed through a 250 cc glass reservoir (E) as a means of dampening perturbations.

The vapor generator system was placed in a Blue-M Magni Whirl water bath maintained to within 32.0°C 0.1°C. Special care was taken to avoid condensation after the permeant vapor passed through the glass reservoir. Hereafter, this will be referred to as the permeant stream.

The permeation cell and most of the tubing interfacing the generator and the cell were placed in a second Blue-M Magni Whirl water bath to maintain the required temperature 0.1°C.

A Hewlett-Packard Model No. 5830 gas chromatograph equipped with dual-flame ionization detection, linked to a 18850A GC Hewlett-Packard terminal was used as a detection means. The HP 5830 gas

Figure 7. Experimental process flow diagram and photograph.

- (A) Experimental process flow diagram
  - A water bath for generation of vapor permeant
  - B water bath for cell
  - C cell
  - D cylinder with liquid permeant
  - E 250 cc glass flask
  - F gas flow bubble meter
  - G porous glass tube
  - H high pressure gas regulator
  - N needle valve
  - R rotameter
  - S sample port
  - T three-way valve
  - W water manometer
- (B) Photograph of the diffusion system

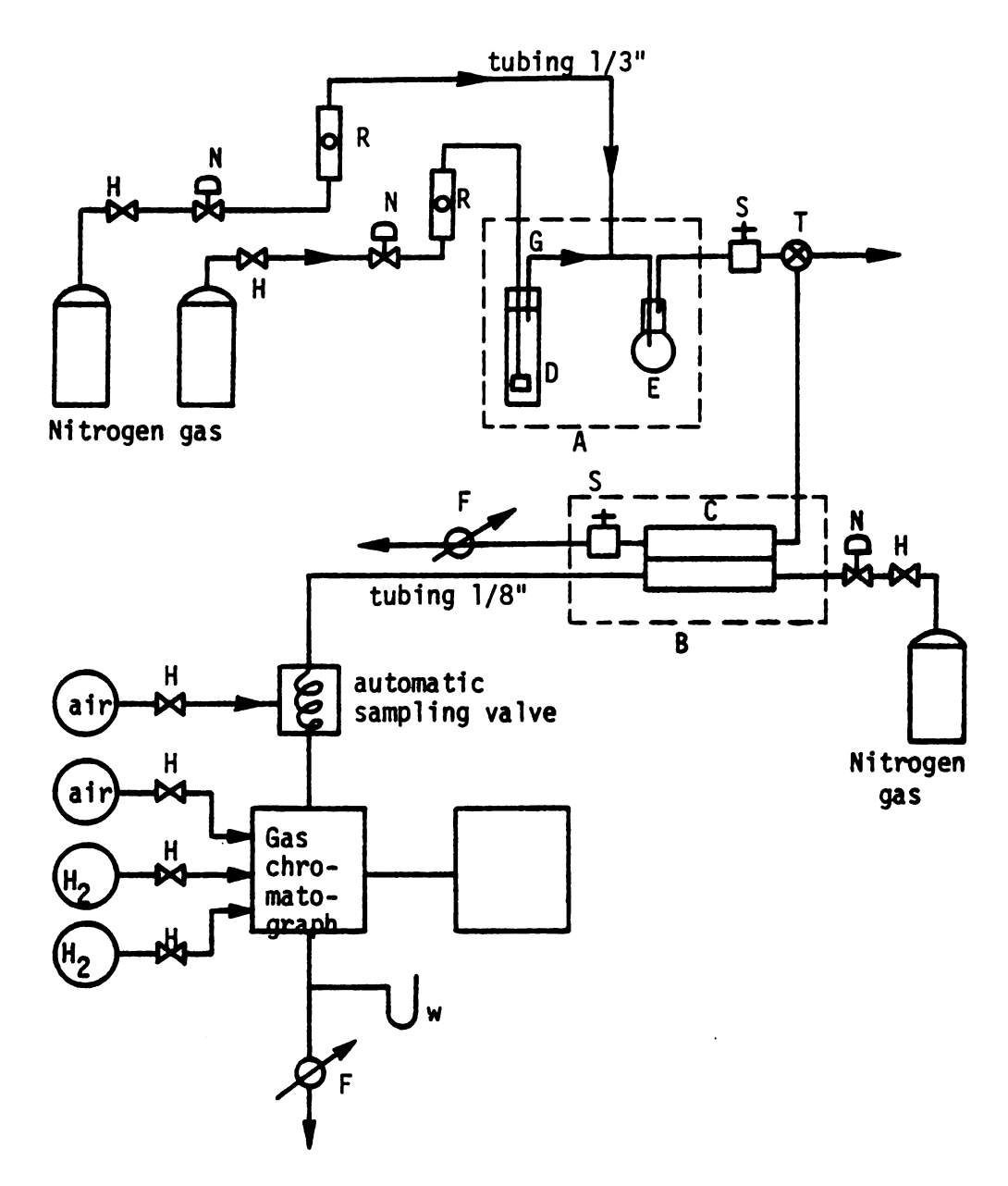


Figure 7A. Experimental process flow diagram.

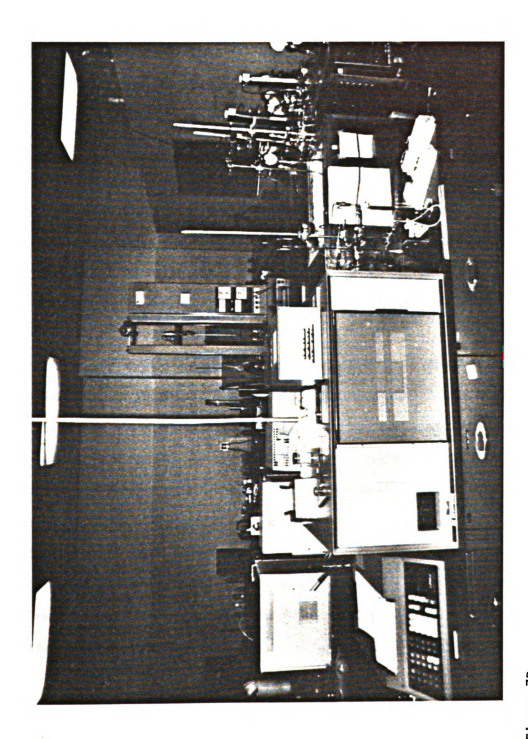


Figure 7B.

chromatograph is a keyboard-controlled instrument that houses a multifunction digital processor.

working with values entered via the keyboard on the terminal unit, the processor established the required injection, oven and detector temperatures for the analysis. A printed output with a plot of the amount of material detected in function of time, the area under this curve (expressed in area units) and the retention time was obtained. Stainless steel tubing (1/16<sup>m</sup> O.D.) conveying the diffusant from the cell was connected to the automatic gas sampling 6-port valve housed within the gas chromatograph. Figure 8 shows the connection between the sampling valve and the sample stream during the fill position (de-actuated valve) and the injection position (actuated valve).

A 6' x 1/8" stainless steel column packed with 5% SP-2100 on 100/120 Supelcoport (Supelco SP-2100 methylsilicone fluid) was used. It exhibited low bleed at high temperature and had low viscosity through its usable range. This gave a high efficiency column, very well suited for analysis of toluene. A 100/120 mesh diatomite was used as support (Supelco, 1984). Conditions under which the gas chromatograph (GC) was run are shown in Table 4.

Flow of gases was regulated with a NUPRO needle valve type B-2SG. These valves gave acceptable constant flows in the order of 2 cc/min. Accurate measure of the flow of gases was performed at

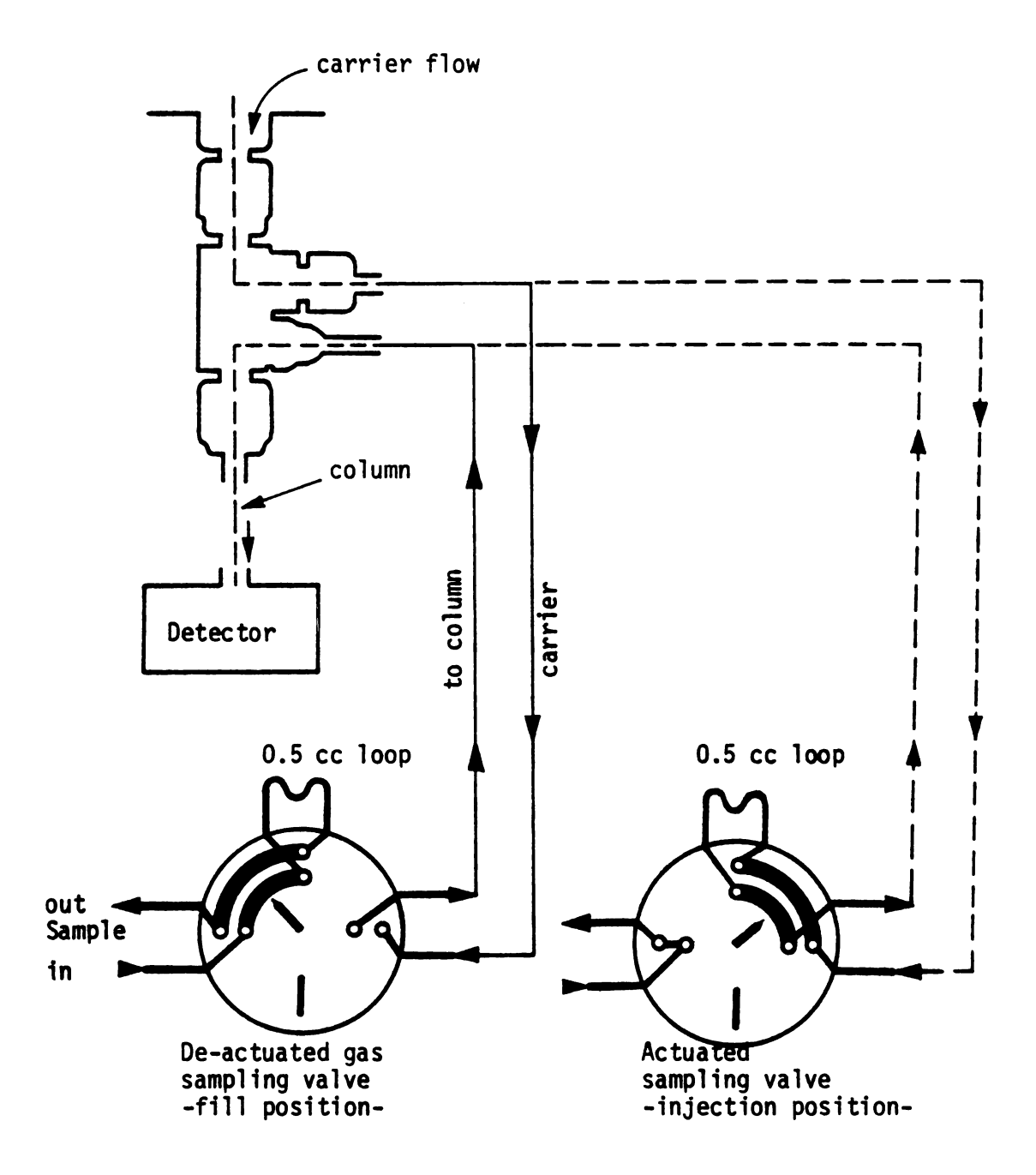


Figure 8. Sampling valve.

TABLE 4. Conditions under which GC was run

Carrier flow	30 cc/min
Oven maximum temperature	225 °C
FID temperature	350°C
Injection temperature	200°C
Temperature	175°C

atmospheric pressure by using a 10cc gas flow bubble meter from Supelco.

Rotameters were used to provide a continuous indication that a constant flow rate was maintained. A Chromel-Alumel thermocouple connected to a Wheatstone bridge was used to measure the temperature in the 6-port gas sampling valve to within 1.0°F.

Unless otherwise stated, 1/8" Q.D. by 1.65 mm I.D. copper tubing was used to connect the different components of the test system. The connection between the cell and the gas sampling valve on the chromatograph was made with SS capillary tubing 1/16" Q.D. and 0.762 mm I.D. with a total length of 40 cm, giving a dead volume of 0.2 cc. Swagelsk brass tube fittings were used to provide a tight system during the long period of the experiments (Crawford, 1980). Glass-to-glass connections were made with stoppers and tubing made of silicone rubber. A GCA Precision Scientific timer model 69230 was used in computing the flow rate of gases. Temperatures were measured with a mercury thermometer to within 0.1°C.

# 6.2.2 Operation

A run was considered as the set of data taken from the moment that the constant concentration permeant flow contacted the film until a steady state of the diffusional process was clearly reached, at a given temperature.

Before a run was started, the system was prepared as follows:

In order to purge the lower chamber of the cell, the capillary tubing and the automatic sampling valve of residual toluene vapor, an aluminum foil disk was mounted in the permeability cell and nitrogen was continually flowed through the lower cell chamber and the connected gas sampling valve.

The system was considered "clean" when the signal from the G.C. was less than 1,000 units/area, corresponding to a toluene concentration of 0.004 ppm in the pump gas stream.

To insure a steady and constant concentration of permeant vapor, carrier gas  $(N_2)$  was continually passed through the vapor generator and the vapor concentration monitored. This step was carried out concurrently with purging the cell. As shown in Figure 7A, a 3-way valve was placed in the line so that the upper cell chamber was bypassed until the cell was free of residual vapor and the experiment was initiated.

During this period the toluene vapor was diverted to the hood.

It was found that several days could be required until a constant concentration of toluene vapor was maintained. The concentration of toluene was monitored by removing a sample via a gas-tight syringe

from a sampling port (see Figure 7) and analyzing the gas sample by direct column injection into the chromatograph, bypassing the cell through the valve (T).

Once the lower cell chamber was free of residual vapor and the permeant concentration constant, the aluminum foil disk was removed from the cell, the film to be tested was mounted between the chambers, and the valve was turned to the position that allowed the flow to go towards the upper chamber of the cell. The timer was set at time zero, and simultaneously the bubble flow meter was used to detect any leakage.

The film sample to be tested was taken from the original sheet and its position was recorded. The sample weight was determined with a Mettler analytical balance, and its density and surface area also recorded.

An automatic sampling program was set for the G.C. via the terminal. Normally, a sample was taken each 60 minutes, with the valve being actuated between the first and third minute. A record was made of the test temperature, permeant concentration, flow rate of the

permeant vapor and flow rate of the nitrogen stream passing through the lower cell chamber.

Values of the permeant stream concentration were determined by sampling through a gas-sampling port with a gas-tight syringe (see Figure 7) and analysis by gas chromatography. The 0.5 ml syringe used had a Supelco Gastight 1750 side-pore needle to avoid clogging with material from the septa. The possibility of taking measurements of the permeant concentration through the automatic sampling valve was ruled out due to possible contamination and interference caused by sorption of toluene vapor by the tubing and sampling valve followed by a slow rate of desorption.

Because of these considerations, an independent method was developed for monitoring the concentration of toluene in the permeant stream.

#### 6.2.3 Precision of the measurements

In order to estimate the uncertainty in the diffusion coefficient, it was necessary to have an estimate of the uncertainty in the measurement performed by the apparatus, i.e., the error associated for each value of the organic vapor concentration determined by the gas chromatograph (expressed in units of area) as a result of the continuous diffusion process and mixing with the sweeping stream of nitrogen.

An analysis of the error propagation was quite complicated since it had to include a careful evaluation of the incidence of at least the following factors:

- (a) Uncertainty of the permeant concentration in the cell (depending itself on temperature, bubbling nitrogen flow, bubble diameter, height of organic liquid in the cylinder, etc.)
- (b) Uncertainty of the amount of nitrogen flowing through the lower chamber.
- (c) Uncertainty in the automatic sampling valve (volume and pressure).
- (d) Uncertainty in the detector unit.
- (e) Temperature fluctuations.

Considering that most of these variations are random and independent, some compensatory effects take place. A simple way to measure these uncertainties is to analyze the steady-state portion of a run since it includes all the parameters influencing the meter system.

Twenty-five sample points, randomly chosen from the steadystate transmission region of permeation run 4, gave the following values:

Average concentration	1.856 ppm
Standard deviation	0.128 ppm
Standard deviation of the mean	$2.6 \times 10^{-2} \text{ ppm}$
Percentage of uncertainty	1.4%

When only a diluted permeant stream was directed through the automatic sample valve, these values were collected:

Average	8.01 ppm
Standard deviation	0.227 ppm
Standard deviation of the mean	0.045 ppm
Percentage of uncertainty	0.6%

Values for the permeant measured with the syringe were:

Average	90.0 ppm
Standard deviation	4.0 ppm
Standard deviation of the mean	1.0 ppm
Percentage of uncertainty	1.0%

Values for the flow rate of the nitrogen stream sweeping the lower chamber gave:

Average	1.97 cc/min
Standard deviation	0.040 cc/min
Standard deviation of the mean	0.01 cc/min
Percentage of uncertainty	0.5\$

One systematic error that could be identified was due to the mixing process occurring in the lower chamber between the gas and the diffused organic molecules. This resulted in concentration values determined by the G.C. for a given time not corresponding accurately to the actual amount of permeant diffusion through the film in the same time. The net effect would produce a delay with respect to the actual diffusion process. In attempting to evaluate this delay it was considered that a model similar to the continuous stirred tank (CTS) with a step could give an acceptable value.

If F is the flow of gas in cubic centimeters per minute,  $V_0$  the volume of the lower chamber also in cubic centimeters, and  $(C_{1}-C_{0})$  a change in concentration of flow resulting in a change in the amount of vapor permeated (assuming a discrete change), the following equation can be written:

$$F_{1}\overline{C}_{1} - F_{1}\overline{C} = V_{0}\frac{d\overline{C}}{dt} \qquad \overline{C}(0) = \overline{C}_{0}$$
 (34)

Equation 34 has the solution

$$C = C_1 - (C_1 - C_0)e^{-St}$$
 (35)

Where S = 
$$\frac{F}{V_0}$$

The required time for  $\overline{C}$  to reach 0.95  $\overline{C}_1$  is  $t = -\ln \frac{0.05}{S}$ For a typical value of  $S = \frac{2}{5} = 0.4 \text{ min}^{-1}$ , t equals 7.5 min.

If it is considered that the times measured during the diffusion process were in the order of hundreds of hours, the impact of this delay was quite negligible, less than 0.01%. If the measured time were in the order of hours, it could have a more significant role.

# 6.2.4 Accumulative or quasi-isostatic method

In the quasi-isostatic or accumulative method, the lower concentration cell chamber is not subjected to a gas flow. The vapor penetrant for measurement flows through the upper cell chamber at a constant concentration and pressure, normally at atmospheric pressure. The lower chamber cell initially filled with nitrogen at atmospheric pressure is totally closed off. When the experiment is started by flowing permeant through the upper chamber, the diffused molecules that have traversed the film are accumulated in the lower cell chamber.

The permeant concentration in the lower concentration chamber was no higher than 3% of the permeant concentration in the upper cell chamber. This was done to keep to a minimum value the variation of the driving force of the permeant through the film.

At intervals, samples were withdrawn from the lower chamber and permeant concentration was determined. Equal volume of nitrogen was replaced. The variation of the driving force and the variation of the concentration in the lower chamber after each sample was performed, attempted with the exactness of the method, but with special care the error could be kept to a minimum value.

Figure 9 presents a schematic diagram of the permeability cell used for the quasi-isostatic or accumulative method.

# 6.2.5 Density Gradient Column System

#### Scope

This method was used to obtain accurate values of film density and subsequent estimation of the percent crystallinity of the respective film sample through the relationship of density to percent of crystallinity. The density values were also used to estimate the average film thickness.

#### Method

The method employed, a standard procedure (ASTM D1505-68) and (ASTM 1981), is based on observing the level to which a test specimen sinks in a column of liquid exhibiting a density-gradient in comparison with standards of known density. A Cole-Palmer Density Gradient

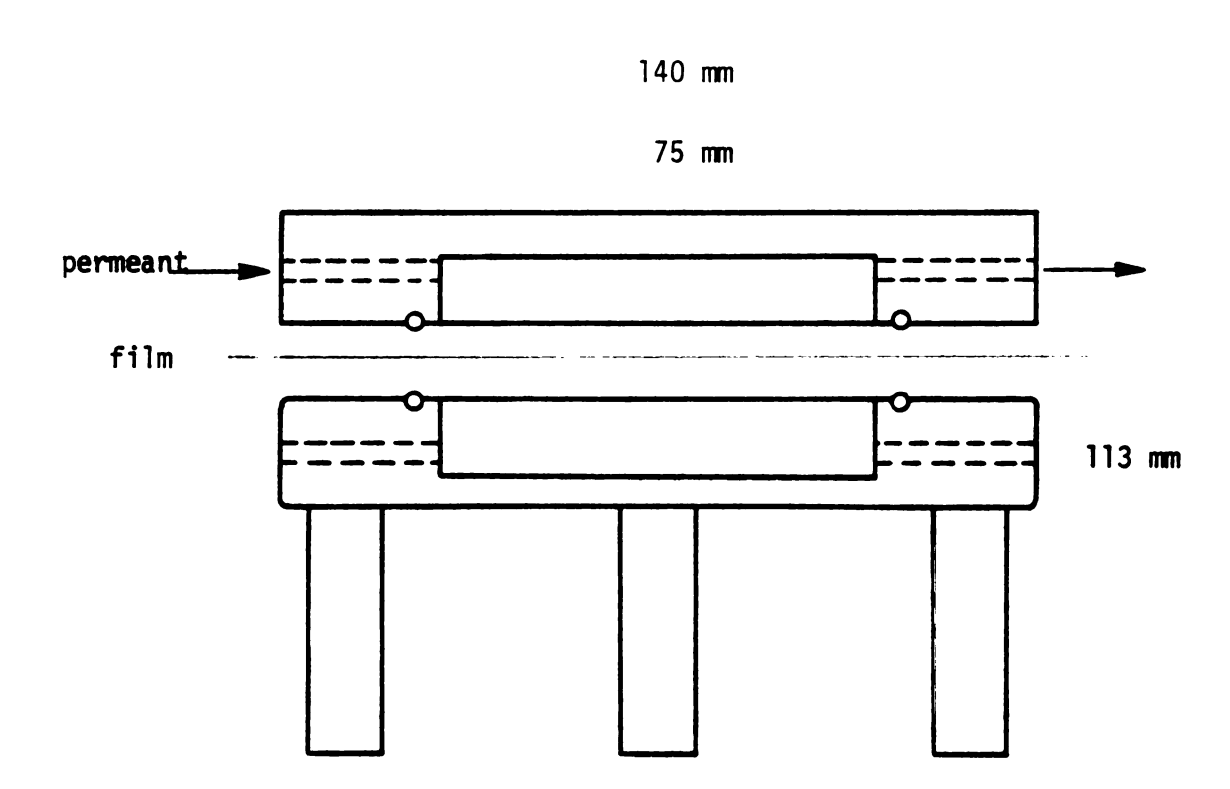


Figure 9. Schematic of the cell for quasi-isostatic method.

apparatus was used which consisted of a graduated glass tube of length 85 cm and 5.0 cm outer diameter which was immersed in a circulating water bath maintained at  $23.0\pm0.2$ °C. The cylinder contained a mixture of two aqueous solutions of calcium chloride of different densities prepared in such a way that there was a linear increasing density gradient from the top to the bottom of the cylinder.

The density of a specimen was determined by observation of its position and linear interpolation from a calibration curve prepared with a set of calibrated glass floats of known densities.

# Operation

Two solutions of CaCl<sub>2.2H2O</sub> in water were prepared (42.3% and 53% w/v respectively) and charged into the column with a mixing device which gave a linear gradient density between 1.304 and 1.400 g/l.

Calibrated glass floats obtained from Lab Glass Inc. were added, and after they reached position equilibrium, a plot of their position in the tube as a function of their respective density value was made. Samples of the film were then carefully submerged. When they reached an equilibrium position, the density was obtained directly from the density vs. position plot. The gradient could be used for several months and each time a determination of density was needed, a recalibration was made.

#### Precision and accuracy

Precision of the data was related to the uncertainty of reading the graduated scale on the glass tube, i.e., 2 mm. This corresponded

to 0.0007 g/cc for a density of 1.3 g/cc. Precision is given by the relative uncertainty 0.0007/1.3 = 0.0005. Accuracy was tested by comparing the obtained data with analysis conducted on similar samples at Eastman Kodak Company Laboratories, Tennessee. Values agreed to within 0.001 g/cc.

# 6.2.6 Calibration of gas chromatograph for toluene

Known amounts of toluene were dissolved in liquid o-dichlorobenzene, suitable for gas chromatography, boiling point 180°C, from Burdoch and Jackson Laboratory Inc., Muskegon, Michigan.

In order to get good separation of the two compounds, the gas chromatograph was set at the conditions given in Table 5.

The average for several determinations gave a factor of 5.27  $\times$   $10^{11}$  units area per gram of toluene. Since the partial pressure of toluene when mixed with nitrogen in the permeation experiment was in the order of  $1 \times 10^{-2}$  atm, applying an ideal gas behavior, the above factor was equivalent to  $3.78 \times 10^{-6}$  g/cc (3.78 ppm) for each  $10^6$  units area in the output of the gas chromatograph.

The correlation coefficient in the least-square fitting to the calibration value was 0.999.

TABLE 5. Conditions under which GC was run for calibration

Temperature 1	175°C
Time 1	0.7 min
Rate	30 °C/min
Temperature 2	200°C
Time 2	5.0 mfn
Injection temperature	200°C
FID temperature	350 °C
Oven maximum temperature	225°C

# 6.2.7 Differential Scanning Calorimetry (DSC)

DSC measurements were conducted in order to determine thermal transitional temperature, Tg, and melting point of PET films.

A DuPont Thermal Analyzer Model 990 was preliminarily used and then most of the samples were tested by Perkin-Elmer Laboratory in Pittsburgh, Pennsylvania using a Perkin-Elmer DSC 4/TADS System.

#### RESULTS AND DISCUSSION

Section 7.1 includes the results of the permeation of toluene through PET films at different temperatures and at different concentrations of toluene (using both continuous flow and accumulative methods); sorption equilibrium experiments; and results of the determination of glass transition temperature of PET.

Discussion of these results is presented in Section 7.2.

# 7.1 Permeation of toluene through PET

Several permeation experiments were conducted in order to investigate the characteristics of the diffusion process of toluene vapor in PET films.

At the time this work was performed, no permeation data for the toluene-PET system was available in the literature. A considerable amount of time was therefore devoted to preliminary experiments. (It was believed that the expected time for a run could be in the order of hours, considering other similar systems.)

Initially, inconsistent results were obtained for the continuous-flow technique. At that time it was felt that a simpler method would be necessary to verify the results of the more complex continuous-flow method. The accumulative or quasi-isostatic method, although considered less accurate, was a simpler method and was therefore used.

Therefore, both continuous-flow and accumulative methods were used as a means to check values by two independent methods.

For all of the experiments, film stretched to 400% elongation at 100°C was used.

Unless otherwise stated, all experiments were conducted at ambient temperature (23°C). Experiment 7 was conducted at 60°C.

While keeping the permeant concentration constant, the goal for each experiment was to calculate the diffusion coefficient and the permeability constant.

Table 10 summarizes the results.

# 7.1.1 Experiment 1

This experiment was carried out at 91 ppm of toluene in the nitrogen-toluene mixture at 23.8°C.

The resultant data are presented graphically in Figure 10 where the total quantity of toluene permeated 0 in g  $\times$  10<sup>6</sup> is plotted as a function of time. The batch or quasi-isostatic method was used.

As can be seen, the general shape of the plot indicates an apparent Fickian behavior. Table 6 gives a summary of the experiment. See Appendix III for calculation of  $D_{\text{Lag}}$ .

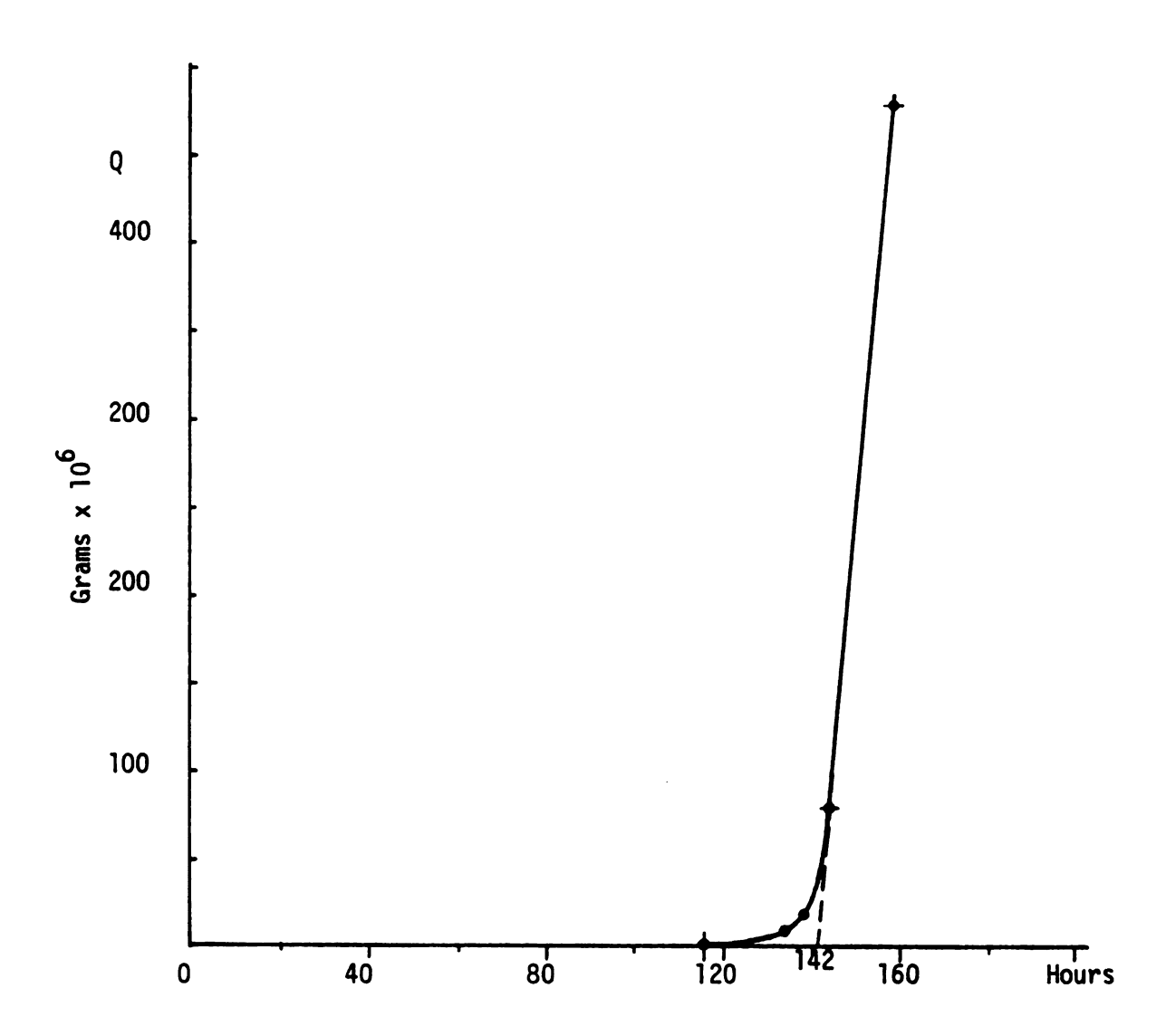


Figure 10. Experiment 1. Total permeated toluene Q versus time.

TABLE 6. Data for Experiment 1

Method: Batch or quasi-isostatic

Temperature: 23.8°C

Toluene concentration:  $\overline{c} = 91 \text{ ppm}$ 

Thickness of the film: =  $3.7 \times 10^{-3}$  cm

Lag time = 142 h

Lag diffusion coefficient  $D_{Lag} = 4.5 \times 10^{-12} \text{ cm}^2/\text{sec}$ 

Permeability constant  $\overline{P} = 0.271 \text{ g.mil/m}^2.\text{day.}100 \text{ ppm}$ 

# 7.1.2 Experiment 2

This experiment was intended to be a replica of Experiment 1.

Temperature and toluene concentration were kept the same, although in the second half of the run, the toluene concentration increased about 14% with respect to the initial value.

Again, the shape corresponded to an apparent Fickian behavior, but the lag was almost twice that of the first experiment. One possible explanation for this result is that this sample was taken close to the corner of the sheet of film.

The resultant data are presented graphically in Figure 11 where the quantity of toluene permeated is plotted as a function of time.

Table 7 gives a summary of the experiment.

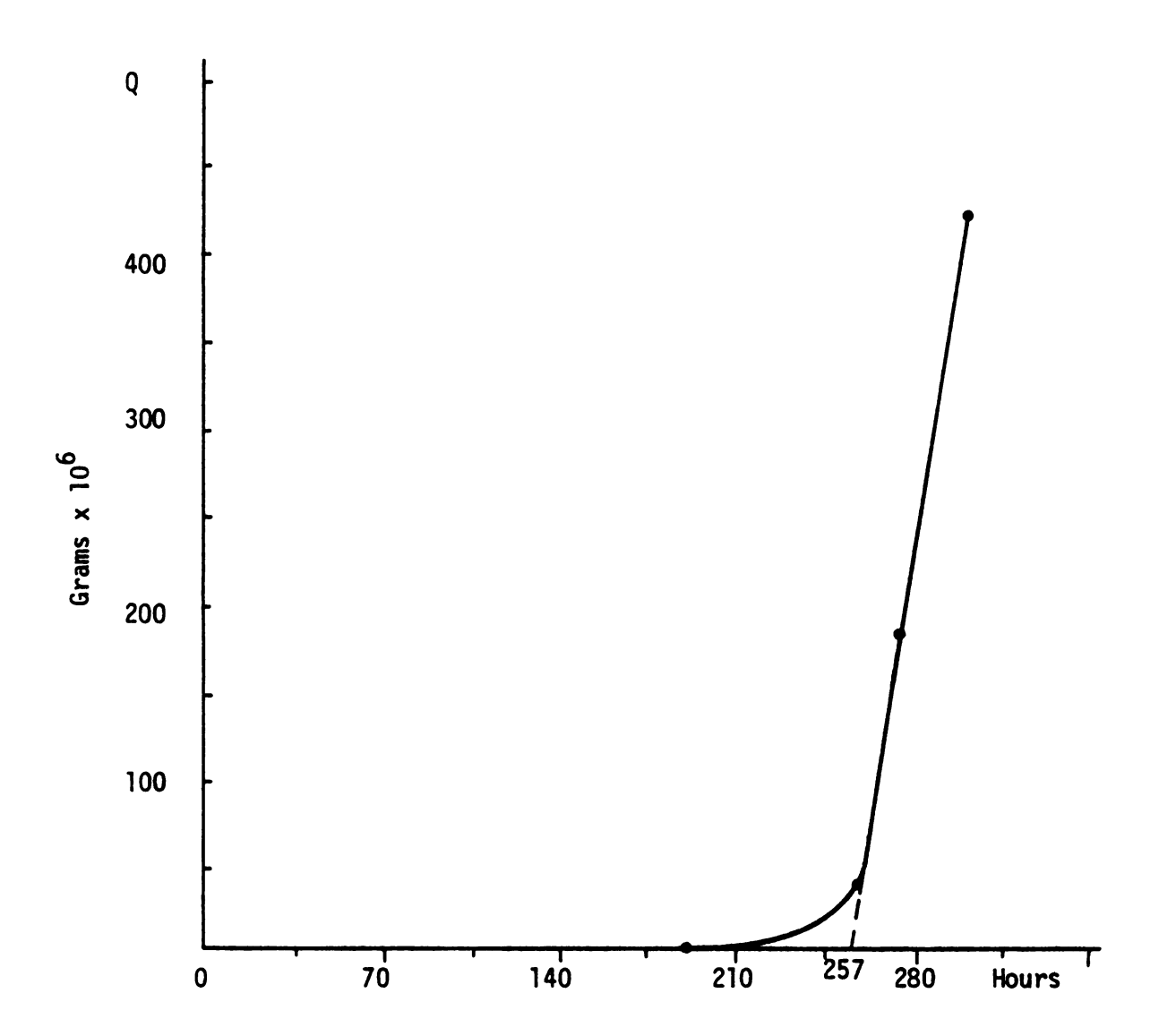


Figure 11. Experiment 2. Total permeated toluene Q versus time.

TABLE 7. Data for Experiment 2

Method: Batch or quasi-isostatic

Temperature: 24.0°C

Toluene concentration:  $\overline{c} = 90$  ppm during first 170 h, then

103 ppm

Thickness of the film: =  $3.57 \times 10^{-3}$  cm

Lag time = 257 h

Lag diffusion coefficient  $D_{Lag} = 2.3 \times 10^{-12} \text{ cm}^2/\text{sec}$ 

Permeability constant  $\overline{P} = 0.051 \text{ g.mil/m}^2.\text{day.}100 \text{ ppm}$ 

# 7.1.3 Experiment 3

After completing the aforementioned batch experiments, experiment 3 was performed by the continuous-flow method. Temperature and toluene concentration remained the same. Data were gathered from most of the unsteady state and steady state regions. Figure 12 presents the flow rate of toluene permeated in grams per hour through the film as a function of time. In Figure 13, the total quantity of toluene permeated is plotted as a function of time. From this the lag time was calculated. The total amount of toluene permeated was obtained by carrying out a graphical integration from Figure 12.

Table 8 gives a summary of the experiment.

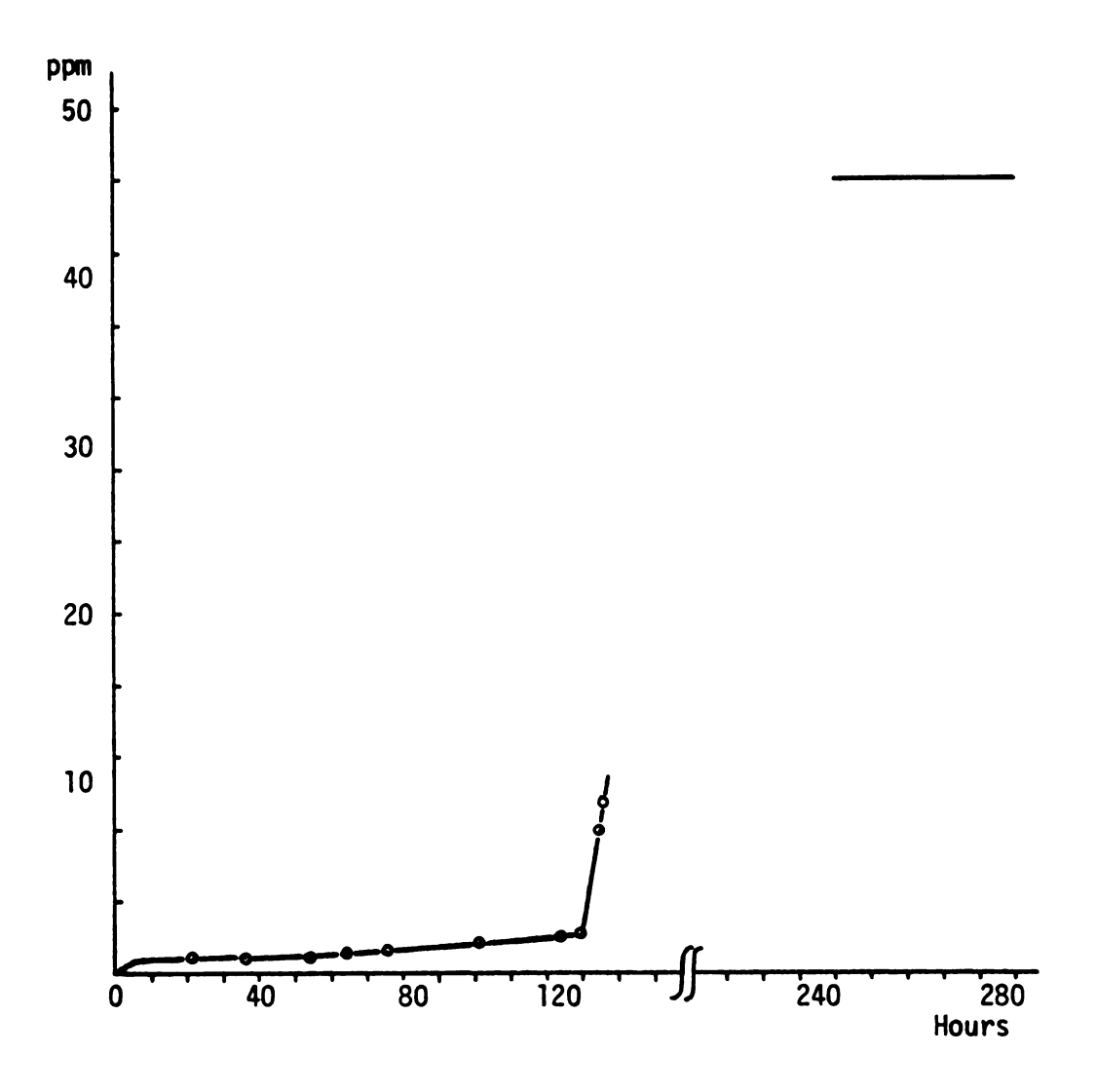


Figure 12. Experiment 3. Concentration of permeated toluene flow versus time.

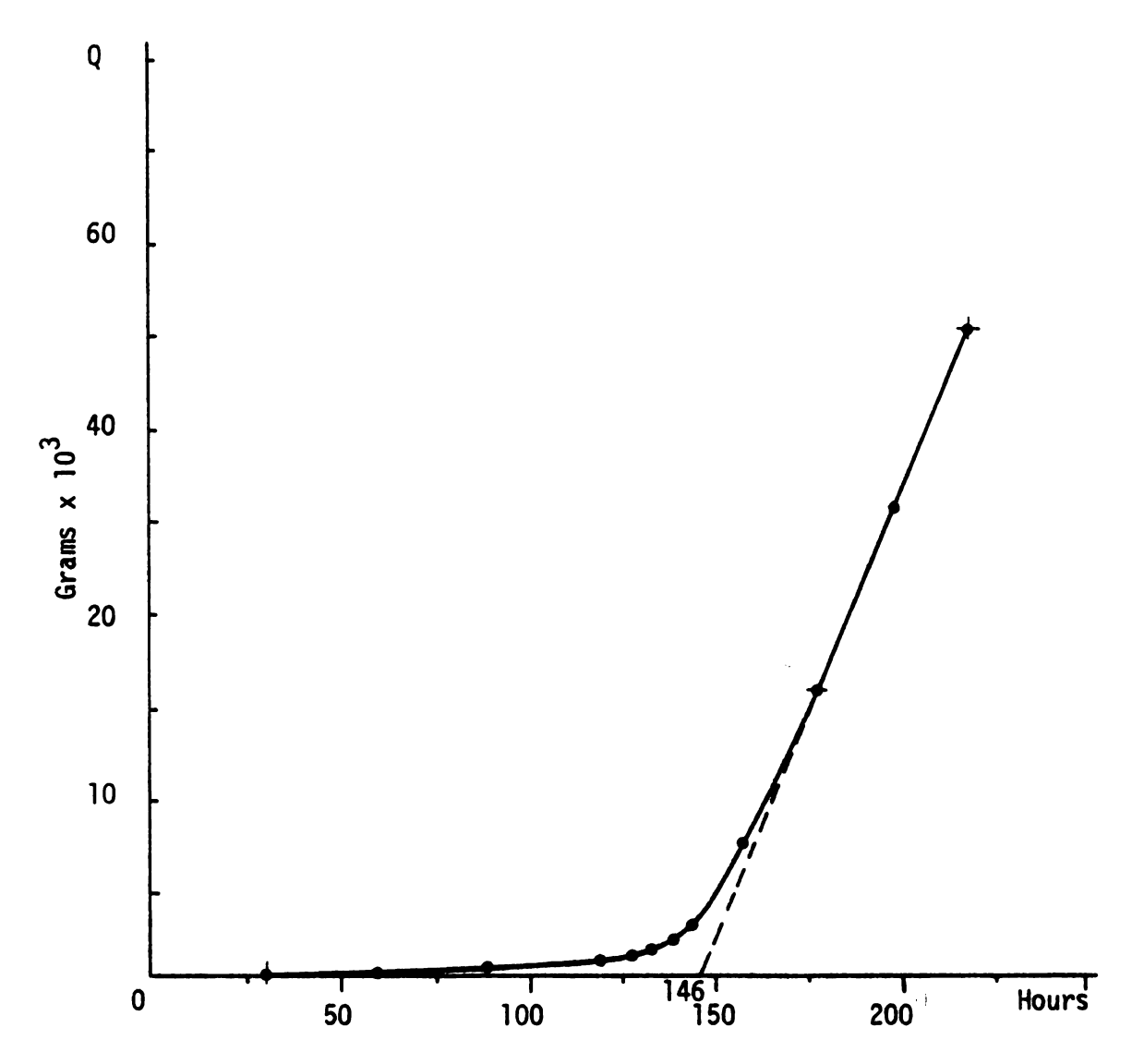


Figure 13. Experiment 3. Total permeated toluene Q versus time.

# TABLE 8. Data for Experiment 3

Method: Continuous-flow

Temperature: 23.0°C

Toluene concentration:  $\bar{c}$  = 92 ppm

Thickness of the film: =  $3.49 \times 10^{-3}$  cm

Lag time = 146.3 h

Lag diffusion coefficient  $D_{Lag} = 3.93 \times 10^{-12} \text{ cm}^2/\text{sec}$ 

Permeability constant  $\bar{P} = 3.17 \text{ g.mil/m}^2.\text{day.}100 \text{ ppm}$ 

# 7.1.4 Experiment 4

This run was a replica of experiment 3. Data collected in this run allowed the calculation of diffusion coefficient by the method of Pasternak et al (1970) and by the lag time method. The actual data are graphically presented in Figure 14 where the permeated flow rate in grams per hour is plotted as a function of time. Figure 15 shows the total amount of toluene permeated as a function of time. To calculate the diffusion coefficient, data presented in Figure 14A were used by applying the Pasternak method. Data from Figure 15 were used to apply the lag time method. Appendices I and II show a sample of the calculation for D.

Table 9 gives a summary of this experiment.

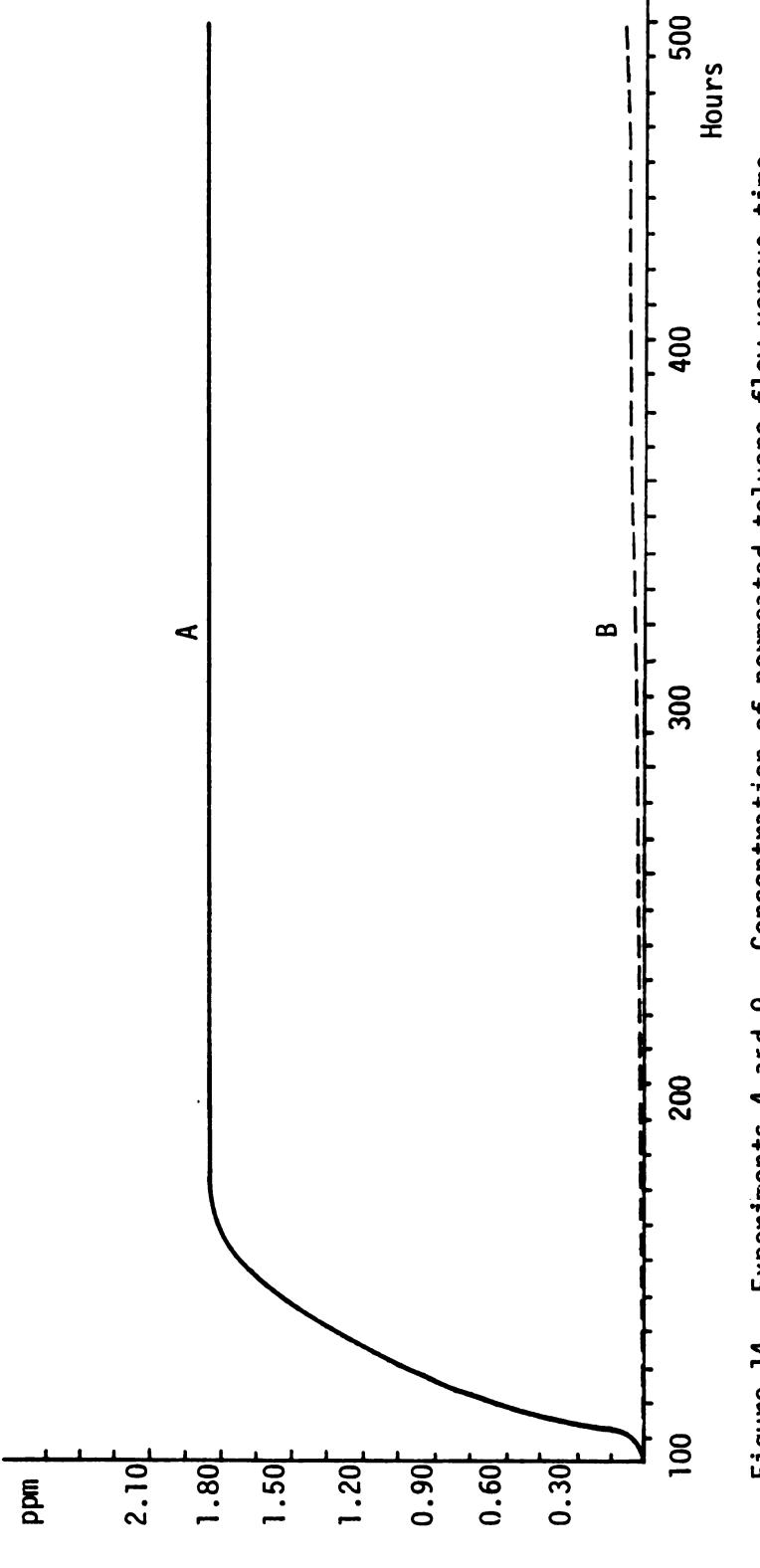


Figure 14. Experiments 4 and 9. Concentration of permeated toluene flow versus time. A - Experiment 4; B - Experiment 9.

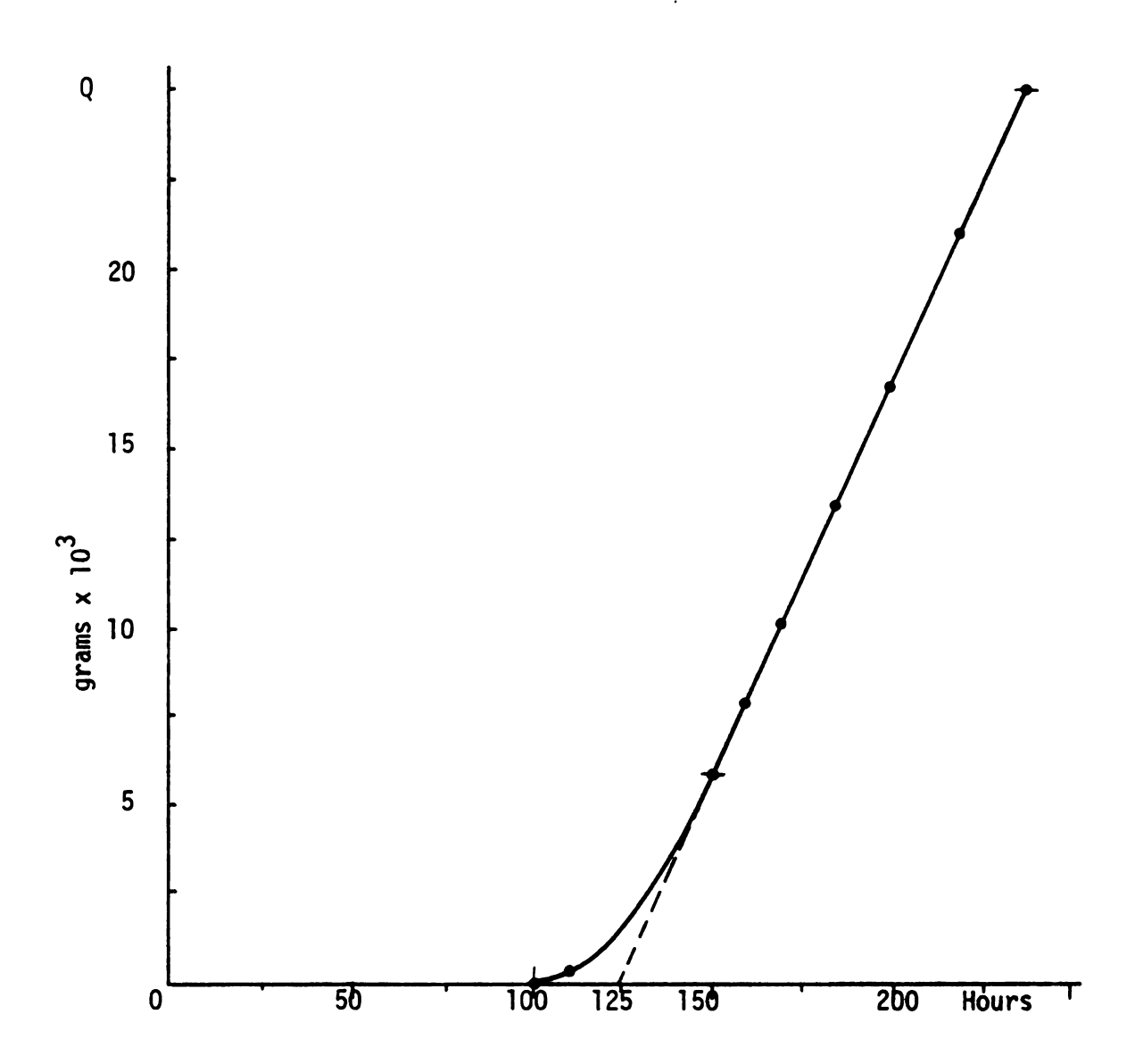


Figure 15. Experiment 4. Total permeated toluene Q versus time.

TABLE 9. Data for Experiment 4

Method: Continuous-flow

Temperature: 23.3°C

Toluene concentration: c = 90 ppm

Thickness of the film:  $3.45 \times 10^{-3}$  cm

Diffusion coefficient:

 $D = 4.67 \times 10^{-12} \text{ cm}^2/\text{sec}$ 

 $D_{Lag} = 4.41 \times 10^{-12} \text{ cm}^2/\text{sec}$ 

Permeability constant:  $\overline{P} = 1.6 \text{ g.mil/m}^2.\text{day.}100 \text{ ppm}$ 

# 7.1.5 Experiments 5 and 6

Experiments 5 and 6 were designed to explore the diffusion process response to a lower toluene concentration than the previous runs. Both methods, batch and continuous-flow, were used simultaneously as a means of verifying results. They were run at the same permeant concentration of 76 ppm and at the same temperature, 27°C.

The continuous-flow system ran for 150 days and the batch apparatus also during 150 days. During these periods of time no toluene was detected as a product of diffusion through the PET film. After these extremely long periods, no permeation occurred at the experimental conditions.

Since it cannot be said that permeation will not take place at these conditions, an upper bound for the  $D_{\text{Lag}}$  was calculated.

Table 10 summarizes these experiments.

TABLE 10. Data for Experiments 5 and 6

	Exp. 5	Exp. 6
Method:	Continuous	Quasi-isostatic
Temperature °C:	27.2	27.2
Toluene concentration, ppm:	76	76
Thickness of film $\times$ 10 <sup>-3</sup> cm	3.45	3.41
Upper bound for D <sub>Lag</sub> cm <sup>2</sup> /sec	1.5 × 10	-13 1.5 × 10 <sup>-13</sup>

# 7.1.6 Experiment 7

The effect of temperature on the diffusion coefficient of toluene through the biaxially oriented PET film was tested in this experiment. The run was carried out by the accumulation method. Some exploratory runs had been made previous to this experiment.

The film was taken from the storage condition at 23-25°C and mounted into the cell. The cell was then placed in a constant temperature oven maintained at 60°C. In order to allow for thermal equilibrium, the permeation run was started two hours later.

Data were obtained after nearly 800 hours of continuously monitoring the diffusion process. Figure 16A is a plot of the total amount of toluene permeated expressed in micrograms as a function of time. As shown, the diffusion process did not appear to reach a

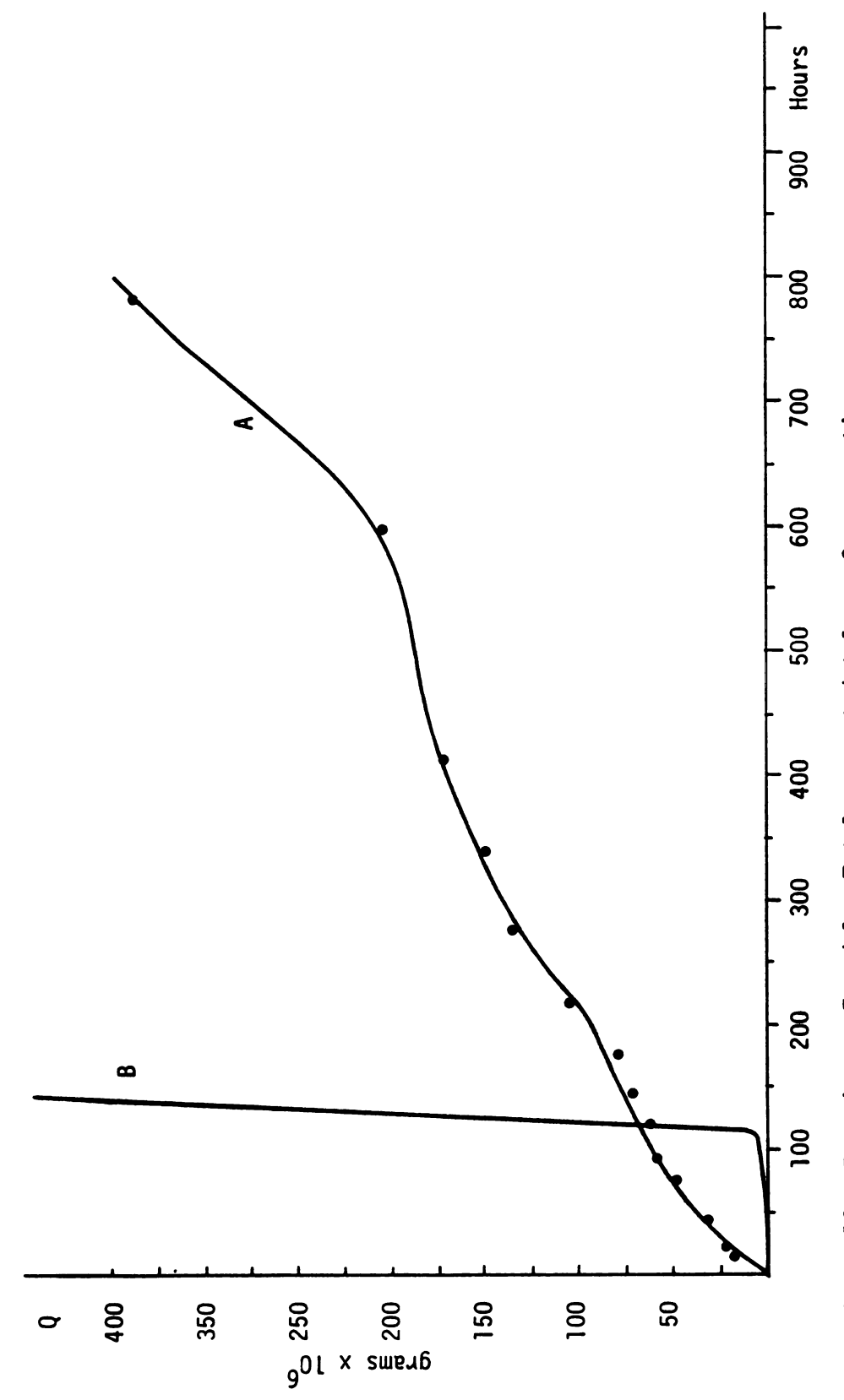


Figure 16. Experiments 7 and 1. Total permeated toluene Q versus time. A - Experiment 7; B - Experiment 1.

steady- state transmission rate. Figure 16B shows the data for Experiment 1, to allow a comparison.

The total amount of toluene permeated after the 800-hour period was a twentieth of the amount which had permeated in less than 300 hours under ambient conditions, even though in the later experiment a lower penetrant driving force concentration was employed (see Experiment 1 for details). The shape of the curve suggests that a non-fickian process took place as compared with Figure 16B in which the curve is typical for a non-Fickian diffusion.

In this case neither the lag-time method nor the Smith and Adams approach could be used to estimate the diffusion coefficient. Here, the small times approximation method developed by Rogers, Buritz and Alpert (1954) and described by Crank (1975) was applied to determine the diffusion coefficient. Meares (1965) also applied this method to a non-Fickian diffusion process. The method is presented in Appendix IV.

For the small times approximation method, the data are presented graphically plotting  $\ln t^{1/2}F$  as a function of  $t^{-1}$ , where t is time in hours and F is flux of toluene through the film. Appendix V gives the numerical value of  $\ln t^{1/2}F$  and  $t^{-1}$  used for graphical presentation and Figure A-1 shows the plot.

Although the points appear to be somewhat scattered, it was assumed that they are represented by a straight line. The diffusion coefficient estimated from the slope of this line is  $D = 2.5 \times 10^{-11}$  cm<sup>2</sup>/sec. The permeability coefficient could not be calculated since

the steady state was not reached. However the permeability rate of the last time interval ( $\Delta t = 102h$ ) is determined as

$$2.3 \times 10^{-4}$$
 g mil m<sup>2</sup>.day.100 ppm

Table 11 presents a summary of this experiment.

TABLE 11. Data for Experiment 7

Method: Accumulative

Temperature: 60°C

Toluene concentration:  $\bar{c} = 102 \text{ ppm}$ 

Thickness of the film:  $3.37 \times 10^{-3}$  cm

Diffusion coefficient:  $2.5 \times 10^{-11}$  cm<sup>2</sup>/sec

Permeability:  $2.3 \times 10^{-4} \frac{\text{g mil}}{\text{m}^2 \cdot \text{day.} 100 \text{ ppm}}$  (at the last interval of time)

Experiments 1 to 7 dealt with PET films that had been kept apart from being in contact with toluene vapor before being mounted into the permeation cell. During these experiments there were some indications that a prior contact between toluene vapor and the film could affect the diffusion process. To verify that observation two experiments were carried out with different degrees of "exposure" of PET to toluene, before the run. These experiments were 8 and 9. In Experiment 8, a sample film was placed in a chamber containing 25 ppm of toluene in nitrogen, during 10 days and at 24°C.

In Experiment 9, the same film was used that was mounted in Experiment 4. After the latter run was over, the film had been left for two months in a toluene-free environment. No attempt was made to remove remaining toluene in a vacuum chamber.

# 7.1.7 Experiment 8

This experiment evaluated the effect on the permeation process of pre-exposure of the PET film to low levels of toluene vapor.

A film sample (4 x 100° B) was pre-exposed by placing the sample in a chamber of 25 ppm toluene vapor and maintaining the sample at this toluene concentration for 10 days at 24°C. Immediately after that, the sample was mounted into the permeation cell and a quasi-isostatic method experiment was carried out. The resultant transmission rate profile curve is shown in Figure 17. It can be seen also that an apparent Fickian behavior, and large lag time characterized this process. The diffusion coefficient calculated from lag time was  $1.6 \times 10^{-12}$  cm which, although the permeant concentration was 98 ppm, can be considered a low value.

Table 12 summarizes this experiment.

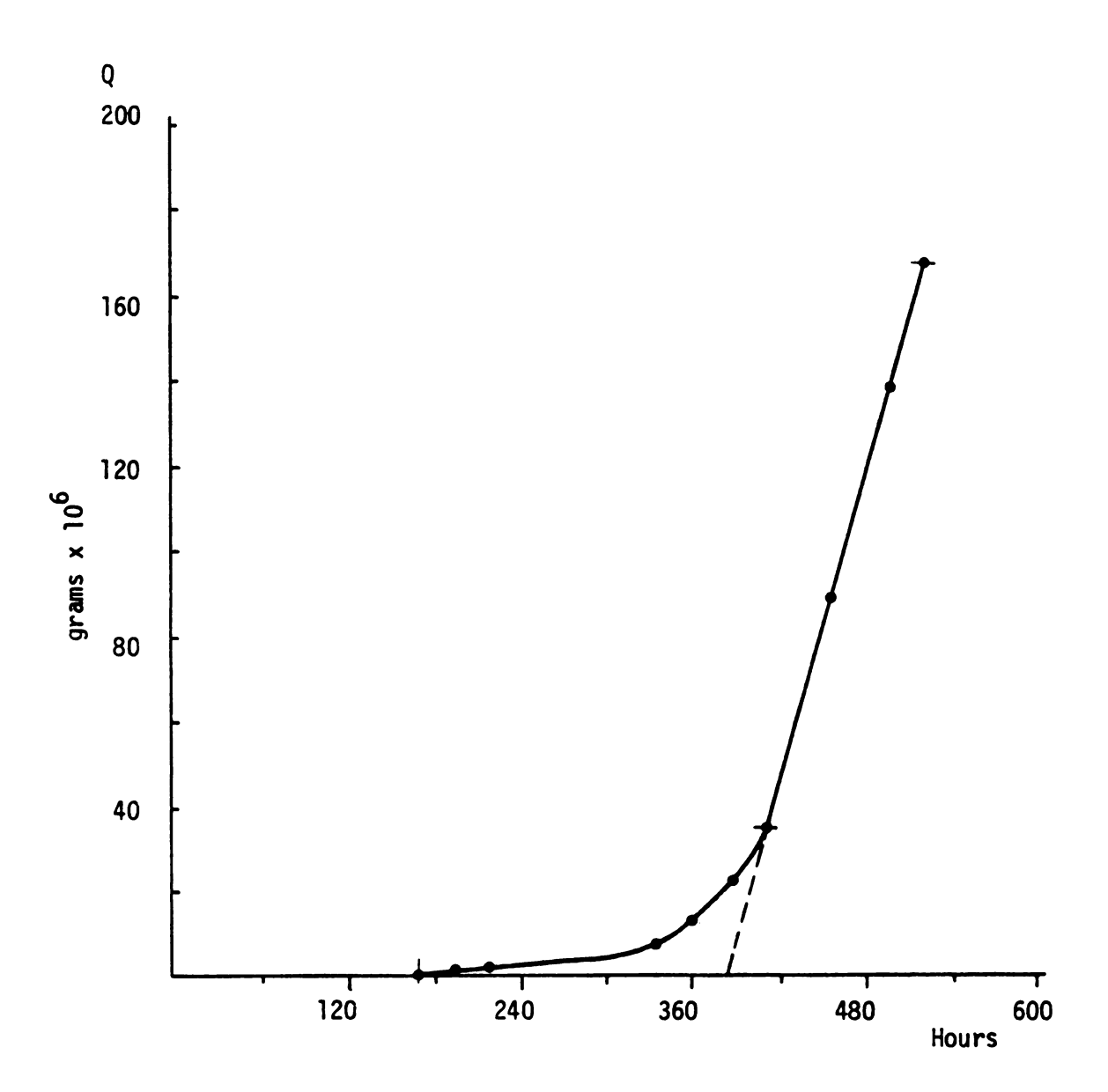


Figure 17. Experiment 8. Total permeated toluene Q versus time.

# TABLE 12. Data for Experiment 8

Method: Quasi-isostataic

Temperature: 23.6°C

Toluene concentration: c = 98 ppm

Thickness of the film:  $3.6 \times 10^{-3}$  cm

Diffusion coefficient:  $D_{Laq} = 1.55 \times 10^{-12} \text{ cm}^2/\text{sec}$ 

Permeability constant:  $\overline{P} = 2.19 \times 10^{-11}$  g mil cm<sup>2</sup>.day.100 ppm

The film was exposed to a very dilute toluene-nitrogen mixture prior to the permeation process.

# 7.1.8 Experiment 9

The objective of this experiment was to evaluate how a film would behave when a second permeation process is conducted on it.

The film from Experiment 4 was used here after being kept in a toluene-free ambient for 60 days.

This experiment was carried out in the same conditions (i.e., permeant concentration and temperature) as Experiment 4. The results are plotted together (see Figure 14B). The difference between the plots is apparent. The rate of permeant was diminished by a factor of 10 and the diffusion coefficient calculated by the small time approximation was  $7.2 \times 10^{-13}$  cm<sup>2</sup>/sec.

This experiment indicated that there was an effect of permeant molecules on the polymer chain configuration. After the film was

submitted to a second permeation experiment, the diffusion process was highly altered. A similar effect on an acetone-cellulose nitrate film system was observed by Drechsel et al (1953) and on a benzene-polysterene system by Long and Kokes (1953). In order to confirm that there was an effective change in the orientation of molecules, birefringency measurements should be carried out. No facilities were available to carry out these measurements at the time of this work.

Table 13 summarizes this experiment.

TABLE 13. Data for Experiment 9

Method: Continuous-flow

Temperature: 24.3°C

Toluene concentration:  $\overline{c} = 91 \text{ ppm (wt/v)}$ 

Thickness of the film:  $3.45 \times 10^{-3}$  cm

Diffusion coefficient:  $7.3 \times 10^{-13}$  cm<sup>2</sup>/sec

Permeability constant:  $\overline{P} = 0.2$   $g \times mil$   $m^2$ .day.100 ppm

This film was the same as that used in Experiment 4.

Table 14 presents a summary of experiments 1 through 9, and Figure 18 is a plot of D as a function of vapor concentration.

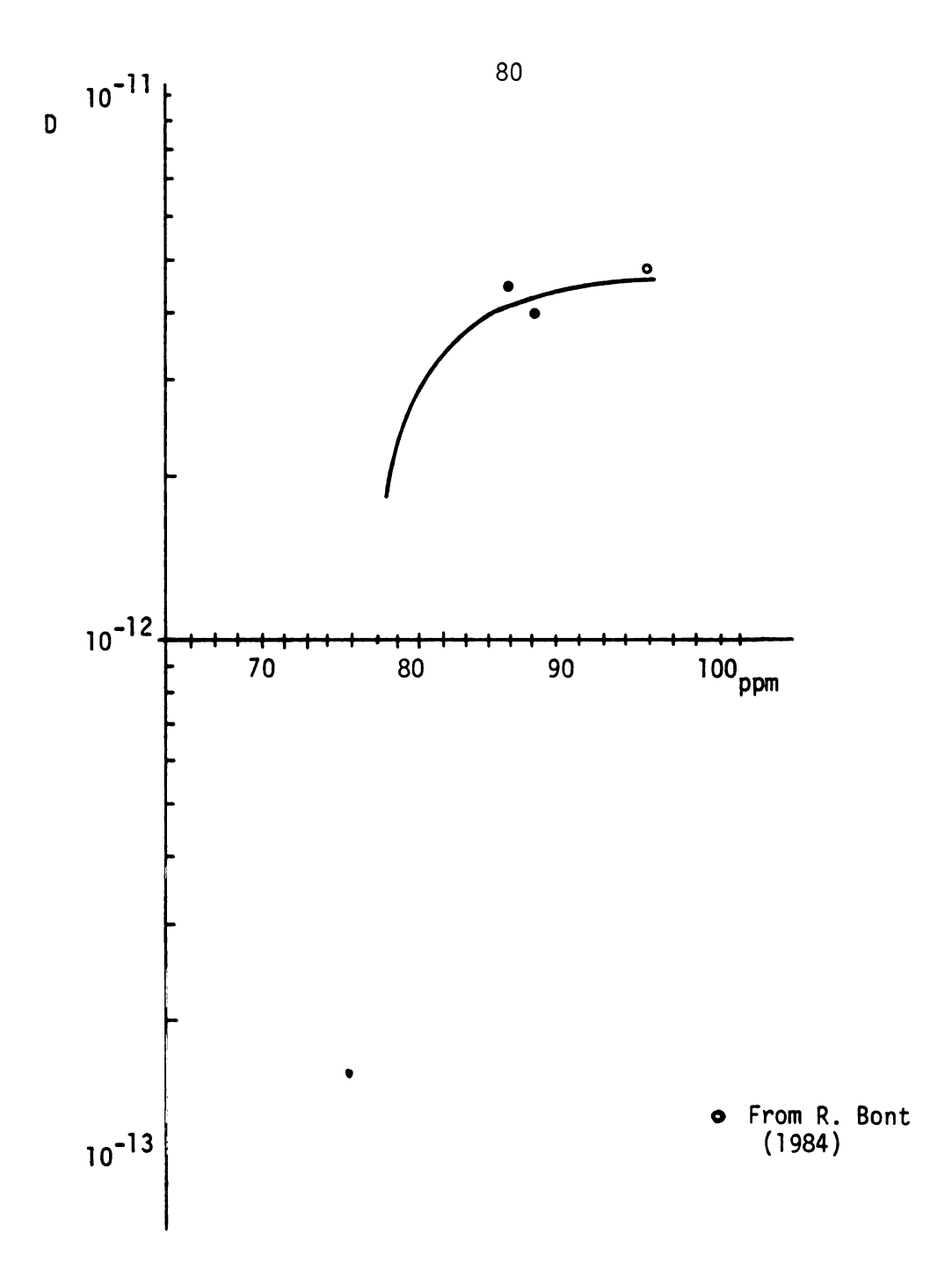


Figure 18. Diffusion coefficient as a function of permeant concentration at 23°C.

Summary data for diffusion of toluene vapor through PET TABLE 14.

27.2 27.2 60.0	
	23.6
	27.2 60.0 23.6 23.6

A, accumulative method; C, continuous-flow method

(a) No permeation after 150 days

(b) Non-steady-state value after 700 hours, limiting diffusion coefficient

### 7.1.9 Sorption equilibrium experiments

Sorption data were obtained by exposing samples of the film to toluene vapor of known concentration. A Mettler analytical balance, within a resolution of 0.1 mg, was used. A more sensitive balance, such as a Cahn electrobalance, was not available at the time of this study. Nevertheless, an acceptable sorption-concentration experimental curve was obtained that showed a non-linear relationship between equilibrium sorption value and sorbate concentration. This is shown in Table 15 and is plotted in Figure 19.

TABLE 15. Solubility data, Toluene vapor-PET

Temperature	W	c
24°C	0.0752	100.5
24°C	0.0157	71.8
24RC	0.0048	51.0
60°C	0.005	101.0

# 7.1.10 Determination of glass transition Temperature, Iq of PET

Two samples of the PET used in the permeation experiments were sent to Perkin-Elmer Instruments in Pittsburgh, Pennsylvania where the Tg was determined by the differential scanning calorimeter (DSC) method. Four values were determined, 81.1, 80.7, 81.0, and 80.0°C, giving an average of 80.7°C.

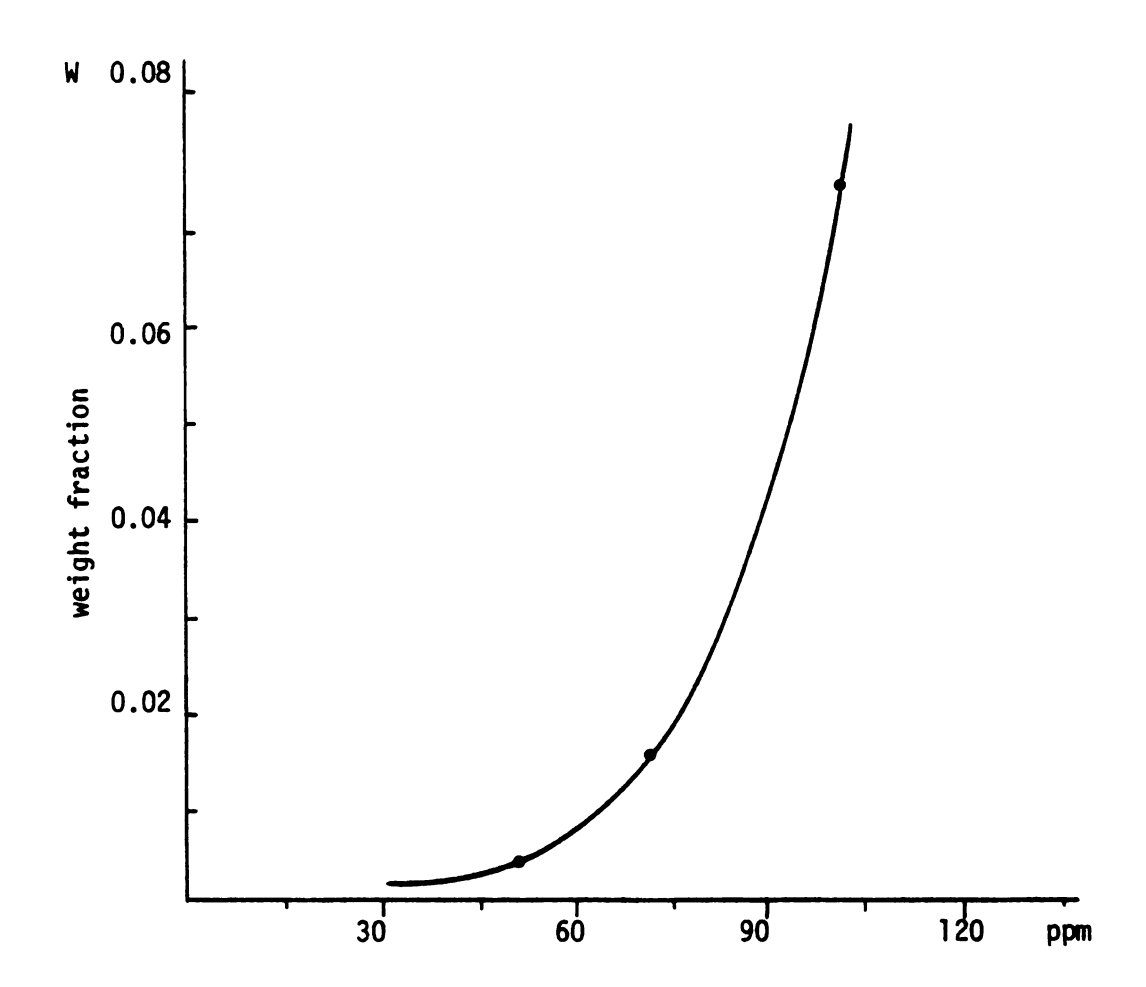


Figure 19. Solubility equilibrium at 23°C. Weight fraction versus permeant concentration.

Figures A2 - A5 in Appendix VI show the plot of MCal/sec versus temperature where the Tg is calculated.

The samples were sealed in standard aluminum DSC sample pans and heated at 40°C/min in a nitrogen atmosphere (20°cc/min), from approximately 30°C to 300°C in a Perkin-Elmer DSC-4/TADS system.

Melting point was also determined, and given a value of 232°C.

#### DISCUSSION

# 7.2 Discussion

# 7.2.1 Deborah number

Vrentas, Jarzebski and Dudas (1975) defined a Deborah number for the diffusion process as

$$(DED)_{D} = \frac{\lambda m}{\theta_{D}}$$
 (36)

Where  $\lambda m$  is a mean relaxation time for a polymer at the conditions of interest and  $\theta_D$  is a characteristic diffusion time, one-dimensional mass transfer in the polymeric film.

For viscoelastic fluid,  $\theta_{\rm f}$  is a measure of the time needed to effect a significant change in the kinematic conditions of a material particle. For unsteady flows, it represents the time needed to proceed from one steady state to another (Astarita and Merruci, 1974).

In this study  $\theta_D$  is taken from the unsteady portion of the permeation experiment and  $\lambda m$  is taken from available literature data.

From the present experiment, it was determined that the highest time required to reach a steady-state diffusion rate, from the time of

initial exposure to the permeant (i.e., toluene) was given 245 h or 8.8  $\times$  10<sup>5</sup> sec. From the work of Meredith and Bay-Sung (1962), the mean relaxation time for PET at 25°C of  $10^{10}$  sec was calculated.

From these values an approximate (DED)D is then given by

$$(DED)_{D} = \frac{\lambda m}{\theta_{D}} = \frac{10^{10}}{8.8 \times 10^{5}} = 1.1 \times 10^{4}$$
 (37)

For (DEB)<sub>D</sub>>>1 a Fickian diffusion is predicted by the Vrentas,
Jarzebski and Dudas (1974) diagram which corresponds to a low penetrant
concentration and a temperature below glass transition (see Figure 5).
This prediction agrees with the experimental Fickian behavior observed
for toluene/PET at the condition of test. Hopfenberg and Frish (1969)
also predicted a Fickian behavior, but in a more qualitative viewpoint,
since they do not use any parameter (see Figure 4).

# 7.2.2 <u>Temperature effect on diffusion coefficient</u>

Experiments that were conducted at ambient temperature, namely experiments 1 through 6, showed an apparent Fickian behavior, as shown in a comparison of Figure 2 and Figures 10, 11, 13 and 15.

Experiment 7 which was carried out at 60°C appeared to be nonfickian (compare Figure 3 and Figure 16A). From the last experiment it was found that the diffusion coefficient increased when compared to the results of the runs carried out at 23°C, meantime the permeability constant sharply decreased when compared to the results of runs carried out at 23°C, contrary to what it was expected. While this phenomenon is not completely understood and warrants further investigation, this change in permeability behavior due to an increase in temperature from well below the polymer glass transition temperature to a temperature approaching Tg suggests that configurational changes on the PET matrix could have taken place that affect the permeability properties.

Although methods such as x-ray, light scattering and birefringency are needed to better evaluate configurational changes, the present results suggest that less "holes" are available within the PET matrix for the permeation of the organic molecule. It should be pointed out that for complex penetrant/barrier film systems like toluene/PET, diffusion experiments should be carried out together with the above-mentioned methods to provide a better understanding of the phenomenon of diffusion and the effect of temperature on polymer diffusivity.

To quantitatively evaluate the effect of temperature on the diffusion process, the mutual diffusion coefficient  $D_{\rm S}$ , calculated from the small times method Rogers, Buritz and Alpert (1954) (See Appendix IV) was used.  $D_{\rm S}$  was calculated for runs 1, 2 and 4 to give a value at 23°C, and for run 7 to provide a value of  $D_{\rm S}$  at 60°C. The calculation procedure is presented for each of the experiments in Appendix V.

The  $\mathrm{D}_{\mathrm{S}}$  values calculated by the small time approximation method are summarized in Table 16.

TABLE 16.	Value of	$D_{s}$ as	a	function	of	temperature
-----------	----------	------------	---	----------	----	-------------

Experiment No.	Temperature °C	$D_{\rm s} \times 10^{12}$ ,cm $^2$ /sec
1	23	0.37
2	23	0.78
4	23	0.34
7	60	24.0

Assuming that the Arrhenius law is followed, the effective activation energy for diffusion  $E_D$  can be derived from the mutual diffusion coefficient  $D_S$  calculated by the small time method, the expression

$$E_{D} = RT^{2} \frac{\partial lnD_{s}}{\partial T}$$
 (38)

Averaging the values for  $D_S$  at 23°C from Table 12 and calculating  $E_D$  from the slope of a plot of log  $D_S$  versus the values presented in Table 17 are obtained, where K is the pre-exponential factor in the expression

$$D_s = K \exp(-E_D/RT)$$

derived from Equation 38.

The different value obtained for Experiment 2 compared with Experiments 1, 3 and 4 for both D values (Table 14) and P values (Table 16) can be attributed to the non-homogeneity of the film samples even when they were stretched at the same conditions and the density

values gave a similar value for the amorphous fraction of PET, and not to experimental error.

TABLE 17. Values for the Arrhenius equation

T, *K	296	233		
$D_{\rm S} \times 10^{12}  {\rm cm}^2/{\rm sec}$	0.50	24.0		
ED	8.9 Kcal/mole			
log K	2.8			

Chen (1974) reported a value of  $E_D$  = 13.8 Kcal/mole for the penetrant/polymer barrier CH<sub>4</sub>/PET, while Michaels et al (1973) reported a value of 12.85 Kcal/mole for the same penetrant/polymer system.

While additional experiments are necessary in order to confirm these results of the toluene/PET system, it can be suggested that the interaction between PET and organic vapor such as toluene should be related to this somewhat low energy of activation.

# 7.2.3 Permeant concentration effect on diffusion coefficient

Values of the diffusion coefficient obtained for the different vapor concentrations assayed are presented in Table 14. The variations of the values of D, for the same experimental conditions, are due to the characteristics of the stretched PET films, and are much bigger than the experimental error due to the method. For the

and the accumulation methods, no diffused toluene vapor was detected after five months of continuous exposure of the film to the permeant. This shows that the driving force created by the concentration gradient of 76 ppm of toluene in the permeant gas phase was not enough to "break through" the barrier posed by the PET film during that period.

This result suggests the possibility of a threshold value within a relatively small range of 76 ppm.

To obtain data for concentration values close to 76 ppm can involve extremely long experiments. The value of D that appears in Table 14 for 76 ppm is only an upper bound calculated for the 5-month period using the lag-time method.

No other permeation data in a range of concentration similar to the ones employed in this work and for a similar system were available at the time of this study.

The diffusion coefficient and permeant concentration of Table 14 may be correlated in several ways. Taking into account the facts above mentioned, the smooth curve in Figure 18 is thought to adequately represent the behavior of D versus permeant concentration in the toluene/PET system.

A behavior similar to that shown in Figure 18 was reported for the toluene/Saran system at 23°C and the same range of permeant concentration (Baner, 1984).

Nevertheless, the observed behavior should have important practical applications, since below some critical permeant concentra-

tion, plastic films can act as non-permeable barriers for long periods of time.

What follows is an attempt to apply quantitatively the free-volume theory by Fujita (1961) to correlate the mutual diffusion coefficient D and permeant concentrations between 80 and 102 ppm of permeant concentration. Although this theory was developed for systems above the glass transition temperature of the polymer, where a Fickian behavior is clearly established, the rationale that supports its application to the toluene-PET system at 23°C is that this system showed an apparent Fickian behavior that is characteristic of the system above Tg. In fact, the repeatedly apparent Fickian behavior in Experiments 1 to 6, and the high value of the Deborah number calculated, suggests its applicability. An attempt to approximately evaluate equation 20,

D = RT Ad (d ln ap/d ln cp)(1-v)exp(- $B_f/f$ )

therefore follows.

In applying the Fujita free-volume theory to the toluene/PET system, the following assumptions were made:

- 1) Since the partial pressure of toluene vapor in the penetrant gas phase is in the order of  $2 \times 10^{-2}$  atm, the activity (ap) is replaced by the partial pressure of toluene in the gas phase p.
- 2) Since toluene vapor produces some swelling of the PET film when dissolved in it, weight fraction values (w) were easier

to obtain than volume fraction values (v). On the other hand, for the value at 80-100 ppm the toluene-PET density data obtained after permeation indicated little variation between them.

#### Therefore,

$$d(\ln ap)/d(\ln v) \approx d(\ln p)/d(\ln w)$$
 (39)

The value of d(|n p)/d(|n w) can be calculated from the sorption equilibrium data. Figure 20 shows a plot of |n p versus |n w, where p is the partial pressure of toluene in the gas phase mixture in contact with the film, and w is the weight fraction of toluene in PET in equilibrium. From the linearity of this plot, it was determined that d (|n p)/d(|n w) was a constant approximately equal to 0.23 for the toluene-PET system and the experimental conditions of interest. Values used to plot Figure 20 are presented in Table 18.

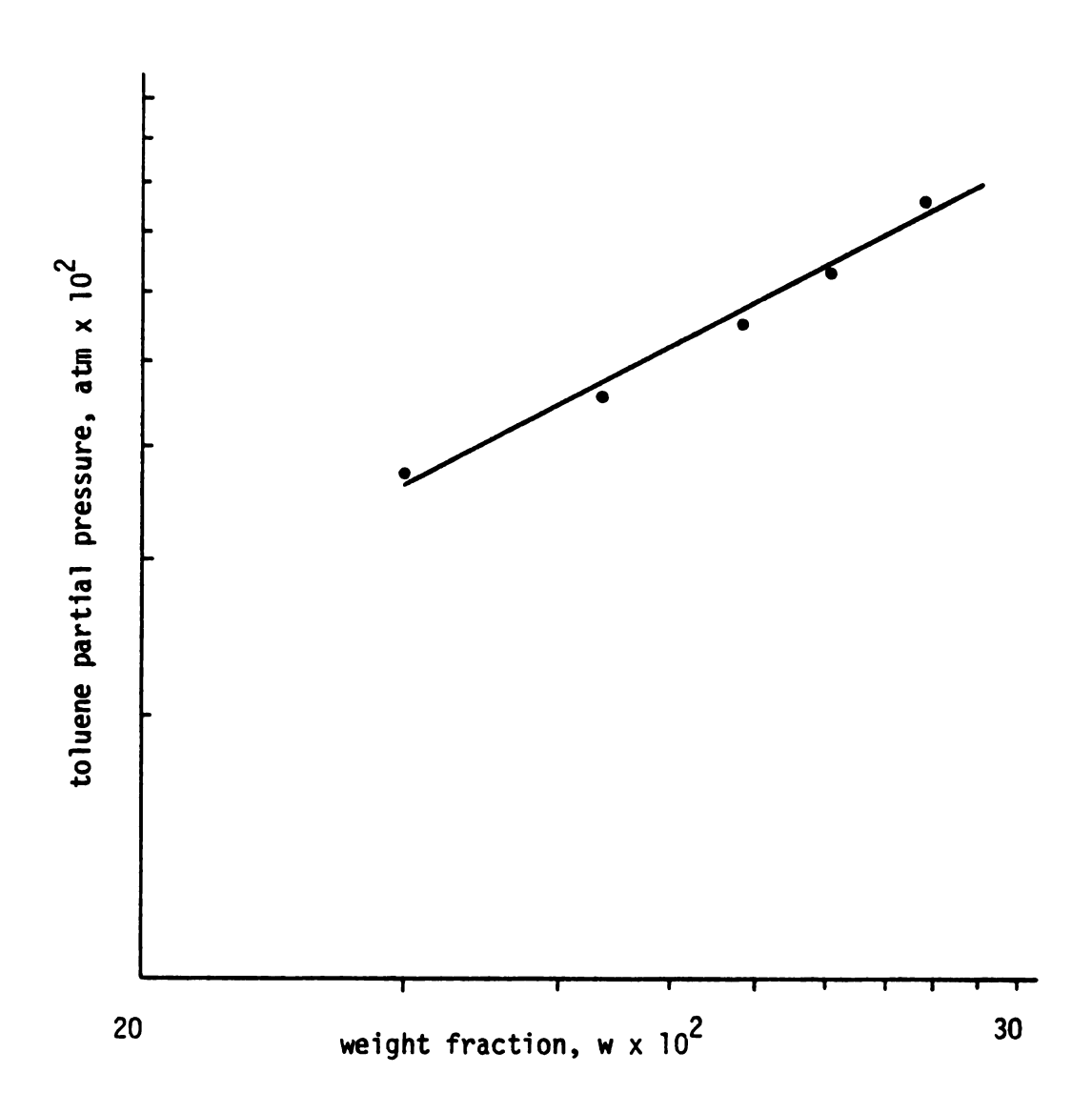


Figure 20. Toluene partial pressure versus weight fraction solution equilibrium at  $23\,^{\circ}\text{C}$ .

TABLE 18. Values of the weight fraction as a function of toluene partial pressure plotted in Figure 20

Toluene concentration ppm	Toluene partial pressure atm $\times 10^2$	Fraction weight $g/g \times 10^2$
80	2.105	2.746
85	2.237	3.669
90	2.368	4.748
95	2.500	5.984
102	2.684	7.974

Since the values of the fraction volume or the weight fraction are much smaller than one, 1-v can be approximated by one.

$$1 - v \approx 1.0 \tag{40}$$

After these substitutions the original expression, equation 20, becomes

$$D = 0.23 D_0 \exp(-B_f/f)$$
 (41)

Where  $D_0 = RT$  Ad

Following Fujita (1961) and Stern and Kulkarin (1983), for a given polymer-penetrant combination, the quantity (f) generally should be a function of both temperature and penetrant concentration, then f can be represented by

$$f(w_p,T) = f^* + [Y(T) - f^*]w_p$$
 (42)

The quantity f\* is the value of f at zero penetrant concentration and represents the average fractional free volume in the pure polymer. The quantity  $\gamma$  may be compared with the fractional free volume of the diluent.

Substituting the last expression into Equation 41 and introducing a factor that takes into consideration the amorphous volume fraction of the polymer,  $\phi_a$ , the following expression is obtained:

$$D = 0.23 D_0 \exp \left[\frac{W}{(B + GW)}\right]$$
 (43)

Where

$$B = \frac{f^{*2} \phi a}{\gamma B_d} \tag{44}$$

$$G = \frac{f^* \phi a}{B_d} \tag{45}$$

 $\phi a = 1$ - percent of crystallinity = 1 - 0.28 = 0.72

In order to derive approximate values for B and G, the value of the limiting diffusion coefficient  $D_0$  equals to  $D_S$  was needed.  $D_0$  was calculated for Experiments 1 and 4, conducted at 90 ppm, and its average value was  $3.4 \times 10^{-13}$  cm<sup>2</sup>/sec.  $D_0$  was determined for a film with  $\phi a = 0.72$ .

Then, from Equation 43

$$\frac{1}{\ln D/0.23D_0} = \frac{B + Gw}{w} = B \frac{1}{w} + G \tag{46}$$

and plotting  $[ln D/0.23D_0]^{-1}$  versus  $w^{-1}$ , the values of G and B can be obtained (see Figure 21).

Values of D as a function of the weight fractions were obtained from Figures 18 and 19, which present D as a function of permeant concentration in the gas phase and solubility equilibrium data, respectively.

Values from 80 to 102 ppm permeant concentration are presented in Table 19.

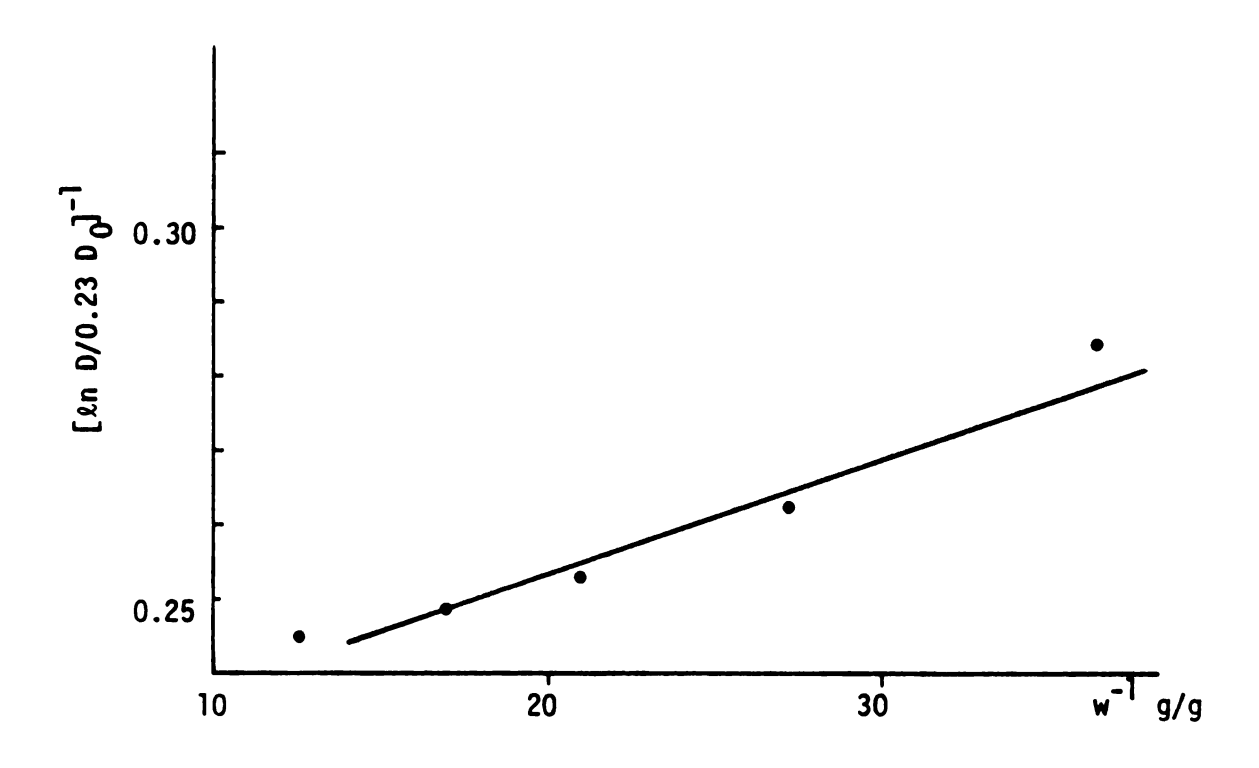


Figure 21. [ $\ln D/0.23 D_0$ ]<sup>-1</sup> versus w<sup>-1</sup> for toluene-PET at 23°C.

TABLE 19. Values of mutual diffusion coefficient as a function of w

Permeant	concentration ppm	Fraction weight w g/g	$0 \times 10^{12}$ cm <sup>2</sup> /sec
	80	0.02746	2.6
	85	0.03669	3.5
	90	0.04748	4.1
	95	0.05984	4.4
:	102	0.07974	4.6

Table 20 presents the values of [ln D/0.23  $D_0$ ]<sup>-1</sup> that are plotted in Figure 21.

From a least-square fitting the slope equals  $1.697 \times 10^{-3}$ , and the y-intercept is 0.2202.

Therefore,

and

$$B = 1.7 \times 10^{-3} \text{ g/g}$$

$$G = 0.22$$

The diffusion coefficient D, for the 4  $\times$  100°C biaxially oriented 72% amorphous PET film-toluene system, at a concentration of

TABLE 20. Values of  $w^{-1}$  and [ln D/0.23 D<sub>0</sub>]<sup>-1</sup>

w-1	[ln D/0.23 D <sub>0</sub> ] <sup>-1</sup>
36.41	0.2854
27.25	0.2631
21.06	0.2526
16.71	0.2481
12.54	0.2454

toluene between 80 and 102 ppm is given by

$$D = 0.78 \times 10^{-13} \exp \left[ \frac{w}{(1.697 \times 10^{-3} + 0.2202 \text{ w})} \right]$$
 (47)

Table 21 compares experimental values of D with value calculated with Equation 47 for  $\phi_a$  = 0.72.

TABLE 21. Comparison of experimental and calculated values of D

Permeant concentration ppm		$D \times 10^{12} \text{ cm}^2/\text{sec}$	
		Experimental	Calculated
	80	2.6	2.7
	85	3.5	3.3
	90	4.1	3.9
	95	4.4	4.4
:	102	4.6	4.9

Values from Table 18 are plotted in Figure 22 to show the relationship between the permeant concentration and the diffusion coefficient, and the agreement between the calculated and the experimental D.

From a least square fitting of sorption equilibrium experiments, w is related to  $\overline{c}$  (in ppm) through the following equation:

$$w = 3.13 \times 10^{-5}(\bar{c})^2 - 33.191 \times 10^{-4}\bar{c} + 92.6717 \times 10^{-3}$$
 (48)

Kulkarni and Stern (1983) developed a semi-empirical correlation to evaluate  $\gamma$ . From experimental data of Fels and Huang (1970), Kulkarni and Stern estimated  $\gamma$  = 0.51 for benzene and  $\gamma$  = 0.63 for hexane at 25°C. Taking a value of  $\gamma$  = 0.5 for toluene it is possible to approximately evaluate the other two parameters, i.e.,  $B_d$  and  $f^*$ . Since  $G^2/B = \gamma/B_d$ , substituting values  $B_d$  = 0.013, from Equation 45 we get  $f^*$  = 0.0040.

Kulkarni and Stern (1983) evaluated f\* = 0.09 for polyethylene, PE. This value is almost 20 times larger than that for PET. Permeability values for PE are also much larger than for PET (see Table 23). No value was available in the literature for PET to allow a better comparison.

# 7.2.4 Considerations on permeability

Permeability constant values (P) presented in Table 22 are listed according to the method of test employed.

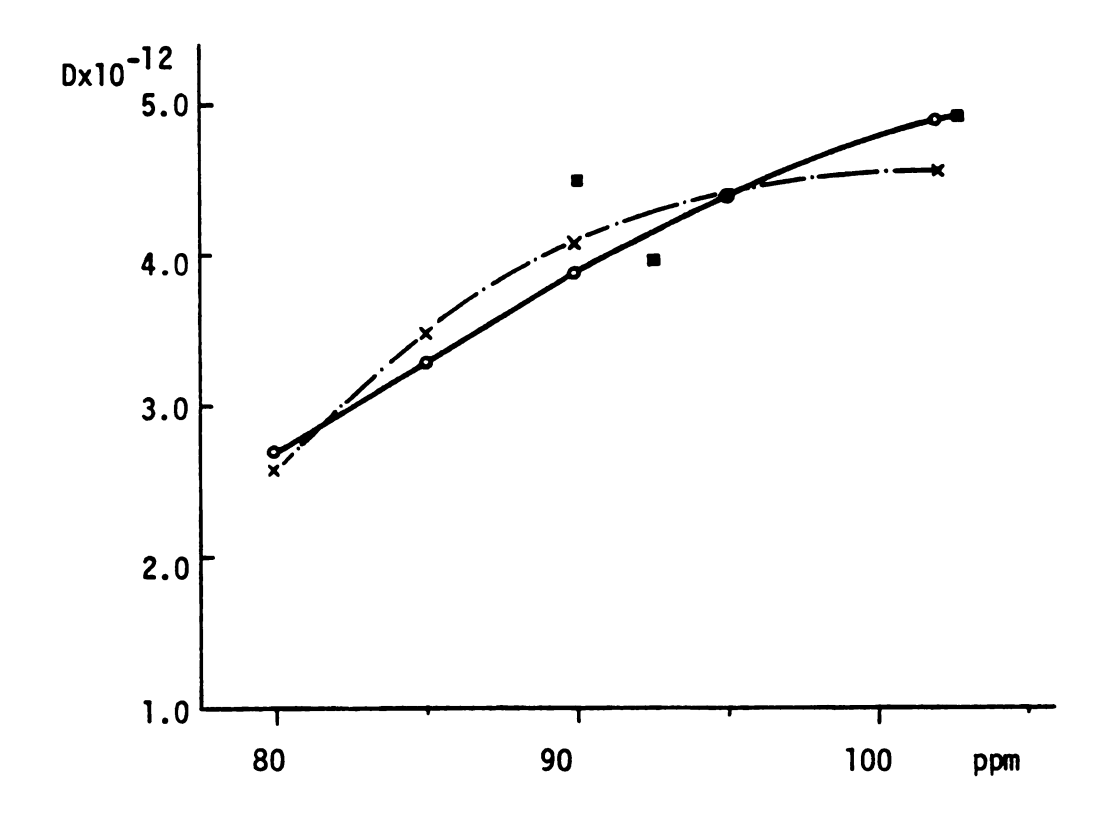


Figure 22. Values of diffusion coefficient versus toluene concentration.

- \_\_\_ predicted values
- --- from smooth curve
  - actual values

TABLE 22. Permeability constants in g.mil/day.m<sup>2</sup>.100 ppm at 23°C.

Accumulation test method (a)	Continuous-flow method (b)	
0.271	3.17	
0.051	1.60	
0.086		

Table 22 shows that in these biaxially oriented PET films, the permeability constant differs not only within the same test method and conditions, but also with the method for its determination.

The average of  $\overline{P}$  values for the accumulation method was 0.136 g.mi1/day.m².100 ppm and ranges from 0.051 to 0.271 g.mi1/day.m².100 ppm, while the average of  $\overline{P}$  values for the continuous-flow method was 1.88 g.mi1/day.m².100 ppm. This lack of reproducibility suggests that orienting partially crystallized PET does not yield the same barrier condition for each of the films. Further, a continuous flowing of nitrogen sweeping the permeated toluene such that existing in the continuous-flow method appeared to have affected the transmission rate of and thus the permeability constant although the diffusion coefficient was not affected. The reason for this latter observation is not fully understood and should be the subject of further investigation.

Table 23 summarizes values of permeability constants for different films. These values were determined at 23°C by the

accumulation technique, with toluene as permeant. All the data, except that for PET that was determined in this study, are taken from Baner, Hernandez, Jayaraman and Giacin (1984).

TABLE 23. Permeability constant for selected films

Toluene concentration ppm	Thickness film mil	Film type	P g,structure/ m <sup>2</sup> .day.100ppm
93	1.0	Oriented polypropilene	12.9
96	1.0	Saran (PV DC)	0.29
94	2.0	Saran/DPP	8.6
88	1.1	Polyethylene (PE)	350.0
93	1.2	PE/Ny lon/PET	$3.9 \times 10^{-4}$
90	1.4	PET	0.14

This table shows that PET can be considered as a very good barrier, when compared with other commercial films under the same test conditions. The temperature effect on the permeability constant for toluene/PET could not be quantitatively evaluated since the  $60^{\circ}$ C run (Experiment 7) had not reached a steady state rate of transmission after 1270 hours of permeation. The value presented in Table 10 is a permeation rate, in units of permeability constant, for the latest interval of time in the run. In that time interval the permeation rate was only  $2.3 \times 10^{-4}$ .g.mil/m².day.100 ppm.

# 7.2.5 Effect of pre-exposing the film to toluene vapor

In Experiment 8, the permeability of a film that was pre-exposed to a toluene vapor-nitrogen mixture with a toluene concentration of 25 ppm for 10 days at 24°C was determined.

In Experiment 9, the permeability data of a film which had been previously mounted for toluene vapor transmission was again determined. The film tested had been used in Experiment 4 and had been exposed to toluene vapor concentration of 90 ppm. A period of two months passed between the end of run 4 and the beginning of run 9.

The values for the diffusion coefficient D, and permeability constant  $\overline{P}$  for the film in run 8 were somewhat lower than those determined in experiments 1, 2 and 3 (see Table 10). As shown by the results of Experiment 9, previous exposure of the PET film to high level (i.e., 90 ppm) of toluene vapor resulted in a significant decrease in the diffusion coefficient and the permeability constant.

In fact, the results from Experiment 4 showed that a preexposure of the PET film to 90 ppm of toluene resulted in a 10-fold
reduction in the diffusion coefficient and permeability constant. It
should be pointed out that there is a similarity in the diffusivity
behavior of the film tested at 60°C (i.e., Experiment 7) and toluenepre-exposed film (i.e., Experiment 9), namely, in the extremely long
unsteady state period and the low permeability values.

As in the case of increase of temperature that produced unexpected results for the permeability constant, a complete understanding of changes produced in the polymer molecular structure as

a result of exposure to toluene vapor for prolonged periods of time can be carried out only by permeation experiments and is beyond the scope of this work. It appears clear that this phenomenon warrants further investigation.

#### CONCLUSIONS

# 8.1 <u>Literature review considerations</u>

- 1. Permeation of gases and vapor through polymer membranes
  presents a wide range of different behaviors. The following elements
  should be taken into account when a diffusional process is considered
  for these systems.
- a. A distinction should be made between glass-polymer systems and subcritical organic vapor. Organic vapor behavior depends on temperature, permeant concentration and polymer.
- b. The glass transition temperature of the polymer, Tg, is a very important parameter when organic vapors are considered.

  Permeation processes near Tg are likely to have a non-Fickian behavior, i.e., the diffusions coefficient is a function of permeant concentration and time.
- c. For most organic vapor/polymer systems, D is a function of permeant concentration and temperature of the experiment.
- 2. Two major theories are available to interpret diffusion processes in penetrant-polymer systems, namely:
- a. Fujita's free-volume theory which is applicable to organic-polymer systems with Fickian behavior and to gas-polymer systems.
- b. Dual sorption theory applicable to gas-polymer systems. There is a lack of data on organic vapor/PET permeation system. No

theory is available to explain non-Fickian behavior. The literature review indicated a lack of experimental data on toluene-PET system.

# 8.2 <u>Equipment considerations</u>

The continuous-flow method interfaced with an automatic gas sampling valve and gas chromatograph with Flame ionization detection appears to be a good method for conducting permeation experiments in organic vapor-polymer film systems. It can also be applied to mixtures of organic vapors with success.

Unsteady-state as well as steady-state data were reliable and a very acceptable error was obtained.

Keeping the permeant concentration constant appeared to be as a major obstacle in running permeation experiments with films for which the diffusion coefficient is very sensitive to the concentration values for long period of time. Working at ambient temperature, a low vapor pressure of the organic liquid limited the range of concentration for the permeant.

The system developed showed a great deal of operatorindependence for long-time runs, and low values for uncertainties.

#### 8.3 Permeation process considerations

The calculated Deborah number which was much larger than unity, and the shape of the permeation curves from Experiment 1 through Experiment 6 clearly indicated that permeation of toluene in PET at 23°C had an apparent Fickian behavior. In this case the relaxation times are much greater than the diffusion times.

When the system was run at 60°C, a temperature close to Tg, the shape of the permeant curve, as expected, showed a non-fickian behavior.

From the diffusivity coefficients at 23°C and at 60°C, the parameters for the Arrhenius expression of D as a function of temperature was calculated. The effective activation energy for diffusion  $E_D$  had a value of 9 Kcal/mole and the logarithm of the pre-exponential factor was 2.8.

Values found in the works of Chen (1974) and Michaels et al (1963) indicate that for PET/CH<sub>4</sub> systems the activation energy has a value of 13 Kcal/mole. A stronger interaction between toluene and PET than  $CH_4/PET$  may account for the observed difference.

Values of the diffusion coefficient versus toluene concentration plotted in Figure 18 showed that D was strongly dependent on the permeant concentration.

The lack of permeation after five months in the experiment run at a toluene concentration of 76 ppm suggested that a "threshold" concentration may be operative within a relatively narrow range around 76 ppm.

No permeation should be expected to occur in experiments carried out at concentration below this "threshold" within reasonable test time (i.e., six months).

Although more experiments are needed to corroborate this finding, it may have important practical packaging applications when dealing with aroma barriers.

When the free-volume theory was applied to approximately correlate the diffusion coefficient to permeant concentration for values above 80 ppm, two equations were developed:

$$D = 0.78 \times 10^{-13} exp \frac{w}{1.7 \times 10^{-3} + 0.22 w}$$
 (47)

$$w = 3.13 \times 10^{-5} \, \overline{c}^2 - 33.191 \times 10^{-4} \, \overline{c} + 92.6717 \times 10^{-3}$$
 (48)

Where D is the diffusion coefficient in cm<sup>2</sup>/sec

- w the weight fraction of toluene in PET in equilibrium with permeant concentration g/g
- c permeant concentration in ppm.

These equations are valid at least for the following conditions: a temperature around 23°C, toluene concentration above 80 ppm, and PET films as described in Section 7.2.3.

Figure 22 presents a comparison between predicted and actual values. As shown, an acceptable agreement is achieved.

Permeability constant values showed variation not only when different test methods were applied, but also between experiments employing the same method and conditions. Values from the accumulation method ranged from 0.05 to 0.27 g.mil/day.m².100 ppm, with an average of 0.14, while the average value for the continuous-flow method was 1.9 in the same units. The reason for this difference is not fully understood but it can have important consequences in packaging industry when designing PET aroma barrier to meet specific requirements.

Besides these variations, PET showed good barrier properties when compared with other commercial film under the same conditions (see Table 19).

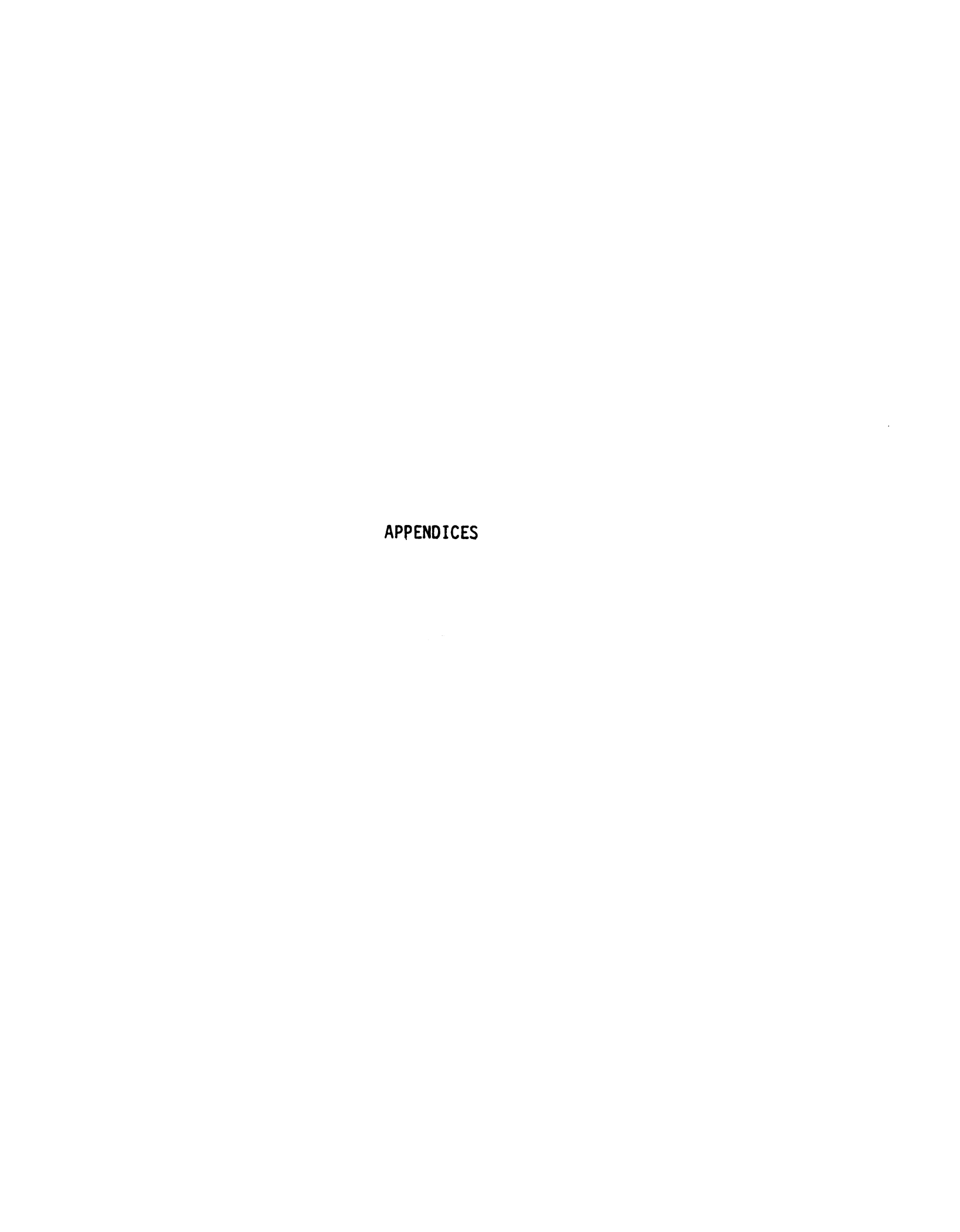
Temperature increase showed that the permeability constant is strongly temperature-dependent. Although the data were taken from an extremely long non-steady state experiment, the estimated permeability constant decreased by three orders of magnitude.

Finally, the effect of pre-exposing the PET film to the permeant vapor showed that concentration as low as 25 ppm had no clear effect on either D or  $\overline{P}$ . However, when the film was re-tested after being pre-exposed to toluene levels of 90 ppm in a previous permeation experiment, a strong hysteresis effect was observed, with values of  $\overline{P}$  being ten times lower than in the first run. Additional experiments are needed to verify these findings.

#### RECOMMENDATIONS

- 1. Fujita's free-volume theory equation developed in this work should be further tested with more data points for the toluene/PET system and with different organic penetrants that can allow a larger range of permeant concentrations. Diffusion coefficient values for the toluene/PET system should be checked for toluene concentration around 85 ppm. A different organic permeant with a lower partial pressure than that of toluene should be employed in order to obtain a larger range of permeant concentration. In this case the model can be submitted to more rigorous conditions always below Tg.
- 2. To confirm whether or not there is a "threshold" concentration for this or in another penetrant/barrier membrane system should be of theoretical and practical interest.
- 3. From 23°C to 60°C there exists a change from apparent Fickian to non-Fickian behavior for the toluene/PET system. More experiments in this range of temperature are needed in order to know whether the change is "smooth" and at what temperature such a transition occurs.
- 4. Methods such as wide-angle x-ray, low-angle light scattering, optical microscopy and birefringence should be applied together with diffusion experiments, to reach a better understanding of the change in the amorphous and crystalline structure of the PET films.

These methods could help to better understand the effect of temperature change below Tg and hysteresis behavior of toluene/PET. The difference among permeability constant values when using apparently similar films could also be better understood.



#### APPENDIX I

# Sample Calculations

Examples are given of calculations from raw data to yield each of the required variables. These calculations are illustrated by Experiment 1 for the quasi-isostatic or accumulation technique and by Experiment 4 for the continuous-flow method.

# Permeability constant, P(\*)

Where q is rate of permeation in the steady-state portion of the experiments in g per day

 $\ell$  is the thickness of the film in  $10^{-3}$  inch or mil

A is the area of permeation,  $m^2$ 

c is the concentration in the upper cell chamber, expressed as ppm. The value of concentration in the lower cell chamber is considered very small compared with the first one.

for q = 
$$8.28 \times 10^{-4}$$
 g/day  
 $\ell = 3.70 \times 10^{-3}$  cm =  $1.457$  mils  
A =  $49.48$  cm<sup>2</sup> =  $49.48 \times 10^{-4}$  m<sup>2</sup>  
 $\overline{c}$  =  $91.3$  ppm

<sup>(\*)</sup>The units in which  $\vec{P}$  is expressed are of common use in packaging engineering.

# Total amount of material permeated, Q

#### Accumulative case:

From the calibration curve,  $1 \times 10^6$  area units should be multiplied by 3.78 in order to get ppm, since the volume of the lower cell chamber is 50 cc.

$$Q = L \times 3.78 \times 50$$
 in micrograms

Where Q is the total amount permeated in micrograms

L is the output from the GC, in area units  $\times 10^{-6}$ 

# For continuous-flow method

$$Q = 3.78 \int L.Fd \qquad (A-2)$$

Where F is the flow rate of the toluene-nitrogen mixture continuously leaving the lower cell chamber

F is considered constant. The integration was carried out graphically.

#### Rate of Permeation

From two pair of values Q and time on the steady-state portion of the process,  $Q_1$ ,  $Q_2$ ,  $t_1$  and  $t_2$ , where

$$Q_2 > Q_1$$
 and  $t_2 > t_1$ 

#### APPENDIX II

### Model for the continuous-flow calculation of D

The permeation flux F through the membrane of thickness  $\ell$  is given by:

$$F(x) = -D \frac{\partial c}{\partial x} \tag{A-3}$$

where c is the concentration of the permeant in the membrane at a position x. In order to solve approximately our system, it is assumed that the diffusion coefficient D is not a function of the concentration, that the surface concentration is proportional to the pressure of the permeant, and that swelling of the membrane is negligible. According to the geometry of the system only flux at is of interest. The concentration of the permeant was kept constant during the permeation process.

The following boundary conditions complete the description of the system:

$$c = c_0$$
 at  $x = 0$   $t = 0$  (A-4)

$$c = c_1 = 0$$
 at  $x = l$  t > 0 (A-5)

$$c = c_1 = 0$$
 at  $x = \ell$   $t > 0$  (A-5)  
 $c = c_2 \frac{\ell - x}{\ell}$  at  $0 < x < \ell$   $t = \infty$  (A-6)

where c  $_{0}$  is the concentration at  $\ell$  =  $\times$  in equilibrium with the permeant flow. These boundary conditions represent the change from one steadystate, t = 0 and  $c_1 = 0$ , to the final  $c_2$  at  $t = \infty$ , with the pressure of permeant on the downstream side of the membrane always kept at zero, since pure nitrogen is continuously flowed.

Solution for equations A-3 to A-6 is already given in the literature, Pasternak et al (1970):

$$F = \frac{Dc_1}{\ell} + \frac{D(c_2 - c_1)}{\ell} \frac{4}{\sqrt{\pi}} \left(\frac{\ell^2}{4Dt}\right)^{1/2} \int_{0}^{\infty} \exp\left(\frac{-n^2 \ell^2}{4Dt}\right)$$
 (A-7)

Since the second term contributes less than 2% to the sum, it is reasonable to retain only the first term. This condition is satisfied for  $\Delta F/\Delta F\infty$  < 0.97 where  $\Delta$  F represents the change in flux at time t and  $\Delta F\infty$  at t =  $\infty$ .

The first order approximation of equation A-7 is:

$$\frac{\Delta F}{\Delta F \infty} = (4/\sqrt{\pi})(\ell^2/4Dt)^{1/2} \exp(-\ell^2/4Dt)$$
 (A-8)

that can be written in the following form:

$$\frac{\Delta F}{\Lambda F \infty} = (4/\sqrt{\pi}) x^{1/2} \exp(-x) \tag{A-9}$$

where  $X = \ell^2/4Dt$ 

For each value of  $\Delta F/\Delta F \infty$  an X can be calculated, and plotting  $\chi^{-2}$  versus t a straight line is obtained. The slope of this line equals  $4D/\ell^2$ .

To solve equation A-9 for each value of  $\Delta F/\Delta F \infty$  a Newton-Rawson method was employed:

If

$$G = X^{1/2} e^{-X} - A$$
 (A-10)

where 
$$A = \frac{\sqrt{\pi}}{4} \frac{\Delta F}{\Delta F \infty}$$
 (A-11)

$$x^{(k+1)} = x^{(k)} - \frac{[x^{(k)}]^{1/2} e^{-x^{(k)}} - A}{\exp[-x^{(k)}]^{\frac{1}{2}} [x^{(k)}]^{1/2} - [x^{(k)}]^{1/2}}$$
(A-12)

Where  $X^{(k+1)}$  is the k+1 interaction for X value.

From data of Experiment 4,

 $\Delta F^{\infty} = 3.656 \, \mu g/min$ 

TABLE A-1. Values for Experiment 4

t in hours	ΔF(t),μg/mm	Δ Ϝ/ΔϜ∞	A	X
109.8	1.264	0.3458	0.1532	0.02466
118.0	1.675	0.4582	0.2030	0.04510
135.6	2.673	0.7311	0.3240	0.13847
145.6	3.141	0.8591	0.3807	0.2292

Figure A-1 shows X vs t, slope = 0.0056543 h<sup>-1</sup>
Then D =  $\frac{\text{slope x } \ell^2}{4 \text{ x } 3600}$  = 4.67 x 10<sup>-12</sup> cm<sup>2</sup>/sec.

Smith and Adams (1980) used this approach to calculate the diffusion coefficient of gases in glassy polymers (nitrogen-polycarbonate). Also Chen (1974), working with propane and PET, calculated the diffusion coefficient by this method.

A similar procedure was applied to data from Experiment 3 to calculate D.

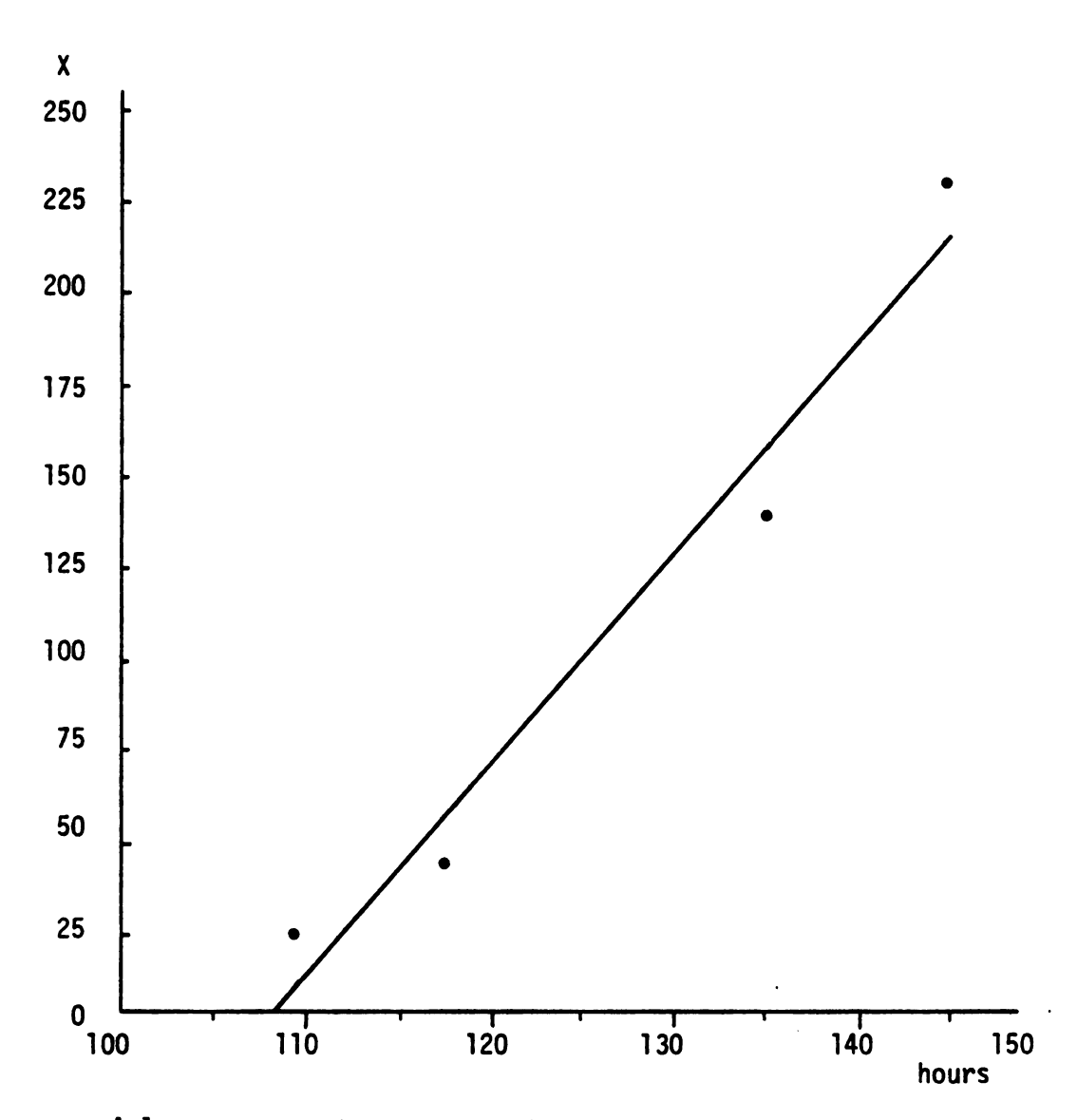


Figure A-1. X versus time for Experiment 4.

#### APPENDIX III

#### Model for lag-time method

During the accumulative, batch or quasi-isostatic experiment, the total amount of toluene permeated from time zero to t is recorded.

The permeant concentration remains constant during the experiment. The concentration of the permeated material increases from zero to a few percent of the permeant concentration at the end of the run.

The rate of passage of diffusant through the membrane is plotted as an amount/time curve, whose final slope allows P to be calculated. There is an interval before the steady state can be approached due to the finite diffusion velocity of permeant within the membrane. The intercept  $\theta$ , between t = 0 and the intersection of the line for steady-state for large time extrapolated back to t-axis, provides an easy way of evaluating D. When D is considered independent of concentration, it is usually called the "lag time."

The solution of Fick's law
$$\frac{\partial c}{\partial t} = D \frac{\partial^{2} c}{\partial x^{2}}$$
(A-13)

when the boundary conditions are:

$$c = c_0$$
 at  $x = 0$   $t = 0$  (A-14)

$$c = c_2 \text{ at } x = \ell$$
  $t > 0$  (A-15)

$$c = f(\xi) = c_1 \quad 0 < \xi < \ell \quad t = 0$$
 (A-16)

Given already in the literature, Barrer (1939).

To get the intersection of Q with the t-axis, equation A-17 should be equaled to zero, i.e., Q = 0, then t becomes  $\theta$ .

$$(c_2 - c_0)\theta = \frac{\ell^2}{D} \left[ \frac{c_2}{6} + \frac{c_0}{3} - \frac{c_1}{2} \right]$$
 (A-18)

In our actual case  $c_1 = c_0 = 0$ , therefore,

$$Q = \frac{\ell^2}{6D} \tag{A-19}$$

 $\theta$  is practically determined by the intersection of the projection of the steady-state portion of the curve Q vs on the t-axis.

From the above,

$$D_{\text{Lag}} = \frac{\ell^2}{6\theta} \tag{A-20}$$

#### APPENDIX IV

# Model for small-time approximation method

In the accumulation method, when the time is inconveniently long to reach the steady state, equations A-13 to A-16 are more conveniently solved by a transformation formula attributed to Holstein by Rogers, Buritz and Alpert (1954) of the form, when D is assumed constant:

$$\frac{dp}{dt} = \frac{2A}{V_0} \text{ sp } (D/\pi t)^{1/2} \int_0^\infty \exp \left[-\ell^2/4Dt\right) (2m+1)^2 ]$$
 (A-21)

Because of the inverted placement of t in the exponentials, this series converges most rapidly for small values of t rather than for large values. For relatively short times, equation A-21 may be approximated by neglecting all of the terms beyond the first.

Multiplying by  $t^{1/2}$  and taking logarithms on both sides, we have

$$\ln t^{1/2} \frac{dp}{dt} = \ln[(2 \text{ As p/V}_0)(D/\pi)^{1/2}] - (\ell^2/4Dt)$$
 (A-22)

Then by plotting  $\ln(t^{1/2} \frac{dp}{dt})$  versus  $t^{-1}$  we should get a straight line of slope  $(-\ell^2/4D)$ .

To obtain the true value of D from this plot, it is necessary to have values of time which are relatively small compared with the time required to reach the steady state as it happens in experiments.

This equation was applied by Meares (1965) to the permeation of allyl chloride in poly(vinyl acetate) where D is dependent of concentration of the permeant and time.

As Meares pointed out, when the extrapolation data of D as a function of  $t^{-1}$  is extrapolated toward t=0 (i.e.,  $1/t=\infty$ ) one finds the limiting slope of  $\ln t^{1/2}$  dp/dt versus  $t^{-1}$ . This extrapolation is towards the time when vapor has not penetrated beyond the ingoing face of the membrane. Thus the limiting slope of a plot of equation A-22 gives  $-\ell^2/4D_0$ , where  $D_0$  is the limiting diffusion coefficient of the polymer.

Calculation of  $D_O$  using the method of small time for Experiments 1, 2, 4 and 7 in order to estimate the effect of temperature on diffusion coefficient is presented in Appendix V. In this case dp/dt has been substituted by  $N = \Delta Q/\Delta t$  where  $\Delta Q$  is the amount of permeant in g during a  $\Delta t$  time in hours.

Values of  $\ln(t^{1/2})$  versus  $t^{-1}$  were algebraically fitted by a least-square method to a straight line.

# APPENDIX V Small-time method calculation

For these calculations,  $N = \Delta Q/\Delta t$ 

Experiment 1: Values for experiment 1 are given in Table A-2.

TABLE A-2. Values for small-time method Experiment 1

t in hours	t <sup>-1</sup> × 10 <sup>3</sup>	ln(t <sup>1/2</sup> N)
136.75	7.313	3.690
142.0	7.042	4.743
151.5	6.600	5.941
160.0	6.750	6.367

From a least-square fitting of  $ln(t^{1/2} N)$  versus  $t^{-1}$ , slope = 2.528  $h^{-1}$   $D_s = 3.74 \times 10^{-13} \text{ cm}^2/\text{sec}$ 

Experiment 2. Values for Experiment 2 are given in Table A-3.

TABLE A-3. Values for small-time method Experiment 2

t in hours	$t^{-1} \times 10^3$	]n(t <sup>1/2</sup> N)	
262.0	3.817	4.65	
265.0	3.774	4.703	
276.0	3.623	4.627	
294.3	3.398	5.154	

Slope =  $-1130 h^{-1}$ 

 $D_s = 7.83 \times 10^{-13} \text{ cm}^2/\text{sec}$ 

Experiment 4. Values for Experiment 4 are given in Table A-4

TABLE A-4. Values for small-time method Experiment 4

t in hours	$t^{-1} \times 10^3$	In(t <sup>1/2</sup> N)
102.8	9.728	4.685
103.9	9.625	5.315
104.8	9.542	5.564
106.8	9.363	6.174
107.8	9.277	6.363
108.8	9.191	6.543
110.8	9.025	6.767
112.8	8.866	6.884

Slope =  $-2.460 \text{ h}^{-1}$ 

 $D_s = 3.36 \times 10^{-13} \text{ cm}^2/\text{sec}$ 

Experiment 7. Values for Experiment 7 are given in Table A-5.

TABLE A-5. Values for small-time method Experiment 7

t in hours	$t^{-1} \times 10^3$	ln(t <sup>1/2</sup> N)
33.25	30.070	4.890
59.75	11.740	5.213
108.75	9.200	4.470
143.55	6.970	4.530
194.25	5.150	6.036
302.00	3.310	5.057
505.5	1.980	5.230
696.0	1.440	6.840

Slope =  $-32.8 h^{-1}$ 

 $D_s = 2.4 \times 10^{-11} \text{ cm}^2/\text{sec}$ 

## APPENDIX VI

## <u>Differential Scanning Calorimetric (DSC) Plots</u>

Figures A-2, A-3, A-4 and A-5 show the value of Tg for two samples, a and b, not exposed to toluene (Figures A-2 and A-3) and two samples, c and d, that were used in a diffusion experiment and were preheated before the DSC test (Figures A-4 and A-5).

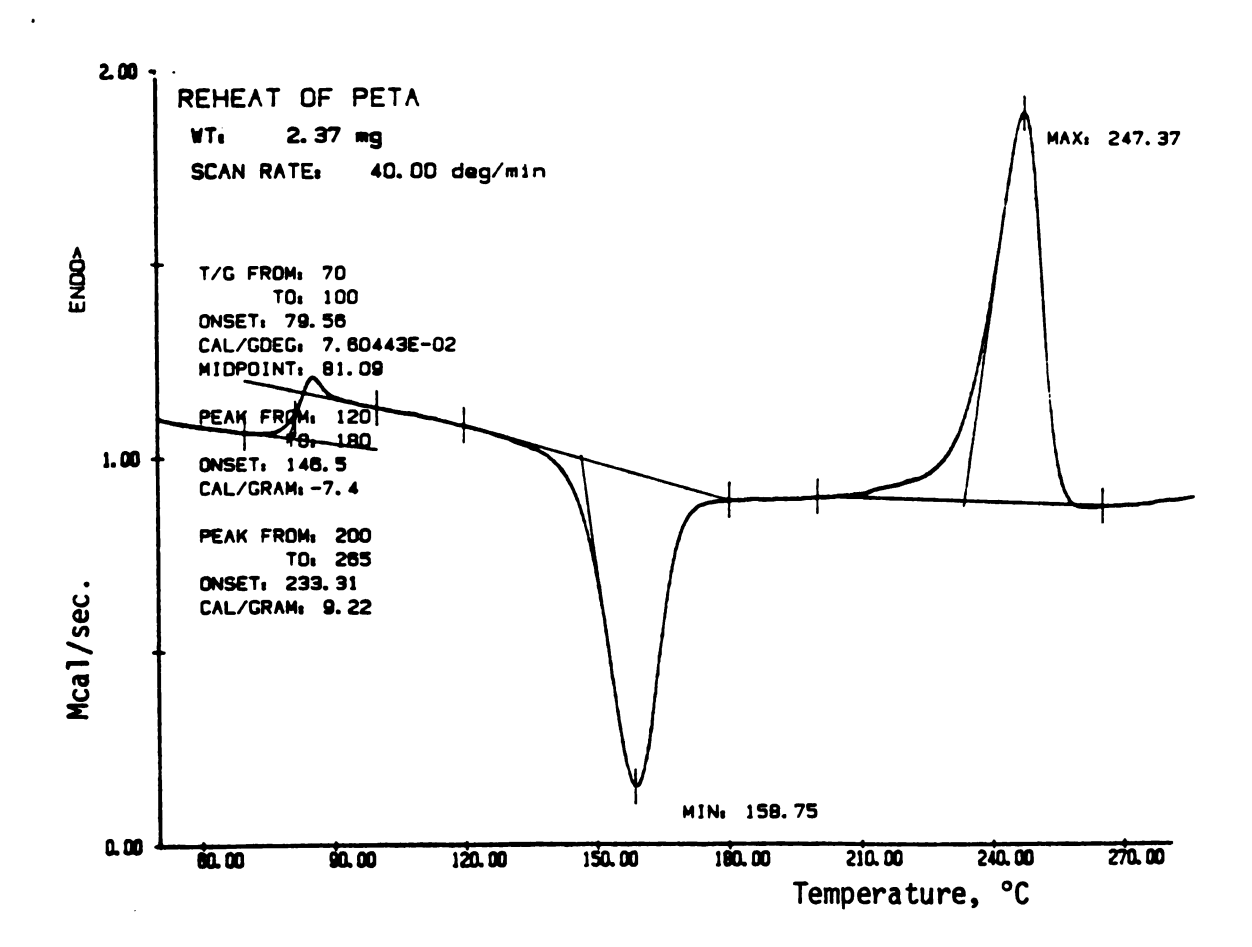


Figure A-2. DSC plot for sample a.

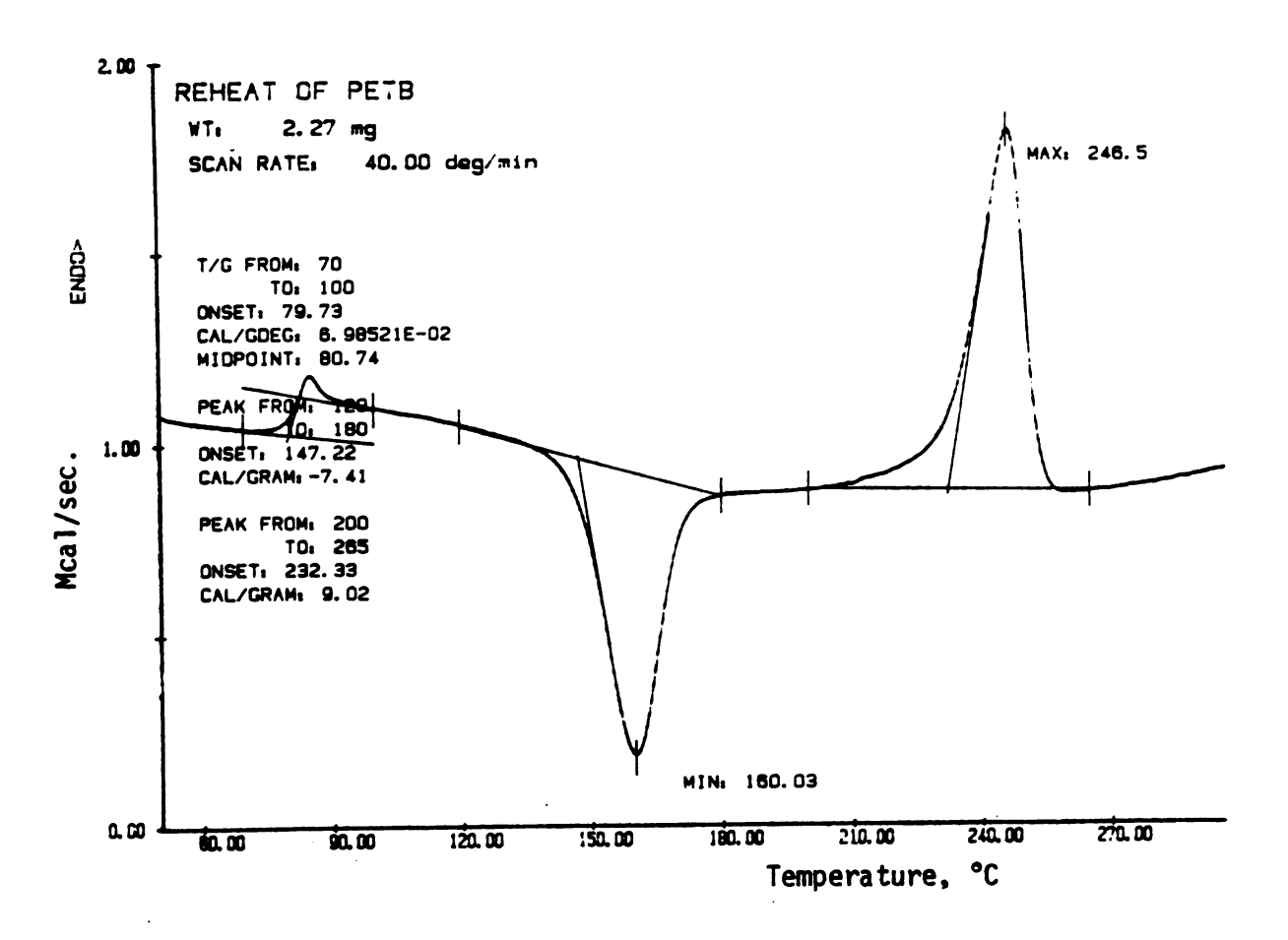


Figure A-3. DSC plot for sample b.

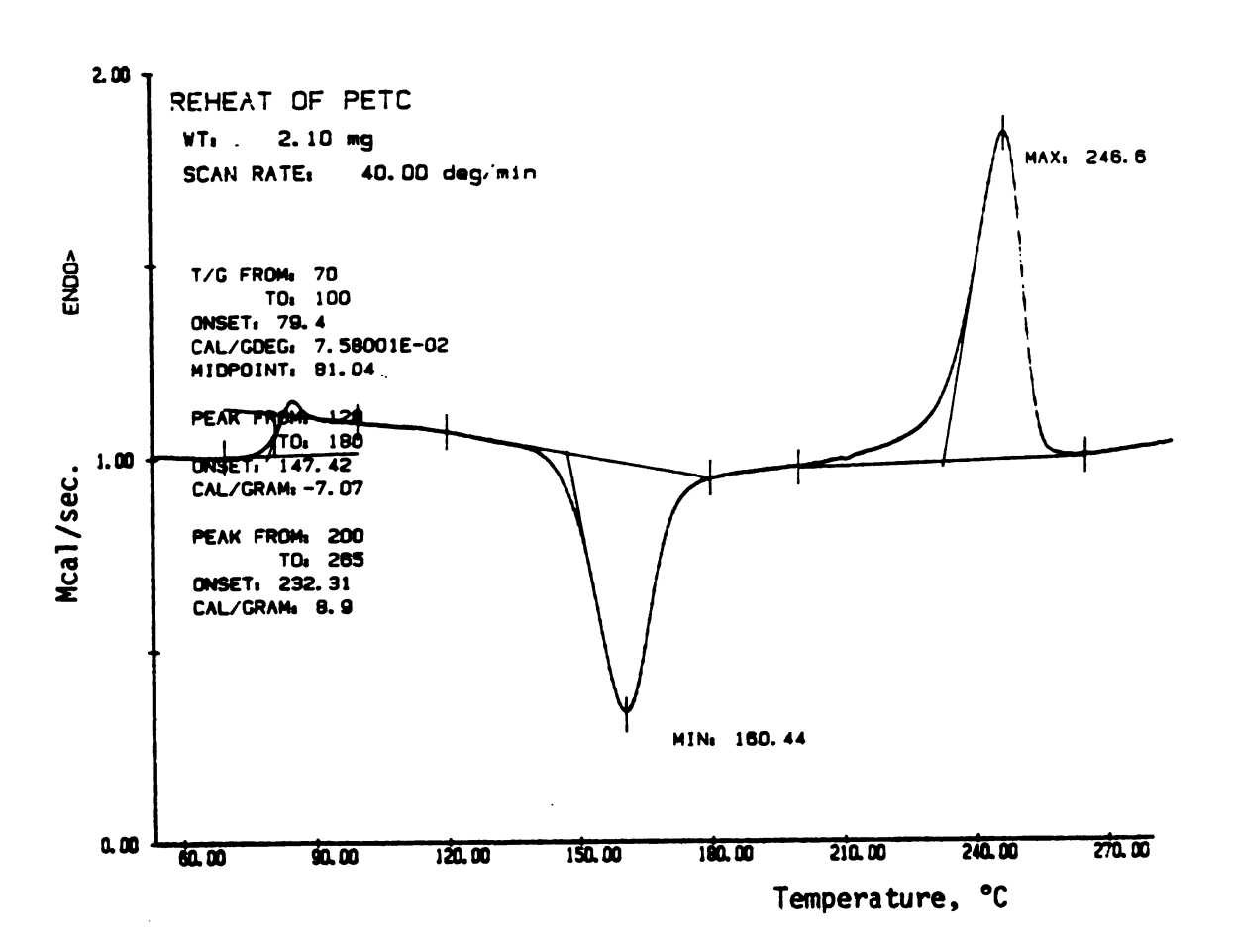


Figure A-4. DSC plot for sample c.

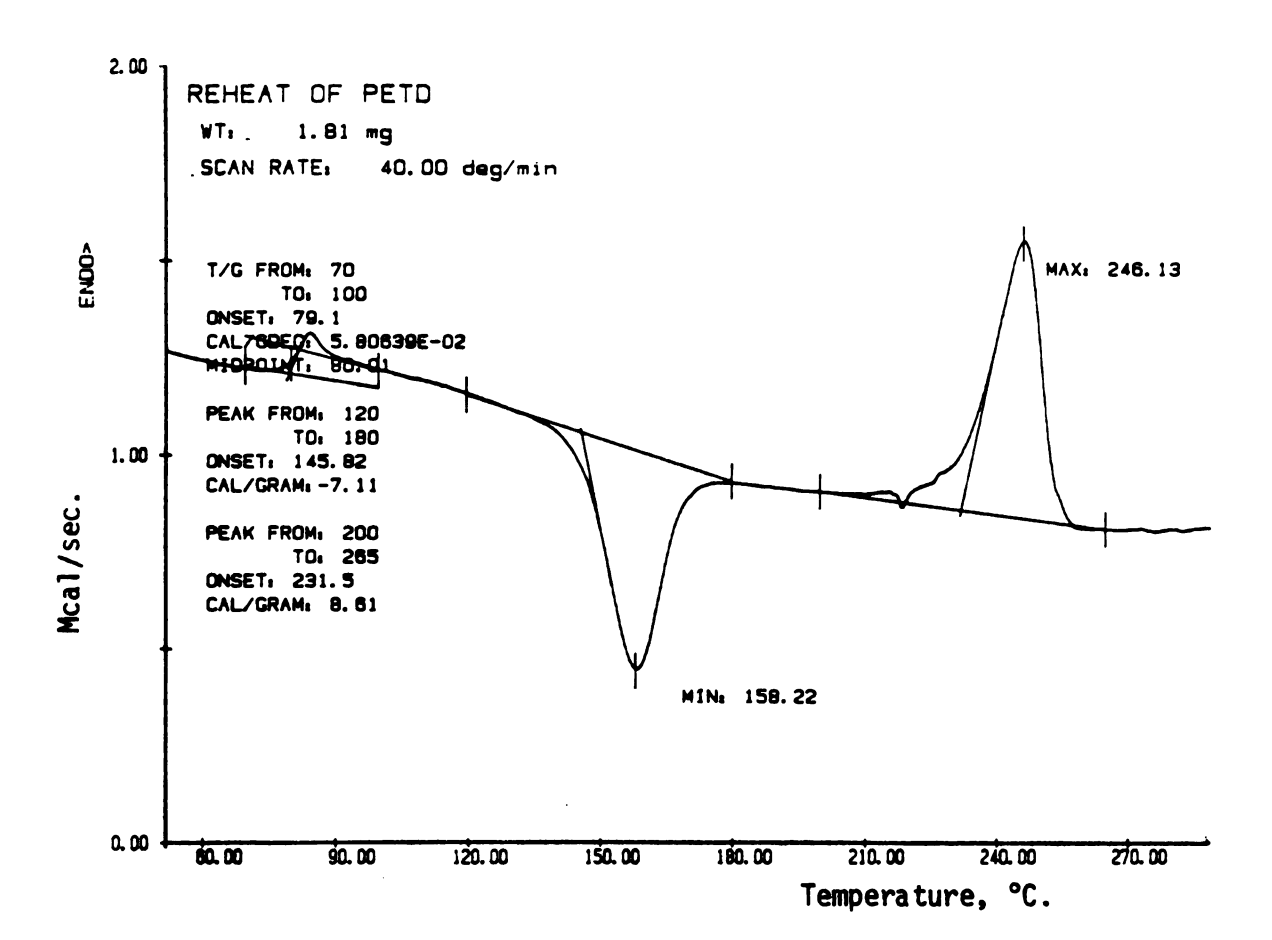
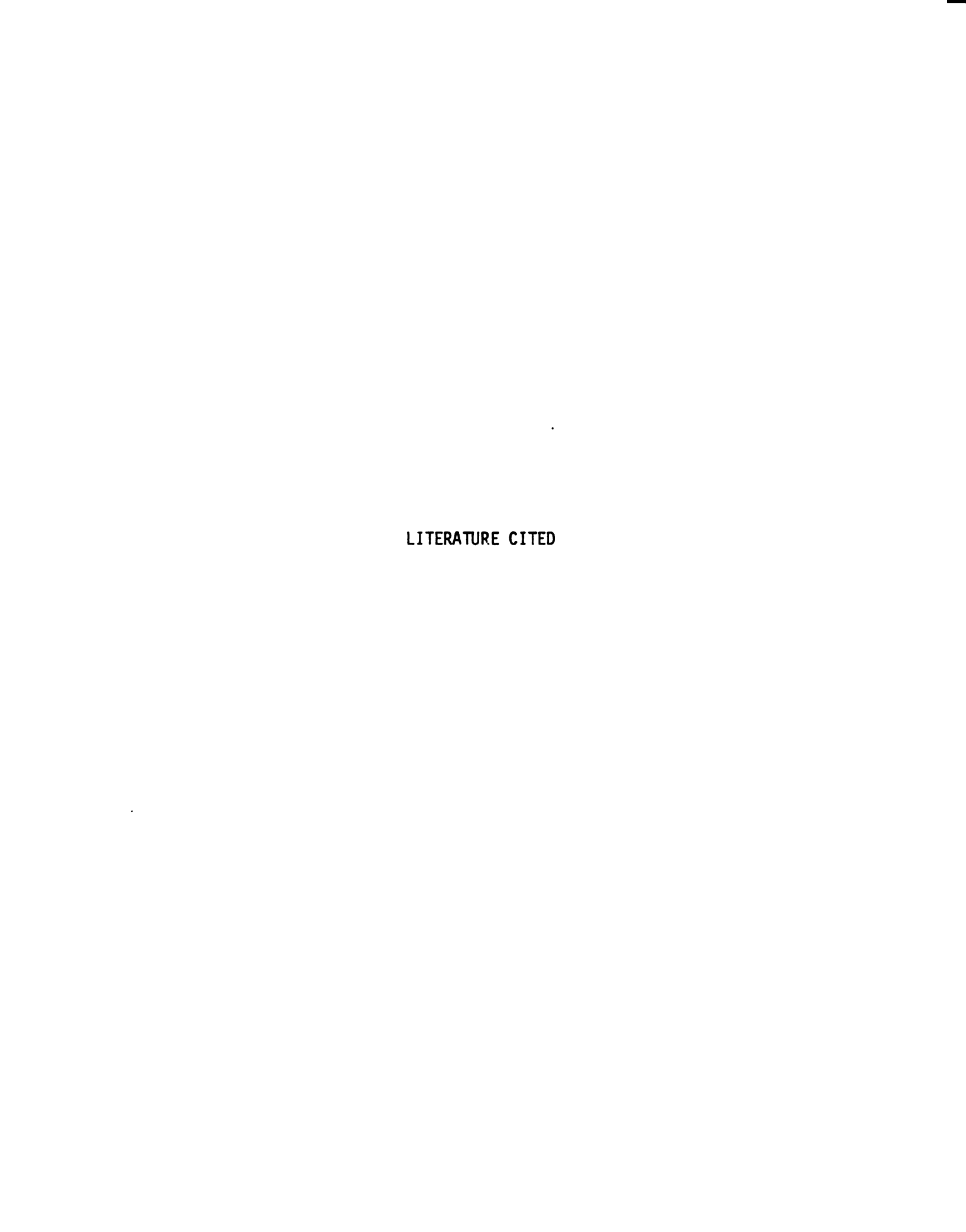


Figure A-5. DSC plot for sample d.



## LITERATURE CITED

- Alfrey, T., E.F. Gurnee, W.G. Lloyd, "Diffusion in Glassy Polymers,"

  J. Polym. Sci. C12, 249 (1966).
- Astarita, G., G. Marucci, <u>Principles of Non-Newtonian Fluid</u>
  <u>Mechanics</u>, McGraw-Hill, London: 1974.
- ASTM part 35, 1981, Annual Book of ASTM Standards, American Society for Testing Materials, Library of Congress
- Baner, L.A., "The Concentration Dependent Diffusion of Toluene Vapor Through Oriented Polypropylene and Polyvinylidene Chloride,"
  Master of Science thesis, School of Packaging, Michigan State University, 1984.
- Baner, L.A., R.J. Hernandez, K. Jayaraman, J.R. Giacin, Symposium on Current Technologies in Flexible Packaging, St. Charles, Illinois, 1984.
- Barrer, R.M., "Permeation, Diffusion and Solution of Gases in Organic Polymers," <u>Trans. Faraday Soc. 35</u>, 628 (1939).
- Barrer, R.M., <u>Diffusion in Polymers</u> Chap. 6, Edited by J. Crank and G.S. Park, 4th edition, Academic Press, London-New York: 1981.
- Barrer, R.M., J. Barrier, J. Slater, "Sorption and Diffusion in Ethyl Cellulose, Part I, History-Dependence of Sorption Isotherms and Permeation Rates," J. Polymer Sci. 23, 315 (1957).
- Barrer, R.M., R.R. Fergusson, "Diffusion of Benzene in Rubber and Polyethylene," <u>Trans. Faraday Soc.</u> 54, 989 (1958).
- Bird, R.R., W.E. Steward, E.N. Lightfoot, <u>Transport Phenomena</u>, John Wiley and Sons Inc., New York: 1960.
- Bont, R., "The Influence of Thermal Mechanical History on the Permeation of Toluene in Glassy Poly(ethylene) Terephthalate," Master of Science thesis, School of Packaging, Michigan State University, 1984.
- Chen, S.P., "Effect of Volume Relaxation, Temperature, and Chemical Structure on Diffusion of Gaseous Hydrocarbons through Glassy Polymers," Polymer Preprints 15, 1, 77-83 (1974).

- Cobbs, W.H., R.L. Burton, "Crystallization of Polyethylene Terephthalate," J. Polymer Sci. 10, 3, 275-290 (1953).
- Cohen, M.H., D. Turnbull, "Molecular Transport in Liquids and Glasses," J. Chem. Phys. 31, 1164-1169 (1959).
- Crank, J., <u>The Mathematics of Diffusion</u>, 2nd edition, Clarendon Press, Oxford: 1975.
- Daubeny, R. de P., C.W. Bunn, C.J. Brown, "The Crystal Structure of Polyethylene Terephthalate," <u>Proc. R. Soc. London, Ser. A</u>, 226, 531 (1955).
- Drechsel, P., J.L. Hoard, F.A. Long, "Diffusion of Acetone into Cellulose Nitrate Films and Study of the Accompanying Orientation," J. Polymer Sci. 10, 241-252 (1953).
- Dumbleton, J.H., "Chain Folding in Oriented Poly(ethylene)
  Terephthalate," J. Polymer Sci. A-2, 7, 667 (1969).
- Encyclopedia of Polymer Science and Technology, Interscience Publisher, John Wiley and Son Inc., New York: 1965.
- Fang, S.M., S.A. Stern, H.F. Frisch, "A 'Free Volume' Model of Permeation of Gas and Liquid Mixtures through Polymeric Membranes," Chem. Eng. Sci. 30, 773-780 (1975).
- Fels, M., R.Y.M. Huang, "Diffusion Coefficients of Liquids in Polymer Membrane by a Desorption Method," J. Appl. Polym. Sci. 14, 523 (1970).
- Ferry, J.D., <u>Viscoelastic Properties of Polymers</u>, 2nd edition, John Wiley and Sons, Inc.: 1970.
- Fujita, H., "Diffusion in Polymer-Diluent Systems," <u>Fortsch-Hochpolym-Forsch</u> 3, 1 (1961).
- Fujita, H., <u>Diffusion in Polymers</u>, 4th edition, Edited by J. Crank and G.S. Park, Academic Press, London: 1981.
- Hartley, G.S., Crank, J., "Some Fundamental Definitions and Concepts in Diffusion Processes," <u>Trans. Faraday Soc. 45</u>, 801 (1949).
- Haward, R.N., <u>The Physics of Glassy Polymers</u>, Applied Science Publishers, Ltd., London: 1973.
- Hayes, M.J., G.S. Park, "The Diffusion of Benzene in Rubber, Part II, High Concentration of Benzene," <u>Trans. Faraday Soc.</u> 52, 949 (1956).

- Hopfenberg, H.B., V. Stannett, "The Diffusion and Sorption of Gases and Vapor and Glassy Polymers," Chapter 9 in <u>The Physics of Glassy Polymers</u> edited by R.N. Haward, Applied Science Publishers, London: 1973.
- Hopfenberg, H.B., H.L. Frisch, "Transport of Organic Micromolecules in Amorphous Polymers," Polymer Letters 7 405-409 (1969).
- Kishimoto, A., Enda, Y., "Diffusion of Benzene in Polyarylates,"

  J. Polym. Sci. Al, 1799 (1963).
- Kishimoto, A., K. Matsumoto, "Effect of Film Thickness upon the Sorption of Organic Vapors in Polymers Slightly Above their Glass Transition Temperature," J. Polym. Sci. part A2, 679-687 (1964).
- Koros, W.J., D.R. Paul, "Transient and Steady-State Permeation in Poly(ethylene Terephthalate) Above and Below Glass Transition,"

  J. Polymer Sci. Physics Ed. 16, 2171-2187 (1978).
- Kulkerni, S.S., S.A. Stern, "The Diffusion of CO<sub>2</sub>, CH<sub>4</sub>, C<sub>2</sub>H<sub>4</sub>, and C<sub>3</sub>H<sub>8</sub> in Polyethylene at Elevated Pressures," <u>J. Polymer Sci. Physics Ed. 21</u>, 441-465 (1983).
- Lasoski, S.W., W.H. Cobbs, "Moisture Permeability of Polymers,
  A Role of Crystallinity and Orientation," J. Polymer Sci. 36,
  21-33 (1959).
- Long, F.A., R.J. Kokes, "Diffusion of Benzene and Methylene Chloride Vapors into Polysterene," <u>J. Am. Chem. Soc. 75</u>, 2232 (1953).
- Makarewicz, P.J., G.L. Wilkes, "Diffusion Studies of Poly(ethylene)
  Terephthalate," <u>J. Polymer Sci., Physics Ed. 16</u>, 1529-2544
  (1978).
- Meares, P., "The Diffusion of Gases Through Polyvinil Acetate,"

  <u>J. Am. Chem. Soc.</u> 76, 3415 (1954).
- Meares, P., "Diffusion of Allyl Chloride in Polyvinyl-acetate,"

  <u>J. Polymer Sci. 27</u>, 391 (1958).
- Meares, P., "Transient Permeation of Organic Vapors Through Polymer Membranes," J. Appl. Polym. Sci. 9, 917-932 (1965).
- Meredith, R., Bay-Sung Hsu, "Stress Relaxation in Nylon and Terylene: Influence of Strain, Temperature, and Humidity,"

  J. Polymer Sci. 61, 253-270 (1962).

- Michaels, A.S., W.R. Vieth, J.A. Barrie, "Solution of Gases in Polyethylene Terephthalate," <u>J. Applied Physics</u> 34, (1), 1-12 (1963-a).
- Michaels, A.S., W.R. Vieth, J.A. Barrie, "Diffusion of Gases in Polyethylene Terephthalate," <u>J. Applied Physics 34</u>, (1), 13-30 (1963-b).
- Michaels, A.S., H.J. Bixler, H.L. Fein, "Gas Transport in Thermally Conditioned Linear Polyethylene," J. Appl. Physics 35, (11), 31-65 (1964).
- Misra, A., R.S. Stein, "Stress-Induced Crystallization of Poly(ethylene) Terephthalate," J. Polymer Sci., Polym. Phy. Ed. 17, 235-257 (1979).
- Overbergh, N., H. Berghmans, G. Smets, "Crystallization of Isotactic Polystyrene Induced by Organic Vapours," <u>Polymer 16</u> 703 (1975).
- Park, G.S., <u>Diffusion in Polymers</u> Chapter 5 edited by J. Crank and G.S. Park, 4th edition, Academic Press, London-New York: 1981.
- Pasternak, R.A., J.F. Schmimscheimer, J. Heller, "A Dynamic Approach to Diffusion and Permeation Measurements," J. Polymer Sci. Part A-2 8, 467-479 (1970).
- Paul, D.R., D.R. Kemp, "The Diffusion Time Lag in Polymer Membranes Containing Adsorptive Fillers," J. Polymer Sci. Symposium 41, 79-93 (1973).
- Paul, D.R., W.J. Koros, "Effect of Partially Immobilizing Sorption on Permeability and the Diffusion Time Lag," J. Polymer Sci., Polym. Phys. Ed. 14, 675-685 (1976).
- Peterlin, A., "Dependence of Diffusive Transport on Morphology of Crystalline Polymers," J. Macromol. Sci. Phys. B11(1), 57-87 (1975).
- Petropolous, J.H., "Quantitative Analysis of Gaseous Diffusion in Glassy Polymers," J. Polymer Sci. A-2, 8, 1797 (1970).
- Prager, S., F.A. Long, "Diffusion of Hydrocarbons in Polyisobutylene,"

  <u>J. Am. Chem. Soc. 73</u>, 4072 (1951).
- Pye, D.G., H.H. Hoehn, M. Panar, "Measurements of Gas Permeability of Polymers II. Apparatus for Determination of Permeabilities of Mixed Gases and Vapor," J. Applied Polymer Sci. 20, 287-301 (1976).

- Richards, R.B., "The Phase Equilibrium Between a Crystalline Polymer and Solvents," <u>Trans. Faraday Soc. B42</u>, 12 (1946).
- Richman, D., F.A. Long, "Measurements of Concentration Gradients for Diffusion of Vapor in Polymers," J. Am. Chem. Soc. 82, 509 (1960).
- Rogers, W.A., R.S. Buritz, D. Alpert, "Diffusion Coefficient, Solubility and Permeability for Helium in Glass," J. Appl. Phys. 25, 868 (1954).
- Rodriguez, F., <u>Principles of Polymer Science</u>, 2nd edition, McGraw-Hill Book Co. 1982.
- Smith, T.L., R.E. Adam, "Effect of the Tensile Deformation on Gas Transport in Glassy Polymer Films," <u>Polymer 22, 3</u>, 299-304 (1981).
- Stern, S.A., S.M. Fang, H.L. Frisch, "Effect of Pressure on Gas Permeability Coefficients. A New Application of 'Free Volume' Theory," J. Polymer Sci. A-2 10, 201-219 (1972).
- Stern, S.A., P.A. Gareis, T.F. Sinclair, P.H. Mohr, "Performance of a Versatile Variable-Volume Permeability Cell. Comparison of Gas Permeability Measurements by the Variable-volume Method and Variable-pressure Method," J. Applied Polym. Sci. 7, 2035-2051 (1963).
- Stern, S.A., S.S. Kulkarni, "Test of a 'Free-volume' Model of Gas Permeation through Polymer Membrane Pure CO<sub>2</sub>, CH<sub>4</sub>, C<sub>2</sub>H<sub>4</sub> and C<sub>3</sub>H<sub>8</sub> in Polyethylene," <u>J. Polymer Sci. Polym. Phys. Ed. 21</u>, 467-481 (1983).
- Stern, S.A., T.F. Sinclair, P.J. Gareis, "An Improved Permeability Apparatus of the Volume-Volume Type," <u>Modern Plastics 42</u>, 154 (1964).
- Van Amerongen, G.J., "Solubility, Diffusion and Permeation of Gases in Gutta-percha," J. Polym. Sci. 2, 381 (1947).
- Vrentas, J.S., J.L. Duda, "Diffusion in Polymer-Solvent System I Reexamination of the Free-volume Theory," J. Polym. Sci. Phys. Ed. 15, 403-416 (1977a).
- Vrentas, J.S., J.L. Duda, "Diffusion in Polymer-solvent Systems II.

  A Predictive Theory for the Dependence of Diffusion Coefficient on Temperature, Concentration and Molecular Weight," J. Polym. Sci. Polym. Phys. Ed 15, 417-439 (1977b)

- Vrentas, J.S., C.M. Jarzebski, J.L. Duda, "A Deborah Number for Diffusion in Polymer-solvent System," AICHE Journal 25(5), 894-901 (1975).
- Zobel, M.G.R., "Measurement of Odour Permeability of Polypropylene Packaging Films at Low Odourant Levels," <u>Polymer Testing 3</u>, 133-142 (1982).



## MATERIAL BIBLIOGRAPHY

Burdick and Jackson Laboratories Inc.

Solvent Guide (1980)

Muskegon, Michigan

Crawford Fitting Co. 29500 Solon Road

Catalog C-578 (1980)

Hewlett Packard

Solon, Ohio 44139

5830A Gas Chromatograph Instrument Manual

Lab Glass Inc.

Fort Henry Drive Kingston, Tennessee 37663

Calibrated Density Floater

Supe1 co

Catalog 22 (1984)

Chromatography Supplies

